OXYGEN-MEDIATED REGULATION OF CHOLESTEROL SYNTHESIS

THROUGH ACCELERATED DEGRADATION OF

HMG COA REDUCTASE

APPROVED BY SUPERVISORY COMMITTEE

Russell DeBose-Boyd, Ph.D.

Richard Bruick, Ph.D.

Michael Brown, M.D.

Zhijian Chen, Ph.D.

George DeMartino, Ph.D.

To my family

For their love and support

OXYGEN-MEDIATED REGULATION OF CHOLESTEROL SYNTHESIS THROUGH ACCELERATED DEGRADATION OF HMG COA REDUCTASE

by

ANDREW TUAN DUC NGUYEN

DISSERTATION

Presented to the Faculty of the Graduate School of Biomedical Sciences

The University of Texas Southwestern Medical Center at Dallas

In Partial Fulfillment of the Requirements

For the Degree of

DOCTOR OF PHILOSOPHY

The University of Texas Southwestern Medical Center at Dallas

Dallas, Texas

May, 2009

OXYGEN-MEDIATED REGULATION OF CHOLESTEROL SYNTHESIS

THROUGH ACCELERATED DEGRADATION OF

HMG COA REDUCTASE

Andrew Tuan Duc Nguyen, Ph.D.

The University of Texas Southwestern Medical Center at Dallas, 2009

Supervising Professor: Russell A. DeBose-Boyd, Ph.D.

Endoplasmic reticulum-associated degradation of the enzyme 3-hydroxy-3-methylglutaryl CoA reductase represents one mechanism by which cholesterol synthesis is controlled in mammalian cells. The key reaction in this degradation is binding of reductase to Insig proteins in the endoplasmic reticulum, which is stimulated by the methylated cholesterol precursors lanosterol and 24,25-dihydrolanosterol. Conversion of these sterols to cholesterol requires the removal of three methyl groups, which consumes

nine molecules of O_2. Here, we report that oxygen deprivation (hypoxia) slows the rate of demethylation of lanosterol and its reduced metabolite 24,25-dihydrolanosterol, causing both sterols to accumulate in cells. These methylated sterols serve as one signal to stimulate rapid Insig-mediated degradation of reductase.

In addition, hypoxia increases the expression of Insig-2 in a response mediated by hypoxia-inducible factor. Our analysis of the mouse *Insig-2* gene revealed the presence of a functional hypoxia response element in the first intron. Importantly, hepatic Insig-2a expression is upregulated in three independent mouse models of hypoxia. These studies establish that Insig-2 is a target gene of hypoxia-inducible factor. The hypoxia-dependent increase in Insig levels confers cells with enhanced sensitivity to sterol-induced degradation of reductase. In this way, hypoxia-inducible factor-mediated induction of Insig-2 provides a second signal for stimulating reductase degradation.

To address the specificity of methylated sterols in promoting reductase degradation, we reconstituted Insig-dependent, sterol-accelerated degradation of the membrane domain of mammalian reductase in *Drosophila* S2 cells. Studies in this system revealed that 24,25-dihydrolanosterol, and lanosterol, is active in accelerating degradation of reductase. These results were confirmed by examining ubiquitination of reductase *in vitro* using permeabilized mammalian cells.

Collectively, these studies show that under hypoxic conditions reductase undergoes accelerated Insig-dependent degradation as the combined result of two events: 1) accumulation of 24,25-dihydrolanosterol and 2) hypoxia-inducible factor-mediated upregulation of Insig-2. Degradation of reductase ultimately slows a rate-determining step in cholesterol synthesis. These results highlight the importance of 24,25-

dihydrolanosterol as a physiologic regulator of reductase degradation and define a novel oxygen-sensing mechanism in the mammalian cholesterol biosynthetic pathway.

ACKNOWLEDGEMENTS

I thank my mentor Russell DeBose-Boyd for teaching me everything that he has during the past four years. I am deeply grateful for his guidance, support, and perspective. I feel very fortunate to have had such a wonderful mentor.

I would also like to thank the members of my dissertation committee: Richard Bruick, Michael Brown, Zhijian Chen, and George DeMartino. I appreciate the helpful insights and advice that they provided about my dissertation research.

Next, I must acknowledge numerous members of the laboratory and department who have helped me in different ways. I thank our department chairs, Michael Brown and Joseph Goldstein, for their encouragement and advice. It has been a great honor to have studied in their department. I thank Kristi Garland and Tammy Dinh for excellent technical assistance. I thank Lisa Beatty, Marissa Infante, Ly Le, Shomanike Head, Angela Carroll, and Ijeoma Onwuneme for invaluable help with tissue culture. I also thank Jeff Cormier for help with real-time PCR analysis, Debra Morgan for help with metabolic labeling studies, Chris Li for help with isolation of primary rat hepatocytes, Y.K. Ho for help with antibody production, Linda Donnelly and Meryl Davis for help with luciferase assays, and Krista Matthews for help with *Drosophila* S2 cells.

Additionally, I thank the following people for reagents that were critical for these studies: the Core Medicinal Chemistry Laboratory for synthesizing the RS-21607 compound; Elhadji Dioum and Joseph Garcia for HIF cells lines and plasmids; and Peter Ratcliffe for HIF-1α-deficient cells.

I also thank our collaborators: Richard Bruick for hypoxia experiments in cultured cells; Jeffrey McDonald and Daniel Smith for analysis of lipids; James Brugarolas, Nicholas Wolff, and Blanka Kucejova for hypoxia and *VHL*$^{f/f}$ mouse experiments; and William Kim and Samuel Heathcote for DMOG mouse experiments.

I thank the Integrative Biology Graduate Program; I would like to especially acknowledge Yi Liu for his dedication to the students in this program. I thank all the faculty members who have taught in the core course and advanced courses, as well as those who facilitated journal club discussions. I also thank Melanie Cobb for her encouragement and advice. I thank Nancy McKinney, Deborah Evalds, and Priyarama Sen for help with administrative matters. I thank my wonderful friends for all of the good times that we have had together throughout graduate school. I thank the Graduate School of Biomedical Sciences and the Division of Cell and Molecular Biology Training Program (NIH T32GM008203) for financial support.

I would like to also acknowledge my previous research mentors: Tohru Fukai, Janice Chou, and David Pallas. Each has taught me important skills and concepts that I continue to apply to my current research. I thank Tohru Fukai and Janice Chou for their continued encouragement and support. I am especially indebted to Tohru Fukai for helping me discover my true passion for research.

Last, but certainly not least, I would like to thank my family, to whom I dedicate this dissertation. I am forever grateful to them for their endless love and support.

TABLE OF CONTENTS

PRIOR PUBLICATIONS

Nguyen, A.D., Kucejova, B., Heathcote, S.A., Kim W.Y., Brugarolas, J., and DeBose-Boyd, R.A. Transcriptional regulation of Insig-2 by Hypoxia-Inducible Factor. (in preparation)

Nguyen, A.D., Lee, S.H., and DeBose-Boyd, R.A. Insig-mediated, sterol-accelerated degradation of the membrane domain of hamster 3-hydroxy-3-methylglutary coenzyme A reductase in insect cells. (in preparation)

Nguyen, A.D., McDonald, J.G., Bruick, R.K., and DeBose-Boyd, R.A. (2007). Hypoxia stimulates degradation of 3-hydroxy-3-methylglutaryl-coenzyme A reductase through accumulation of lanosterol and Hypoxia-Inducible Factor-mediated induction of Insigs. J. Biol. Chem. *282*, 27436-27446.

Lee, P.C., Nguyen, A.D., and DeBose-Boyd, R.A. (2007). Mutations within the membrane domain of HMG CoA reductase confer resistance to sterol-accelerated degradation. J. Lipid Res. *48*, 318-327.

Kim, S.Y., Nguyen, A.D., Gao, J.L., Murphy, P.M., Mansfield, B.C., and Chou, J.Y. (2006). Bone marrow-derived cells require a functional glucose-6-phosphate transporter for normal myeloid functions. J. Biol. Chem. *281*, 28794-28801.

Nguyen, A.D., Pan, C.J., Weinstein, D.A., and Chou, J.Y. (2006). Increased scavenger receptor class B type I-mediated cellular cholesterol efflux and antioxidant capacity in the sera of glycogen storage disease type Ia patients. Mol. Genet. Metab. *89*, 233-238.

Nguyen, A.D., Pan, C.J., Shieh, J.J., and Chou, J.Y. (2005). Increased cellular cholesterol efflux in glycogen storage disease type Ia mice: potential mechanism that protects against premature atherosclerosis. FEBS Lett. *579*, 4713-4718.

Nguyen, A.D., Itoh, S., Jeney, V., Qin, Z., Yanagisawa, H., Fujimoto, M., Ushio-Fukai, M., and Fukai, T. (2004). Fibulin-5 is a novel binding protein for extracellular superoxide dismutase. Circ. Res. *95*, 1067-1074.

Hink, H.U., Santanam, N., Dikalov, S., McCann, L., Nguyen, A.D., Parthasarathy, S., Harrison, D.G., and Fukai, T. (2002). Peroxidase properties of the extracellular superoxide dismutase: role of uric acid in modulating in vivo activity. Arterioscler. Thromb. Vasc. Biol. *22*, 1402-1408.

LIST OF FIGURES

CHAPTER ONE

CHAPTER TWO

LIST OF TABLES

LIST OF APPENDICES

LIST OF DEFINITIONS

ChIP – chromatin immunoprecipitation

CHO – Chinese hamster ovary

CMV – cytomegalovirus

COX – cytochrome *c* oxidase

DMOG – dimethyloxalylglycine

dsRNA – double-stranded RNA

ER – endoplasmic reticulum

ERAD – ER-associated degradation

GAPDH – glyceraldehyde 3-phosphate dehydrogenase

GC-MS – gas chromatography-mass spectroscopy

GLUT – glucose transporter

HIF – hypoxia-inducible factor

HMG – 3-hydroxy-3-methylglutaryl

HPLC-MS – high performance liquid chromatography-mass spectrometry

HRE – hypoxia response element

25-HC – 25-hydroxycholesterol

IgG – immunoglobulin G

Insig – insulin-induced gene

LDL – low density lipoprotein

NPC1 – Niemann-Pick type C1

ODD – oxygen degradation domain

PAGE – polyacrylamide gel electrophoresis

PBS – phosphate-buffered saline

RCC – renal cell carcinoma

RNAi – RNA interference

SCAP – SREBP cleavage-activating protein

SDS – sodium dodecyl sulfate

siRNA – small interfering RNA

SREBP – sterol regulatory element-binding protein

tk – thymidine kinase

TLC – thin layer chromatography

VEGF – vascular endothelial growth factor

VHL – von Hippel-Lindau

CHAPTER ONE

OXYGEN-MEDIATED REGULATION OF CHOLESTEROL SYNTHESIS THROUGH ACCELERATED DEGRADATION OF HMG COA REDUCTASE

ABSTRACT

Endoplasmic reticulum-associated degradation of the enzyme 3-hydroxy-3-methylglutaryl CoA reductase represents one mechanism by which cholesterol synthesis is controlled in mammalian cells. The key reaction in this degradation is binding of reductase to Insig proteins in the endoplasmic reticulum, which is stimulated by the cholesterol precursors lanosterol and 24,25-dihydrolanosterol. Conversion of these methylated sterols to cholesterol requires removal of three methyl groups, which consumes nine molecules of O_2. Here, we report that oxygen deprivation (hypoxia) slows demethylation of lanosterol and its reduced metabolite 24,25-dihydrolanosterol, causing both sterols to accumulate in cells. In addition, hypoxia increases the expression of Insig-2 in a response mediated by hypoxia-inducible factor. Accumulation of 24,25-dihydrolanosterol together with upregulation of Insig-2 accelerates degradation of reductase, which slows a rate-determining step in cholesterol synthesis and ultimately decreases cholesterol production. These results define a novel oxygen-sensing mechanism mediated by the combined actions of methylated intermediates in cholesterol synthesis and the transcription factor hypoxia-inducible factor.

INTRODUCTION

The enzyme 3-hydroxy-3-methylglutaryl (HMG) CoA reductase catalyzes reduction of HMG CoA to mevalonate, a rate-determining step in synthesis of cholesterol and nonsterol isoprenoids that are indispensable for cell function (Goldstein and Brown, 1990). HMG CoA reductase is embedded in membranes of the endoplasmic reticulum (ER) through an N-terminal domain that contains eight membrane-spanning helices separated by short loops (Roitelman et al., 1992). The catalytic domain of reductase projects into the cytosol (Gil et al., 1985; Liscum et al., 1985). Sterol and nonsterol end-products of mevalonate metabolism exert stringent feedback control on reductase through multiple mechanisms (Brown and Goldstein, 1980). This complex feedback control system permits continuous production of essential nonsterol isoprenoids while avoiding overproduction of cholesterol and potentially toxic cholesterol precursors. One mechanism for feedback control involves rapid degradation of reductase, which is mediated by a pair of ER membrane proteins called insulin-induced gene (Insig)-1 and Insig-2 (Sever et al., 2003b). Accumulation of sterols in ER membranes triggers binding of the membrane domain of reductase to a subset of Insigs that carry a membrane-anchored ubiquitin ligase called gp78, which initiates ubiquitination of reductase (Song et al., 2005b). Ubiquitination marks reductase for proteasomal degradation, reducing the half-life of the protein from 12 h in sterol-depleted cells to less than 1 h under sterol-replete conditions.

Sterol regulatory element-binding proteins (SREBPs), a family of membrane-bound transcription factors, constitute another mechanism for feedback regulation of

reductase (Goldstein et al., 2006). In sterol-deprived cells, SREBPs are transported from the ER to the Golgi, whereupon they encounter proteases that release soluble fragments from membranes into the cytosol. Processed forms of SREBPs migrate to the nucleus and enhance transcription of genes encoding reductase and other enzymes known to be required for cholesterol synthesis (Horton et al., 2002a). Translocation of SREBPs from the ER to Golgi requires the sterol-responsive escort protein called SREBP cleavage-activating protein (SCAP) (DeBose-Boyd et al., 1999; Nohturfft et al., 2000; Rawson et al., 1999). SCAP, like reductase, contains a hydrophobic N-terminal domain that spans the membrane eight times and a C-terminal domain located in the cytosol that mediates association with SREBPs (Nohturfft et al., 1998; Sakai et al., 1997). Sterols trigger binding of Insigs to a region in the membrane domain of SCAP that comprises membrane-spanning helices 2-6 and resembles the Insig binding site in reductase (Hua et al., 1996; Yabe et al., 2002; Yang et al., 2002). Insig binding prevents incorporation of SCAP and its bound SREBPs into COPII-coated vesicles that are destined for fusion with the Golgi. In the absence of this transport, SREBPs remain tethered to membranes and are not cleaved; consequently, expression of target genes falls and cholesterol synthesis declines.

With regard to sterol specificity, recent studies have revealed a crucial difference in Insig-mediated regulation of SCAP and reductase (Goldstein et al., 2006). Cholesterol directly binds to the membrane domain of SCAP (Radhakrishnan et al., 2004), inducing a conformational change that triggers Insig binding, thereby blocking exit of SCAP/SREBP from the ER (Adams et al., 2004; Brown et al., 2002). SCAP recognizes the sterol nucleus and the 3β-hydroxyl group of cholesterol; the iso-octyl side chain is dispensable

for binding. Lanosterol and 24,25-dihydrolanosterol, the first sterol intermediates in cholesterol synthesis (Figure 1-1) neither bind SCAP nor block proteolytic activation of SREBPs (Song et al., 2005a). Instead, lanosterol and 24,25-dihydrolanosterol potently stimulate Insig-dependent ubiquitination and degradation of reductase. Methyl groups present in the 4α, 4β, and 14α positions are key determinants for the actions of lanosterol and 24,25-dihydrolanosterol in stimulating reductase degradation. These methyl groups are removed in the conversion of lanosterol and 24,25-dihydrolanosterol to cholesterol; the initial reaction is catalyzed by the cytochrome P450 enzyme lanosterol 14α-demethylase (Gaylor, 2002). Lanosterol demethylation has been implicated as a rate-limiting step in the post-squalene portion of the cholesterol synthetic pathway (Spence and Gaylor, 1977; Williams et al., 1977), thereby situating the reaction as a potential focal point in sterol regulation.

Synthesis of cholesterol is an oxygen-intensive process; 11 molecules of O_2 are consumed by four enzymes during production of one molecule of cholesterol from acetyl-CoA (Bloch, 1952; Summons et al., 2006) (Figure 1-1). A single molecule of O_2 is required for epoxidation of squalene, which is catalyzed by the enzyme squalene monooxygenase. Nine molecules of O_2 are utilized in removal of the 4α, 4β, and 14α methyl groups in lanosterol through successive actions of lanosterol 14α-demethylase and C4-methyl sterol oxidase. The final oxygen-requiring step in cholesterol synthesis is catalyzed by sterol 5-desaturase and consumes one molecule of O_2, resulting in reduction of lathosterol to 7-dehydrocholesterol.

In the fission yeast *S. pombe*, orthologs of mammalian SREBP and SCAP called Sre1 and Scp1, respectively, function in a mechanism that uses sterol synthesis as an

indicator of oxygen availability (Hughes et al., 2005) Oxygen deprivation (hypoxia) inhibits synthesis of the fungal sterol ergosterol, which triggers Scp1-dependent proteolytic activation of Sre1. In the nucleus, processed forms of Sre1 modulate transcription of genes encoding enzymes that catalyze oxygen-dependent steps in synthesis of ergosterol to maintain sterol homeostasis. Other Sre1 target genes include those that encode oxygen-requiring enzymes in heme, sphingolipid, and ubiquinone synthesis (Todd et al., 2006). Hypoxia has been reported to inhibit cholesterol synthesis in mammalian cells (Mukodani et al., 1990), but a role for SREBP and SCAP has not been demonstrated. However, an intriguing possibility exists that degradation of reductase is modulated by low oxygen in mammalian cells, considering that demethylation of lanosterol consumes the majority of molecular oxygen required for cholesterol synthesis.

In the current studies, we explored the consequences of hypoxia on regulation of reductase in cultured Chinese hamster ovary (CHO) cells. Our results show that hypoxia triggers accumulation of lanosterol and its metabolite 24,25-dihydrolanosterol, due to inhibition of lanosterol 14α-demethylase. The accumulation of methylated sterols serves as one signal for rapid degradation of reductase, which ultimately reduces flow through early steps of cholesterol synthesis when oxygen is limiting. The other signal is provided by hypoxic induction of Insig-2. Pharmacologic and genetic data presented in these studies indicate that the hypoxic induction of Insigs requires the oxygen-sensitive transcription factor hypoxia-inducible factor (HIF)-1α (Schofield and Ratcliffe, 2004; Semenza, 2004; Wang and Semenza, 1995). Moreover, our analysis of the mouse *Insig-2* gene identified a hypoxia responsive element (HRE) in the first intron that is necessary

for induction by HIF. Considered together, these results not only highlight the importance of lanosterol and/or 24,25-dihydrolanosterol as physiologic regulators of reductase degradation, but they also establish a new connection between cholesterol synthesis and oxygen sensing in mammalian cells.

EXPERIMENTAL METHODS

Materials

We obtained hydroxypropyl-β-cyclodextrin from Cyclodextrin Technologies Development; bovine serum albumin, the squalene monooxygenase inhibitor NB-598, insulin, dexamethasone, and 3,3′,5-triiodo-l-thyronine were from Sigma; [^{14}C]pyruvate, [^{14}C]acetate, and [^{3}H]cholesterol were from American Radiolabeled Chemicals; silica gel thin layer chromatography (TLC) plates were from Macherey-Nagel; cell culture media and reagents were from Mediatech; doxycycline was from Clontech. Dimethyloxalylglycine (DMOG) was obtained from Frontier Scientific. The lanosterol 14α-demethylase inhibitor RS-21607 (Swinney et al., 1994; Walker et al., 1993) was synthesized by the Core Medicinal Chemistry Laboratory, University of Texas Southwestern Medical Center. Other reagents, including lipoprotein-deficient serum (d > 1.215 g/ml), sodium compactin, and sodium mevalonate, were prepared or obtained from sources as described previously (DeBose-Boyd et al., 1999).

Cell Culture

CHO-7 cells, a subline of CHO-K1 cells selected for growth in lipoprotein-deficient serum (Metherall et al., 1989), were maintained in medium A (1:1 mixture of Ham's F-12 medium and Dulbecco's modified Eagle's medium containing 100 units/ml penicillin and 100 μg/ml streptomycin sulfate) supplemented with 5% (v/v) lipoprotein-deficient serum. SRD-15 and SRD-17 cells are mutant cell lines derived from CHO-7 cells. SRD-15 cells were maintained in medium A containing 5% lipoprotein-deficient serum and 2.5 μM 25-

hydroxycholesterol (Lee et al., 2005). SRD-17 cells were grown in medium A containing 5% lipoprotein-deficient serum and 10 μM SR-12813 (Lee et al., 2007). C4.5 cells are CHO-K1 cells that stably express the cell surface marker E-selectin under transcriptional control of HREs. Mutant Ka13 cells were derived from C4.5 cells and lack HIF-1α (Wood et al., 1998). C4.5 and Ka13 cells were cultured in medium A supplemented with 5% fetal calf serum. SV-589 human fibroblast cells and HepG2 human hepatoma cells were maintained in medium B (Dulbecco's modified Eagle's medium containing 100 units/ml penicillin and 100 μg/ml streptomycin sulfate) supplemented with 10% fetal calf serum. AML12 mouse hepatocytes (Wu et al., 1994) were maintained in medium A supplemented with 10% fetal calf serum, 5 μg/ml insulin, 5 μg/ml transferrin, 5 ng/ml selenium, and 40 ng/ml dexamethasone. Inducible HIF-1α and HIF-2α cells lines (provided by Drs. Elhadji M. Dioum and Joseph A. Garcia, UT Southwestern Medical Center) were maintained in medium B supplemented with 10% fetal calf serum. These cell lines were generated using the HEK293-based T-REX System (Invitrogen). In these cells lines, doxycycline treatment induces the expression of mutant forms of either human HIF-1α or human HIF-2α, containing the HA epitope at the C-terminus. In these mutant proteins, two key proline residues (402 and 564 of HIF-1α; 431 and 531 of HIF-2 α) were mutated to alanines; consequently the proteins are not subject to oxygen-dependent degradation (Schofield and Ratcliffe, 2004; Semenza, 2004).

All mammalian cell lines used in this study were grown in monolayer at 37 °C. CHO-7, SRD-15, SRD-17, C4.5, Ka13, and HepG2 cells were maintained in incubators filled with 8-9% CO_2; SV-589, AML12, and HEK293 cells were maintained in incubators filled with 5% CO_2. Hypoxia treatments were performed at 37 °C in a

humidified hypoxic chamber (Coy Laboratory Products) filled with 1% O_2 and 5% CO_2 and balanced with N_2. Control cells were incubated at 37 °C under normoxic conditions in 21% O_2 and 5% CO_2. RS-21607, NB-598, and DMOG were added to the culture medium in DMSO at a final concentration of 0.1% (v/v). 25-Hydroxycholesterol was added in ethanol at a final concentration of 0.1%.

Metabolic Labeling Studies

Incorporation of [^{14}C]pyruvate and [^{14}C]acetate into sterols and fatty acids was determined as described (Brown et al., 1978) with minor modifications. CHO-7 cells were set up for experiments on day 0 and treated as described in the figure legends. On day 1, cells were refed 2 ml of medium A containing 5% lipoprotein-deficient serum and 6.25 μCi of [^{14}C]pyruvate or 10 μCi of [^{14}C]acetate; cold pyruvate and acetate were added to achieve final concentrations of 2 and 0.5 mM, respectively. After incubation at 37 °C for the times indicated in the figure legends, cell monolayers were washed twice with 2 ml of cold buffer containing 5 mM Tris-HCl pH 7.4, 0.15 M NaCl, and 0.2% (w/v) bovine serum albumin and then twice with 2 ml of cold buffer containing 5 mM Tris-HCl pH 7.4, and 0.15 M NaCl. Cells were harvested and dissolved in 1 ml of 0.1 N NaOH at room temperature for at least 30 min. Cholesterol, lanosterol, and squalene dissolved in chloroform/methanol (2:1) were added to each sample as carrier sterols, and ~40 μCi of [^{3}H]cholesterol was added as an internal standard. Lipids were saponified in 15% KOH, 40% ethanol at 80 °C for 1 h. Lipids were extracted twice with 4 ml of petroleum ether, and the organic phase was evaporated under nitrogen gas with heat. Lipids were resuspended in heptane and separated by thin layer chromatography on plastic-backed

silica gel TLC plates developed in 100% chloroform. For fatty acids, 2 ml of H_2O was added to the remaining aqueous phase before acidifying with 2 ml of concentrated HCl. After adding 2 ml of ethanol, fatty acids were extracted twice with 4 ml of petroleum ether, and the amount of radioactivity in each was measured by scintillation counting. Values were corrected for recovery and background from parallel dishes incubated at 4 °C. An aliquot of each sample was taken prior to saponification for protein determination using the BCA protein assay reagent (Pierce). The mean values from triplicate dishes are presented as nmol of [^{14}C]pyruvate incorporation/mg of protein.

Analysis of Cellular Cholesterol Intermediates

Cells were set up for experiments on day 0 as described in the figure legends. Treatment conditions prior to harvest of the cells are also described in the figure legends. Following treatments, cells were harvested, washed twice with phosphate-buffered saline (PBS), and stored at -80 °C until analyzed. Lipids were extracted with chloroform/methanol (Bligh and Dyer, 1959), and relative amounts of sterols were determined by high performance liquid chromatography-mass spectrometry (HPLC-MS). Values were normalized for protein amount, and data are presented as fold changes relative to the amount of sterols at time = 0 h. These values are given in the figure legends.

Cell Fractionation and Immunoblot Analysis

Following incubations as described in the figure legends, cells from 3-5 dishes were pooled, washed with PBS, and subjected to cellular fractionation. Cells were homogenized by passing through a 22.5 gauge needle 30 times in 0.5 ml Buffer A1 (10

mM HEPES-KOH pH 7.6, 0.25 M sucrose, 10 mM KCl, 1.5 mM $MgCl_2$, 5 mM EDTA, and 5 mM EGTA) containing protease inhibitors (0.1 mM leupeptin, 5 μg/ml pepstatin A, 2 μg/ml aprotinin, 25 μg/ml N-acetyl-leucinal-leucinal-norleucinal, 0.5 mM phenylmethylsulfonylfluoride, 0.5 mM Pefabloc, and 0.25 mM dithiothreitol). The cell homogenates were subjected to centrifugation at 1000 × g for 7 min at 4 ºC. The pellets were resuspended in 0.3 ml of Buffer C (20 mM HEPES-KOH pH 7.6, 25% (v/v) glycerol, 0.42 M NaCl, 1.5 mM $MgCl_2$, 1 mM EDTA, and 1 mM EGTA) containing protease inhibitors, rotated at 4 ºC for 1 h, and then subjected to centrifugation at 10^5 × g for 30 min at 4 ºC in a Beckman TLA 100.2 rotor. The resulting supernatants, designated as the nuclear extract fractions, were precipitated with acetone and subsequently resuspended in 100 μl sodium dodecyl sulfate (SDS)-lysis buffer (10 mM Tris-HCl pH 6.8, 1% (w/v) SDS, 100 mM NaCl, 1 mM EDTA, and 1 mM EGTA). The membrane fractions were isolated by subjecting the post-nuclear supernatants to centrifugation at 2 × 10^4 × g for 15 min at 4 ºC. The membrane pellets were resuspended in 50 μl SDS-lysis buffer.

Protein concentrations of the nuclear extract and membrane fractions were determined using the BCA protein assay reagent (Pierce). Aliquots of the membrane fractions were mixed with an equal volume of a buffer containing 62.5 mM Tris-HCl pH 6.8, 15% (w/v) SDS, 8 M urea, 10% (v/v) glycerol, and 100 mM dithiothreitol. Subsequently, 5× sample buffer (0.25 M Tris-HCl pH 6.8, 10% (w/v) SDS, 50% (v/v) glycerol, 0.05% (w/v) bromophenol blue, and 12.5% β-mercaptoethanol) was added to the nuclear extract fractions and membrane fractions to achieve a final concentration of

1×. Following incubation at 37 ºC for 20 min, samples were separated by 8% SDS-polyacrylamide gel electrophoresis (PAGE) and transferred to Hybond C-Extra nitrocellulose filters (Amersham). Following incubations with primary antibodies described below and horseradish peroxidase-conjugated secondary antibodies (Jackson ImmunoResearch) as indicated in the figure legends, immunocomplexes were visualized with SuperSignal Pico Chemiluminescent Substrate (Pierce).

Primary antibodies used for immunoblotting were as follows: immunoglobulin G (IgG)-A9, a monoclonal antibody against the catalytic domain (amino acids 450-887) of hamster reductase (Liscum et al., 1983); IgG-R139, a rabbit polyclonal antibody against hamster SCAP (amino acids 54-277 and 540-707) (Sakai et al., 1997); IgG-7D4, a monoclonal antibody against the N-terminus of hamster SREBP-2 (Yang et al., 1995); a monoclonal antibody against human HIF-1α (amino acids 432-528; Upstate Biotechnology); and a rabbit polyclonal antibody against human calnexin (amino acids 575-593; Novus Biologicals).

RNA Isolation and Quantitative Real-Time PCR Analysis

The protocol for quantitative real-time PCR was identical to that described previously (Liang et al., 2002). Total RNA was isolated using the RNeasy kit (Qiagen) and treated with DNase to remove contaminating DNA (Qiagen). Then, 2 μg of the purified RNA was subjected to reverse transcription reactions using TaqMan Reverse Transcription Reagents (Applied Biosystems) with random hexamers. Triplicate samples of resulting cDNAs were subjected to quantitative real-time PCR using SYBR Green (Applied

Biosystems) in 384-well plates. The sequences of the primers used are listed in Appendix A. Relative amounts of mRNAs were calculated using the comparative C_T method.

Animal Studies

All studies involving animals were conducted in accordance with NIH guidelines for the care and use of live animals and followed protocols approved by the IACUC committees of the institutions at which the experiments were performed. Animal studies involving hypoxia treatment of mice and *VHL*$^{f/f}$ mice were done in collaboration with Dr. James Brugarolas (University of Texas Southwestern Medical Center). All animal procedures were performed in the Brugarolas laboratory. For the hypoxia treatments, 4-6-week old female C57Bl/6J mice were placed in a hypoxic chamber which was equilibrated to atmospheric conditions. Over a 40-min period, the oxygen level was decreased in a step-wise manner to 6% O_2 by displacement with N_2. Mice were subsequently maintained at 6% O_2 for 6 h. Control mice were kept in normal atmospheric conditions within the same room. Food and water were removed during the treatment period.

VHL$^{f/f}$ mice carry a conditional *VHL* null allele and have been described previously (Haase et al., 2001). *VHL*$^{f/f}$ mice and age-matched wild-type control mice were injected with adenovirus encoding for Cre recombinase driven by the albumin promoter to achieve liver-specific recombination. Mice were analyzed 4 days after injection.

Animal studies involving DMOG treatment of mice were done in collaboration with Dr. William Kim (University of North Carolina at Chapel Hill). All animal procedures were performed in the Kim laboratory. DMOG was dissolved in PBS and

administered by oral gavage to 8-week old female mice at a dose of 8 mg/day for 5 consecutive days. Control mice received the vehicle PBS by oral gavage.

At the end of these treatment periods, mice were sacrificed; the livers were removed and snap frozen in liquid N_2. Upon receiving the liver samples, analysis of gene expression was performed in our laboratory. RNA isolation and quantitative real-time PCR analysis was carried out as described above. Statistical analysis was performed using the unpaired *t*-test. Differences were considered statistically significant when $p < 0.05$. Data are presented as means ± SEM.

Generation of Insig-2 Reporter Plasmids

Sequences containing the 5'-flanking region and the first intron of the mouse *Insig-2* gene (see Figure 1-11) were amplified by PCR with the Phusion DNA polymerase kit (New England Biolabs). Mouse genomic DNA, isolated from the liver of a C57BL/6 mouse, was used as the template. The primers used for these amplification reactions are listed in Appendix B. The PCR products were gel purified, subjected to restriction digestion, and subcloned into the multiple cloning site of the promoterless pGL4 vector (Promega, pGL4.10) upstream of a synthetic luciferase coding sequence. Site-directed mutagenesis of the candidate HREs was performed using the QuikChange XL kit (Stratagene) using the pGL4-Insig-2 #2 plasmid as the template and the primers listed in Appendix B. The pGL4-tk-Renilla Luciferase vector, in which Renilla luciferase is constitutively expressed under the control of the thymidine kinase (tk) promoter, was obtained from Promega (pGL4.74). pCMV-HIF-1α encodes for a stable version of human HIF-1α with the HA epitope at the C-terminus (as described above). pCMV-HIF-1α was

generated by subcloning the mutant HIF-1α cDNA (provided by Drs. Elhadji M. Dioum and Joseph A. Garcia, UT Southwestern Medical Center) into the pcDNA3.1 vector (Invitrogen), in which expression is driven by the cytomegalovirus (CMV) promoter. The integrity of each plasmid was confirmed by DNA sequencing.

Isolation and Transfection of Primary Rat Hepatocytes

Hepatocytes were isolated by the collagenase method from nonfasted 250-g male Sprague-Dawley rats, as previously described with minor modifications (Horton et al., 1999). Rats were anesthetized with isoflorane, and the liver was perfused *in situ* via the portal vein with 200 ml of prewarmed Liver Perfusion Medium (Invitrogen) at a flow rate of 10 ml/min. The liver was subsequently perfused with 140 ml of prewarmed Liver Digest Medium (Invitrogen) containing collagenase. The liver was then removed from the animal, the hepatic capsule was stripped, and dissociated cells were dispersed by shaking. Cells were passed through a 100 μm cell strainer (BD Biosciences) into an equal volume of ice-cold medium B supplemented with 5% fetal calf serum. The cells were pelleted and washed twice in the same medium. Cells were plated in collagen I-coated 6-well plates (BD Biosciences) at a density of 1.5×10^6 cells per well in the same medium. After 4 h, cells were washed with PBS and switched to medium C (medium 199 containing 100 units/ml penicillin and 100 μg/ml streptomycin sulfate) supplemented with 100 nM dexamethasone, 100 nM 3,3′,5-triiodo-L-thyronine, and 1 nM insulin.

For reporter assay experiments, cells were washed twice with PBS and transiently transfected on day 1 with 4 μg DNA (1.8 μg of the indicated reporter plasmid and 0.4 μg of pGL4-tk-Renilla Luciferase, without or with 1.8 μg of pCMV-HIF-1α) per

well using 10 μl of Lipofectamine 2000 (Invitrogen) in 2 ml of medium D (RPMI 1640). After 6 h, cells were washed with PBS and refed medium C supplemented with 100 nM dexamethasone, 100 nM 3,3′,5-triiodo-L-thyronine, and 100 nM insulin for 36 h.

Alternatively, for experiments in which mRNA levels were examined, on day 1 cells were washed twice with PBS and refed medium C containing 100 nM dexamethasone and 100 nM 3,3′,5-triiodo-L-thyronine, without or with 1 nM insulin for 6 h.

Luciferase Assays

At the end of the treatment periods, cell monolayers were washed with PBS and lysed in 0.4 ml of Passive Lysis Buffer (Promega) by shaking for 30 min at room temperature. The lysates were transferred to a microcentrifuge tubes and briefly centrifuged to remove insoluble debris. Firefly and Renilla luciferase activities were measured in 96-well plates using 20 μl of the cleared lysates with the Dual-Luciferase Reporter Assay System (Promega). The amount of firefly luciferase activity of the transfected cells was normalized to Renilla luciferase activity. Data are expressed either as this normalized value (firefly luciferase activity/Renilla luciferase activity) or as the fold induction by HIF-1α.

Chromatin Immunoprecipitation Assays

SV-589 human fibroblast cells were set up on day 0 at a density of 5×10^5 cells per 100-mm dish in medium B supplemented with 10% fetal calf serum. On day 1, cells were refed the same medium without or with 1 mM DMOG. On day 2, chromatin

immunoprecipitation (ChIP) assays were performed using the ChIP Assay kit (Upstate) according to the manufacturer's instructions. Briefly, chromatin was crosslinked for 10 min at 37 ºC by adding formaldehyde to the culture medium of cells at a final concentration of 1% (w/v). Cells were then harvested, washed with PBS three times, and lysed on ice for 10 min in 200 µl of a detergent-containing buffer with protease inhibitors as described above. Cell lysates were subjected to sonication on ice for 10 sec intervals four times at 30% maximum power. After clearing insoluble debris by centrifugation, the lysates were diluted and incubated with 2.5 µg of the indicated antibody at 4 °C. The antibodies used were: preimmune rabbit IgG as a negative control; polyclonal anti-HIF-1α IgG (Bethyl Laboratories); and polyclonal anti-HIF-2α IgG (Stratagene). After 1 h, 60 µl of salmon sperm DNA/protein A agarose slurry was added, and the mixture was incubated overnight at 4 °C. After washing the protein A agarose/antibody/chromatin complexes, histone complexes were eluted from the antibody by incubating in a buffer containing 1% SDS and 0.1 M $NaHCO_3$. Histone/DNA crosslinks were reversed by adding NaCl at a final concentration of 0.2 M and incubating at 65 °C overnight. The following day, the samples were treated with 20 µg of proteinase K at 45 °C for 1 h, and DNA was recovered in 50 µl using the PCR purification kit (Qiagen). PCR analysis was performed using the Advantage-GC PCR kit (Clontech) with 5 µl of the purified DNA and the primers listed in Appendix C. Mouse genomic DNA was used as a positive control for the PCR reactions.

RESULTS

Accumulation of Endogenous Lanosterol and 24,25-Dihydrolanosterol Stimulates Degradation of HMG CoA Reductase

The experiment of Figure 1-2A compares effects of the reductase inhibitor compactin (Brown et al., 1978), the squalene monooxygenase inhibitor NB-598 (Horie et al., 1990), and the lanosterol 14α-demethylase inhibitor RS-21607 (Swinney et al., 1994) (see Figure 1-1) on lipid synthesis in CHO-7 cells. CHO-7 cells are a subline of CHO-K1 cells selected for growth in lipoprotein-deficient serum (Metherall et al., 1989). The cells were grown in the absence of exogenous cholesterol and then metabolically labeled with [^{14}C]acetate. Lipids extracted from the labeled cells were separated by thin layer chromatography (TLC), and incorporation of the radiolabel into squalene, lanosterol, and cholesterol was determined. In untreated cells, time-dependent incorporation of [^{14}C]acetate into cholesterol was observed; small amounts of radioactivity (<10% of that incorporated into cholesterol) were found in squalene and lanosterol. As expected, compactin prevented incorporation of [^{14}C]acetate into squalene, lanosterol, and cholesterol. NB-598 abolished incorporation of [^{14}C]acetate into lanosterol and cholesterol; the majority of the radiolabel was found in squalene. RS-21607 treatment led to complete inhibition of [^{14}C]cholesterol synthesis with concomitant accumulation of [^{14}C]lanosterol, a result attributable to inhibition of lanosterol 14α-demethylase activity.

The next experiment was designed to determine whether accumulation of lanosterol and 24,25-dihydrolanosterol that results from RS-21607 treatment stimulates degradation of reductase (Figure 1-2B). Activity through the cholesterol biosynthetic

pathway was stimulated by first subjecting cells to treatment with hydroxypropyl-β-cyclodextrin, a reagent that removes cholesterol from the plasma membrane (Kilsdonk et al., 1995). The cells were then incubated in medium containing lipoprotein-deficient serum to allow for maximal expression of SREBP target genes. Following this recovery period, cells were incubated in the absence or presence of RS-21607, after which they were harvested and separated into membrane and nuclear extract fractions. Immunoblotting revealed the complete disappearance of reductase from the membrane fraction of cells treated for 6 h with RS-21607 (*top panel*, *lane g*); this effect was blocked by compactin (*lanes k-m*). In contrast, RS-21607 treatment did not lead to suppression of SREBP processing, as indicated by equivalent amounts of nuclear SREBP-2 in treated and untreated cells (*bottom panel*; compare *lanes b-d* with *lanes e-g*).

Hypoxia Triggers Accumulation of Lanosterol and 24,25-Dihydrolanosterol and Insig-Mediated Degradation of HMG CoA Reductase

Noting that the demethylation of lanosterol and 24,25-dihydrolanosterol consumes the majority of molecular oxygen required for cholesterol synthesis (Figure 1-1), we next sought to determine whether the reaction becomes inhibited when oxygen is limiting, leading to accumulation of lanosterol and 24,25-dihydrolanosterol in cells. Cells were first subjected to cyclodextrin treatment and subsequently cultured in lipoprotein-deficient serum under hypoxic (1% O_2) or normoxic (21% O_2) conditions. Following incubation for various periods of time, cells were harvested; lipid extracts were prepared and analyzed by high performance liquid chromatography-mass spectrometry (HPLC-MS). The results show that the level of lanosterol was increased 5-fold (to 20 μg/mg

protein) following 6 h of hypoxia treatment (Figure 1-3A). The level of 24,25-dihydrolanosterol, the 24,25-reduced metabolite of lanosterol, was increased 25-fold by hypoxia; however, the absolute amount of 24,25-dihydrolanosterol is low compared with lanosterol. Indeed, based on peak areas, we estimate the amount of lanosterol exceeded that of 24,25-dihydrolanosterol by 26-fold under normoxic conditions. Importantly, accumulation of lanosterol and 24,25-dihydrolanosterol upon hypoxia treatment was blocked by compactin, demonstrating that it required *de novo* sterol synthesis. Intermediates distal to lanosterol (zymosterol, desmosterol, and 7-dehydrocholesterol) tended to decrease in hypoxic cells. The amount of cholesterol was quite high at zero time (42 μg/mg protein) and did not change during the 6 h of hypoxia. When the cells were incubated with [^{14}C]pyruvate, the incorporation of ^{14}C into cholesterol fell, and incorporation into [^{14}C]lanosterol rose during hypoxia (Figure 1-3B). There was no accumulation of [^{14}C]squalene, although its conversion to 2,3-epoxysqualene requires a single molecule of O_2 (Figure 1-1).

An experiment was next designed to determine whether reductase is degraded when lanosterol and 24,25-dihydrolanosterol accumulate in oxygen-deprived cells. Figure 1-4A shows that reductase protein declined markedly after 3 h of hypoxia (*top panel*, *lane i*) and even further at 6 h (*lane j*). This disappearance was prevented by compactin (*lanes k-m*), consistent with the hypothesis that lanosterol accumulation mediates the effect. The amount of processed SREBP-2 in the nuclear extract actually rose after 6 h of hypoxia (*second panel*, *lane j*), and it rose further when compactin was present without or with hypoxia (*lanes g and m*). As expected, oxygen depletion stabilized HIF-1α, one of the three HIF-α subunits that mediate transcriptional responses to hypoxia (Schofield and

Ratcliffe, 2004; Semenza, 2004) (*fourth panel*, *lanes h-m*). HIF-1α is known to be rapidly degraded during normoxia and stabilized upon hypoxia due to an inhibition of its ubiquitination (Huang et al., 1998; Salceda and Caro, 1997). Levels of a control membrane protein, calnexin, were unchanged regardless of culture under normoxic or hypoxic conditions (*fifth panel*). Like compactin, NB-598 prevented oxygen-regulated degradation of reductase (Figure 1-4B, *top panel*, compare *lanes b-d* with *lanes e-j*), but the enzyme continued to become degraded when the hypoxic cells were treated with RS-21607 (*lanes k-m*).

To address the Insig requirement for oxygen-regulated degradation of reductase, experiments were conducted in two lines of mutant CHO cells (Figure 1-4C). SRD-15 cells lack both Insig-1 and Insig-2; thus, neither reductase degradation nor inhibition of SREBP processing is stimulated when these cells are treated with sterols (Lee et al., 2005). SRD-17 cells harbor a point mutation in the membrane domain of reductase (G87R) that prevents its sterol-induced binding to Insigs, thereby abrogating sterol-accelerated degradation of the enzyme (Lee et al., 2007). The results show that, as expected, reductase was degraded in wild-type cells exposed to hypoxia for 6 h (*top panels*, *lanes e-g*). In contrast, reductase was refractory to hypoxia-induced degradation in mutant SRD-15 and SRD-17 cells (*top panels*, *lanes l-n*), although HIF-1α was stabilized in the mutant cells to a level comparable with that in wild-type cells (*bottom panels*, *lanes l-n*).

Degradation of HMG CoA Reductase in Oxygen-Depleted Cells Requires the Presence of HIF-1α

Ubiquitination and subsequent degradation of HIF-α subunits requires hydroxylation of specific proline residues, which enhances their binding to the von Hippel-Lindau (VHL) tumor suppressor protein (Maxwell et al., 1999). The VHL protein is the recognition component of a ubiquitin ligase complex that targets HIF-α for degradation. Prolyl hydroxylation of HIF-α is catalyzed by a class of dioxygenases that use 2-oxoglutarate as a co-substrate and exhibit an absolute requirement for molecular oxygen (Bruick and McKnight, 2001; Epstein et al., 2001; Schofield and Ratcliffe, 2004). When cells are deprived of oxygen, prolyl hydroxylation is suppressed, allowing HIF-α to escape degradation and accumulate to high levels. Stabilized HIF-α subunits associate with the constitutive HIF-β subunit, forming the heterodimeric transcription factor HIF. The HIF-α/β heterodimer binds to HREs present in more than 70 target genes that play a central role in both systemic and cellular responses to hypoxia (Schofield and Ratcliffe, 2004; Semenza, 2004; Wenger et al., 2005).

Rapid degradation of reductase correlated with stabilization of HIF-1α in oxygen-deprived cells (see Figures 1-4 and 1-5), which prompted us to next explore a possible role for HIF activation in reductase degradation. To this end, we employed DMOG, a cell-permeable analog of 2-oxoglutarate that inhibits 2-oxoglutarate-dependent dioxygenases (Jaakkola et al., 2001). In the experiment of Figure 1-5A, DMOG treatment of oxygenated cells stimulated degradation of reductase in a fashion that paralleled enhanced stability of HIF-1α (*top two panels*, compare *lanes a-d* with *lanes e-h* and *i-l*). The response to DMOG was remarkably similar to the hypoxic response shown in Figure 1-4. First, levels of nuclear SREBP-2 were not reduced by DMOG treatment (Figure 1-5A, *third panel*). Second, compactin and NB-598, but not RS-21607, blocked DMOG-

induced degradation of reductase (Figure 1-5B, *top panel*). Finally, DMOG failed to accelerate reductase degradation in mutant SRD-15 and SRD-17 cells (Figure 1-5C, *top panel*, *lanes h-n* and *v-bb*), demonstrating a requirement for the action of Insigs.

Stimulated by the results of Figure 1-5, we next conducted experiments in Ka13 cells, a line of mutant CHO cells that lack HIF-1α (Wood et al., 1998). Hypoxia and DMOG treatment (Figure 1-6, A and B, respectively) for 6 h triggered degradation of reductase in parental C4.5 cells (*top panels*, *lanes a-g*) but not in mutant Ka13 cells (*top panels*, *lanes h-n*). The anti-HIF-1α immunoblot revealed the presence of the protein in parental cells and its absence in mutant cells regardless of hypoxia or DMOG treatment (Figure 1-6, A and B, *middle panels*). Despite their HIF-1α deficiency, the cholesterol synthetic pathway appears intact in Ka13 cells, as was indicated by the accumulation of lanosterol and 24,25-dihydrolanosterol when the cells were depleted of oxygen (Figure 1-6C).

Oxygen-Sensitive Degradation of HMG CoA Reductase Mediated by HIF-Dependent Induction of Insigs

A clue to the identities of HIF target genes required for oxygen-regulated degradation of reductase is provided by studies focused on the transcriptional profile of oxygen-depleted cells. In several DNA microarray analyses, transcripts for Insig-1 and/or Insig-2 have been identified among those induced by hypoxia or DMOG treatment (Elvidge et al., 2006; Kim et al., 2003; Mense et al., 2006; Sung et al., 2007). The quantitative real-time PCR experiment of Figure 1-7A shows a 2-3-fold induction of Insig-1 and Insig-2 mRNAs in C4.5 cells following 12 h of hypoxia or DMOG treatment. A similar level of

induction was observed for vascular endothelial growth factor (VEGF) mRNA, a well established HIF target gene (Semenza, 2004; Wenger et al., 2005). mRNA levels of HMG CoA synthase, reductase, and SCAP were not changed by either treatment. In contrast, as shown in Figure 1-7B, hypoxia- and DMOG-induced expression of Insig-1 and Insig-2 mRNA was absent in Ka13 cells, indicating that the response requires the presence of HIF-1α. We could not determine protein levels for Insig-1 and Insig-2 in these experiments, due to the lack of an antibody capable of detecting the endogenous proteins in hypoxic CHO cells. Moreover, detection of Insig-1 in these experiments is further complicated, because the protein is rapidly degraded in cholesterol-depleted cells; in cholesterol-replete cells, Insig-1 binds SCAP and becomes stabilized (Gong et al., 2006). Considered together, the results of Figure 1-7 provide a plausible mechanism by which HIF-1α mediates oxygen-dependent regulation of reductase degradation.

Insig-2 Expression Is Increased by Hypoxia and DMOG Treatments in Various Cultured Cell Lines

We next examined the expression of Insig-1 and Insig-2 in a panel of cells lines following treatment with DMOG. As shown in Figure 1-8, DMOG treatment led to an increase in Insig-2 mRNA levels in multiple cell lines, including CHO-7 hamster ovary cells, SV-589 human fibroblast cells, HepG2 human hepatoma cells, AML12 mouse hepatocytes, and primary rat hepatocytes. On the other hand, induction of Insig-1 expression by DMOG treatment was only observed in CHO-7 cells and primary rat hepatocytes. As controls, we observed DMOG-dependent upregulation of several established HIF target genes including VEGF, glyceraldehyde 3-phosphate

dehydrogenase (GAPDH), and glucose transporter (GLUT)1 (Semenza, 2004; Wenger et al., 2005).

The DMOG-dependent regulation of Insig-2 expression in multiple cell lines supports the idea that Insig-2 is a HIF target gene. However, these results do not necessarily indicate a direct effect of HIF on Insig-2 expression. To address this question, we used inducible HEK293 stable cell lines in which stable forms of HIF-1α or HIF-2α are expressed upon treatment with doxycycline. In these cell lines, doxycycline-mediated induction of HIF-α or HIF-2α led to upregulation of Insig-2 expression (Figure 1-9); Insig-1 levels were unaffected by the doxycycline treatment. Taken together, these experiments suggest that expression of Insig-2 is regulated by hypoxia in a HIF-dependent manner in cultured cells.

Hepatic Insig-2a Expression is Upregulated in Mouse Models of Hypoxia

We next sought to determine if HIF regulates Insig-2 expression in the liver, which is the primary site of cholesterol metabolism *in vivo*. Previous studies have revealed that two different Insig-2 isoforms are expressed in the liver: Insig-2a and Insig-2b (Yabe et al., 2002; Yabe et al., 2003). These isoforms are transcribed from a single *Insig-2* gene, and they encode for identical proteins. The Insig-2a and Insig-2b mRNA sequences differ only in their non-coding first exons; Insig-2a contains exon 1a, whereas Insig-2b contains exon 1b. This difference leads to differential regulation of Insig-2a and Insig-2b. Insig-2a is expressed specifically in the liver, and its expression is repressed by insulin both in primary rat hepatocytes and *in vivo*. On the other hand, Insig-2b is ubiquitously expressed and is not known to be regulated.

For these studies, we employed oxygen deprivation, pharmacological, and genetic mouse models of hypoxia. In the oxygen deprivation model, we exposed C57Bl/6J mice to hypoxia (6% O_2) for 6 h. Control mice were maintained at normoxia (21% O_2) in the same room. Food was withdrawn from both groups during the treatment period to control for any effect of insulin of Insig-2a expression. Following the treatments, RNA was isolated from the liver and real-time quantitative PCR was performed. In the mice exposed to hypoxia, we observed a significant increase in the hepatic expression of the HIF target genes GLUT1 and aldolase A (Figure 1-10A). While expression of Insig-1 and Insig-2b were not increased, Insig-2a levels were upregulated by 28-fold in the livers of hypoxia-treated mice.

In a pharmacological model of hypoxia, mice were administered DMOG by oral gavage at a dose of 8 mg/day. After 5 consecutive days of treatment, hepatic gene expression was analyzed by real-time PCR. As expected, we observed an increase in the hepatic expression of the HIF target gene VEGF in the DMOG-treated mice (Figure 1-10B). Although GLUT1 levels tended be higher in these mice, the difference was not significant when compared to control mice which received the vehicle PBS. DMOG treatment resulted in an 8-fold increase in hepatic Insig-2a expression. Similar to the changes in the hypoxia-treated mice, we observed a slight decrease in Insig-1 and Insig-2b expression in the livers of DMOG-treated mice.

As a genetic model, we examined Insig-2 levels in $VHL^{f/f}$ mice, which harbor a conditional *VHL* null allele (Haase et al., 2001). The VHL protein is the recognition component of a ubiquitin ligase complex that targets HIF-α for rapid degradation under normoxic conditions (Maxwell et al., 1999). Recombination of the *VHL* allele blocks

degradation of HIF-α and results in constitutive HIF activation. *VHL*$^{f/f}$ mice and control wild-type mice were injected with adenovirus encoding for Cre recombinase driven by the albumin promoter in order to achieve liver-specific recombination. The mice were analyzed 4 days after injection. Expression of the HIF target genes VEGF and GLUT1 were increased in the *VHL*$^{f/f}$ mice, indicating successful recombination in the liver (Figure 1-10C). Hepatic Insig-2a mRNA levels were upregulated 12-fold in the *VHL*$^{f/f}$ mice, compared to levels in wild-type mice. Insig-1 and Insig-2b expression levels were not different between the *VHL*$^{f/f}$ and wild-type mice. Taken together, these results demonstrate that Insig-2a expression is regulated by HIF in the mouse liver.

Identification of a Functional HRE in the Mouse Insig-2 Gene

Based on sequence alignment of HREs found in established HIF target genes, the following consensus HRE was recently reported: 5'-R<u>CGTG</u>X$_{(1-8)}$<u>CAC</u>AG-3' (Fukuda et al., 2007). Importantly, the underlined nucleotides, including the HIF binding site (CGTG), are highly conserved in these HIF target genes. Therefore, we scanned the *Insig-2* gene, including 5 kb upstream of the transcriptional start site, for sequences conforming to 5'-<u>CGTG</u>X$_{(1-8)}$<u>CAC</u>-3'. This sequence analysis revealed that the mouse *Insig-2* gene contains 3 such sequences, as shown in Figure 1-11.

To determine if Insig-2 is a *bona fide* HIF target gene, we generated a series of reporter plasmids in which different regions of the mouse *Insig-2* 5'-flanking region and first intron were cloned upstream of a luciferase coding sequence in the promoterless pGL4 vector. In our reporter assay experiments, we transiently transfected cells with these various reporter plasmids alone or with pCMV-HIF-1α, a plasmid encoding for a

stable version of human HIF-1α. In this mutant form of HIF-1α, prolines 402 and 564 were mutated to alanines, and therefore the protein is not subject to oxygen-dependent hydroxylation, ubiquitination, and degradation (Schofield and Ratcliffe, 2004; Semenza, 2004). We chose to carry out these studies in primary rat hepatocytes for two reasons. First, primary rat hepatocytes are the cultured cells that most closely resemble the liver. Second, primary rat hepatocytes express both of the known Insig-2 isoforms, Insig-2a and Insig-2b (Yabe et al., 2003). It is worth noting that Insig-2a, but not Insig-2b, mRNA levels were upregulated in DMOG-treated primary rat hepatocytes (Figure 1-8).

As shown in Figure 1-12, co-expression of HIF-1α in primary rat hepatocytes did not affect the luciferase activity of cells transfected with the control reporter plasmid (pGL4-empty) or pGL-Insig-2 #1, which contains the 3.64 kb region directly upstream of exon 1a. However, HIF-1α expression led to a ~6-9-fold induction of luciferase activity in hepatocytes transfected with plasmids pGL4-Insig-2 #2-7, which span the intronic region between exon 1a and exon 1b. Although HIF-dependent induction of luciferase activity was also observed in cells transfected with pGL4-Insig-2 #8, the extent of induction was much less. These results indicate the presence of a functional HRE that localizes to a region that is present in pGL4-Insig-2 #7 but absent in pGL4-Insig-2 #8. Within this 234-nucleotide region, there are two sequences that conform to the consensus HRE. We designated the more distal sequence as candidate HRE-1 and the more proximal sequence as candidate HRE-2; these sequences are 5'-CGTGCGTGCGCGCAC-3' and 5'-CGTGGAGCCTGTCAC-3', respectively, with the core components of the consensus HRE underlined. We mutated the candidate HRE-1 and candidate HRE-2 in the context of the pGL4-Insig-2 #2 reporter plasmid to the

following sequences: 5'-TACTTACTCGCGGTA-3' and 5'-TACTGAGCCTGTGTA-3', respectively. As expected, a HIF-mediated induction of luciferase activity was observed with the pGL4-Insig-2 #2 wild-type plasmid (Figure 13A). Similar results were observed with a plasmid in which the candidate HRE-2 was mutated. In contrast, mutation of the candidate HRE-1 completely abolished this effect, demonstrating that candidate HRE-1 is responsible for HIF-mediated induction of the reporter plasmid. Sequence alignment of this region of the *Insig-2* gene from various species reveals that the HRE is highly conserved across species (Figure 1-13B).

We next performed chromatin immunoprecipitation (ChIP) assays to determine if HIF physically interacts with the *Insig-2* HRE. Because commercially available HIF antibodies cannot readily detect HIF-1α and HIF-2α in primary rat hepatocytes, we used SV-589 human fibroblast cells for these studies. When either HIF-1α or HIF-2α was immunoprecipitated, the *Insig-2* HRE was among the HIF-associated DNA fragments (Figure 1-14). Importantly, the 5'-flanking region of *Insig-2* was not immunoprecipitated, indicating that the HIF/*Insig-2* HRE interaction is specific. As a positive control, we observed that DNA fragments corresponding to the HRE of an established HIF target gene, *VEGF*, were also associated with HIF-1α. These results show that endogenous HIF-α subunits interact with the human *Insig-2* gene. Collectively, these data establish that Insig-2 is a HIF target gene.

Insigs play central roles in two feedback regulatory mechanisms, namely sterol-accelerated degradation of reductase and proteolytic processing of SREBPs (Goldstein et al., 2006). Previous studies in cultured cells as well as in animals have shown that increased Insig expression results in greater sensitivity to both of these feedback

mechanisms. Therefore, we expect that HIF-dependent upregulation of Insig-2 should cause cells to be more responsive to sterols. In the experiment of Figure 1-15, we treated CHO cells for 24 h without or with DMOG to activate HIF. As expected, the DMOG-treated were more sensitive to the oxysterol 25-hydroxycholesterol. This is reflected in the ability of these cells to stimulate degradation of reductase and block SREBP processing at lower concentrations of 25-hydroxycholesterol than the control cells that were not treated with DMOG. These results suggest that HIF-mediated induction of Insig can modulate the sensitivity of cells to key feedback mechanisms that regulate cholesterol production.

Our results show that hypoxia triggers accumulation of lanosterol and its metabolite 24,25-dihydrolanosterol, due to inhibition of lanosterol 14α-demethylase (Figure 1-16). The accumulation of methylated sterols serves as one signal for rapid degradation of reductase, which ultimately reduces flow through early steps of cholesterol synthesis when oxygen is limiting. The other signal is provided by HIF-mediated induction of Insig-2, which confers cells with enhanced sensitivity to sterol-induced degradation of reductase. Considered together, these results not only highlight the importance of lanosterol and 24,25-dihydrolanosterol as a physiologic regulator of reductase degradation, but they also establish a new connection between cholesterol synthesis and oxygen sensing in mammalian cells.

DISCUSSION

The current study describes a novel mechanism for oxygen-sensitive feedback regulation of HMG CoA reductase, a rate-determining enzyme for synthesis of cholesterol in mammalian cells. In light of previous studies showing that the methylated cholesterol synthesis intermediates lanosterol and 24,25-dihydrolanosterol potently stimulate degradation of reductase (Song et al., 2005a), we searched for physiologic conditions that trigger an accumulation of these sterols in cells. During this search, we noticed that synthesis of one cholesterol molecule from acetyl-CoA requires 11 molecules of O_2, nine of which are utilized during the demethylation of lanosterol and its reduced metabolite 24,25-dihydrolanosterol by the successive actions of lanosterol 14α-demethylase and C4-methyl sterol oxidase (Figure 1-1). Results of the current study show that when cells are deprived of oxygen, demethylation of lanosterol and 24,25-dihydrolanosterol becomes rate-limiting, and both sterols accumulate (Figure 1-3). Accumulation of lanosterol and 24,25-dihydrolanosterol is accompanied by the disappearance of reductase from membranes of oxygen-deprived cells (Figure 1-4, A and B). This disappearance was blocked by the reductase inhibitor compactin and the squalene monooxygenase inhibitor NB-598 but not by the lanosterol 14α-demethylase inhibitor RS-21607 (Figure 1-4C), which allows for production of lanosterol (Figure 1-2A) and presumably 24,25-dihydrolanosterol. These results indicate that the disappearance of reductase upon exposure to hypoxia is the result of accelerated degradation of the enzyme in response to accumulation of lanosterol and 24,25-dihydrolanosterol. The Insig requirement for oxygen-regulated degradation of reductase

is revealed by results of Figure 1-4D. Reductase was not subject to hypoxia-induced degradation in cells that either lack Insigs (SRD-15 cells) or express a mutant form of reductase that cannot bind Insigs in the presence of sterols (SRD-17 cells).

Although hypoxia (and subsequent accumulation of lanosterol and 24,25-dihydrolanosterol) accelerated reductase degradation, these it failed to block processing of SREBPs within the 6 h treatment period (Figure 1-4, A and B). This finding is consistent with our previous observation that exogenous 4,4-dimethylated sterols stimulate reductase degradation but do not block SREBP processing (Song et al., 2005a). The lack of SREBP inhibition can be rationalized through knowledge of the fact that genes encoding all known cholesterol synthetic enzymes, including those that convert lanosterol and 24,25-dihydrolanosterol to cholesterol, are targets of SREBPs. Under conditions in which lanosterol accumulates, a reduction in SREBP processing would slow conversion of lanosterol to cholesterol. On the other hand, a selective decrease in reductase slows lanosterol production while maintaining high levels of the post-lanosterol enzymes.

A recent study has suggested that 24,25-dihydrolanosterol, and not lanosterol, is the active methylated sterol that stimulates degradation of reductase (Lange et al., 2008). In our studies, we observed increased levels of both lanosterol and 24,25-dihydrolanosterol (Figures 1-3A and 1-6C) in hypoxia-treated cells. Furthermore, in pharmacological studies with the lanosterol 14α-demethylase inhibitor RS-21607, we are unable to separate the effects of lanosterol and 24,25-dihydrolanosterol on reductase degradation (Figure 1-2B). Therefore, to address this issue of sterol specificity in the context of reductase, we reconstituted Insig-dependent, sterol-induced degradation of

reductase in *Drosophila* S2 cells (see Chapter 2). Studies in this system found that 24,25-dihydrolanosterol, but not lanosterol, is active in stimulating reductase degradation (Figure 2-3). Consistent with these results, 24,25-dihydrolanosterol potently stimulated ubiquitination of reductase *in vitro* (Figure 2-4). In contrast, lanosterol was unable to promote ubiquitination of reductase. We believe that earlier studies implicating a role for lanosterol in the ubiquitination and degradation of reductase were confounded by the presence of significant amounts of contaminating 24,25-dihydrolanosterol in the batches of lanosterol that were used (data not shown).

A surprising finding of the current study is the hitherto unappreciated role of HIF-1α in oxygen-regulated degradation of reductase. Remarkably, treatment of cells with the 2-oxoglutarate-dependent dioxygenase inhibitor DMOG not only stabilized HIF-1α as previously reported, but also led to Insig-dependent degradation of reductase in oxygenated cells (Figure 1-5). Although DMOG treatment did not result in the accumulation of lanosterol and 24,25-dihydrolanosterol (data not shown), the effect of the compound on reductase degradation was blocked by compactin and NB-598. Given that DMOG nonselectively inhibits 2-oxoglutarate-dependent dioxygenases, the results of Figure 1-6, A and B, are important in that they provide a direct link between HIF-1α and reductase degradation. The results show that reductase was refractory to hypoxia- and DMOG-induced degradation in HIF-1α-deficient Ka13 cells. Importantly, lanosterol and 24,25-dihydrolanosterol continued to accumulate in hypoxic Ka13 cells (Figure 1-6C), indicating the mutant cells are not defective in sterol synthesis. Moreover, Ka13 cells responded to exogenous sterol treatment by stimulating rapid degradation of reductase

(data not shown). Thus, HIF-1α-dependent gene transcription appears to be a second requirement for rapid degradation of reductase in oxygen-deprived cells.

Figure 1-7 provides evidence that the HIF-1α target genes required for oxygen-dependent regulation of reductase encode for Insigs. Expression of mRNAs for Insig-1 and Insig-2 is enhanced by hypoxia and DMOG treatment through a mechanism that requires the presence of HIF-1α. DMOG-dependent induction of both Insig-1 and Insig-2 expression was also observed in CHO-7 cells and primary rat hepatocytes (Figure 1-8). However, in other cell lines including SV-589 human fibroblast cells, HepG2 human hepatoma cells, and AML12 mouse hepatocytes, only Insig-2 mRNA levels were increased following DMOG treatment. Additional evidence for HIF-mediated regulation of Insig-2 expression comes from HIF-1α- and HIF-2α-inducible cell lines. In both of these cell lines, Insig-2 mRNA levels increased following induction of HIF-1α or HIF-2α by treatment with doxycycline (Figure 1-9). Together, these studies implicate a role for HIF in the regulation of Insig-2 expression in cultured cells.

To determine if Insig-2 is regulated by HIF *in vivo*, we used several different mouse models of hypoxia. In an oxygen deprivation model, we exposed mice to hypoxia (6% O_2) for 6 h. In a pharmacological model, we analyzed mice after treatment with DMOG for five days. Finally, in a genetic model, we analyzed $VHL^{f/f}$ mice four days after inducing liver-specific recombination. Upregulation of hepatic Insig-2a expression was observed in all three of these mouse models (Figure 1-10). The degree of induction of Insig-2a was comparable to that of established HIF target genes including VEGF, GLUT1, and aldolase A (Semenza, 2004; Wenger et al., 2005). These results demonstrate

that Insig-2 is subject to regulation by HIF, both in cultured cells as well as in the livers of animals.

Analysis of the mouse *Insig-2* gene revealed the presence of three sequences conforming to the consensus HRE in the 5'-flanking region and in the first intron (Figure 1-11). We tested these candidate HREs in reporter assays using primary rat hepatocytes. These studies led to the identification of a functional HRE within the intronic region between exon 1a and exon 1b (Figure 1-12). Importantly, mutation of this HRE abolished HIF-dependent induction of reporter luciferase activity (Figure 1-13A). As shown in Figure 1-13B, the Insig-2 HRE is highly conserved across species. Consistent with this, hypoxia and DMOG treatments led to increased Insig-2 mRNA levels in multiple cell lines, including those of human, rat, hamster, and mouse origins (Figures 1-7, 1-8, and 1-9). Finally, employing a ChIP assay, we detected physical interactions between the human *Insig-2* HRE and both HIF-1α and HIF-2α (Figure 1-14). Taken together, these results establish that *Insig-2* is a bona fide target gene of the oxygen-sensitive transcription factor HIF.

Previous studies have shown that Insig-2a and Insig-2b use alternate promoters to produce the respective mRNAs from a single *Insig-2* gene (Yabe et al., 2003). The mouse *Insig-2* HRE identified in these studies is located 4,460 nucleotides downstream of exon 1a and 285 nucleotides upstream of exon 1b (see Figure 1-11). Despite its closer proximity to the Insig-2b promoter, HIF regulates Insig-2a and not Insig-2b in both primary rat hepatocytes and mouse livers (Figures 1-8 and 1-10). This discrepancy may be explained by the fact that transcription factors can modulate gene transcription from distant sites. For example, the classic HIF target gene *erythropoietin* contains a functional

HRE located in the 3' untranslated region (Firth et al., 1994; Wang and Semenza, 1993). Moreover, transcriptional regulation results from the combinatorial effects of multiple transcription factors and cofactors. For example, HIF functions with ATF-1 and CREB-1 to activate transcription of lactate dehydrogenase A (Ebert and Bunn, 1998; Firth et al., 1995), and with AP-1 to regulate VEGF (Damert et al., 1997). It has been suggested that these combined effects of neighboring transcription factors can lead to tissue-restricted activity of an HRE (Wenger et al., 2005). This may further explain why Insig-2a is specifically upregulated by HIF in cell types that express both Insig-2a and Insig-2b (Figures 1-8 and 1-10). In the absence of Insig-2a expression, it appears that HIF is able to regulate Insig-2b. Cell lines derived from extra-hepatic tissues, such as CHO, SV-589, and HEK293 cells, are not known to express Insig-2a. Yet, total levels of Insig-2 mRNA are increased in these cell lines following HIF activation (Figures 1-7, 1-8, and 1-9). These results suggest that there is a factor present in hepatocytes that causes HIF to specifically drive Insig-2a expression; in the absence of this factor, HIF is able to activate transcription of Insig-2b.

HIF-1α-mediated induction of Insigs helps to explain why reductase became degraded upon DMOG treatment without an accumulation of lanosterol (Figure 1-5). This is consistent with unpublished studies in which we observed that increased expression of Insigs through transfection enhances sensitivity of reductase degradation to sterols. Moreover, extended treatment of cells with DMOG rendered reductase more sensitive to the regulatory oxysterol 25-hydroxycholesterol (Figure 1-15). Collectively, the results of the current study indicate that oxygen-regulated degradation of reductase in CHO cells is the combined result of two actions: 1) inhibition of lanosterol 14α-

demethylase and subsequent accumulation of lanosterol and 24,25-dihydrolanosterol and 2) HIF-1α-dependent induction of Insig-2 (Figure 1-16).

Our studies in mouse models of hypoxia reveal that the liver-specific isoform of Insig-2, namely Insig-2a, is regulated by hypoxia *in vivo* (Figure 1-10). With this induction of Insig-2a, we would anticipate a resulting decrease in the expression of SREBP target genes. Indeed, in these mouse models of hypoxia, we observed a consistent trend towards decreased expression of many SREBP target genes. Reductase, low density lipoprotein (LDL) receptor, acetyl CoA carboxylase, and fatty acid synthase are among the genes that were significantly downregulated (data not shown). A likely reason for the small number of SREBP target genes that were significantly affected is that the small cohorts sizes (n=3 or 6 per group) were not sufficient to account for the variability between mice. Recently, DNA microarray analysis was used to compare transcriptional profiles in livers of mice overexpressing nondegradable forms of HIF-1α or HIF-2α and of mice harboring a liver-specific deletion of *VHL* (Kim et al., 2006). Consistent with results of the current study, expression of Insig-2 mRNA was found to be enhanced in livers of all three groups of mice. Further analysis revealed a significant down-regulation of several SREBP target genes, including those encoding reductase, lanosterol synthase, lanosterol 14α-demethylase, and C4-methyl sterol oxidase (unpublished observation). A similar reduction in SREBP target genes was also observed in livers of mice exposed to hypoxia (Dolt et al., 2007); however, an induction of Insig-2 was not observed in that study.

Significant changes in SREBP processing or in the levels of SREBP target genes were not observed during the 6 h hypoxia treatment of CHO-7 cells. However, prolonged

treatment of cells with DMOG in the presence of compactin rendered SREBP processing more sensitive to 25-hydroxycholesterol (Figure 1-15). This discrepancy may be explained by differences in relative levels of SREBP isoforms that are known to exist among different cell types. CHO cells used in this study primarily express the SREBP-1a and SREBP-2 isoforms, whereas SREBP-1c and SREBP-2 predominate in mouse liver (Shimomura et al., 1997). Moreover, sterol regulation in the liver is more complicated, because Insigs are reciprocally regulated (Goldstein et al., 2006; Yabe et al., 2003). Insig-1 expression requires nuclear SREBP, and transcription of SREBP-1c is stimulated by insulin. When animals are fasted, insulin levels drop and hepatic SREBP-1c is not transcribed. As a result, nuclear SREBP-1c declines, thus lowering production of Insig-1 mRNA and protein. In contrast, Insig-2 levels are high, due to the liver-specific Insig-2a transcript that is negatively regulated by insulin. Insulin levels are restored upon refeeding, leading to 1) rapid reduction in Insig 2 mRNA and protein, 2) increased production of SREBP-1c mRNA and restoration of nuclear SREBP-1c, and 3) increased production of Insig-1 mRNA and protein.

In conclusion, we have described a link between cholesterol synthesis and oxygen sensing in animal cells. The link is provided by hypoxia-induced accumulation of the cholesterol biosynthetic intermediates lanosterol and 24,25-dihydrolanosterol and HIF-mediated induction of Insig-2. Convergence of these signals leads to rapid degradation of HMG CoA reductase, thereby limiting synthesis of cholesterol. Considering that cholesterol (an important component of cell membranes) and nonsterol isoprenoids (including the prenyl groups that become attached to many signaling proteins) are essential for cell growth and viability, we envision accelerated degradation

of reductase as part of a protective mechanism that guards against wasting of oxygen and inappropriate cell growth in the face of hypoxia. Further insight into oxygen-regulated degradation of reductase will be provided by future studies focused on determining the consequences of hypoxia on cholesterol metabolism in the liver (the major site of cholesterol synthesis *in vivo*) as well as other tissues of whole animals.

FIGURES

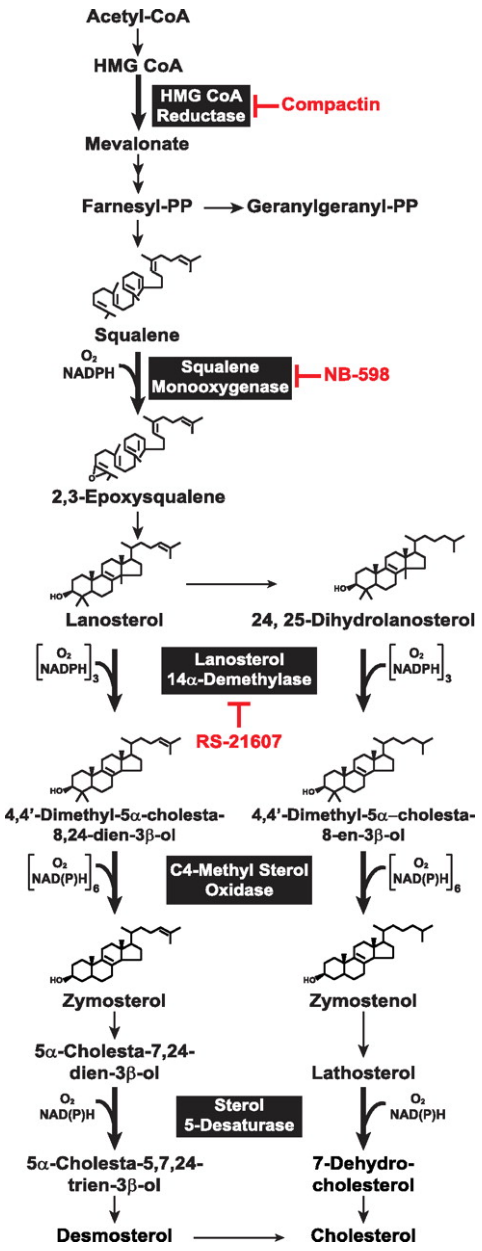

Figure 1-1. Schematic representation of the cholesterol synthetic pathway in mammalian cells. Reactions that require O_2 are indicated, and specific inhibitors of various enzymes in the pathway are highlighted in red.

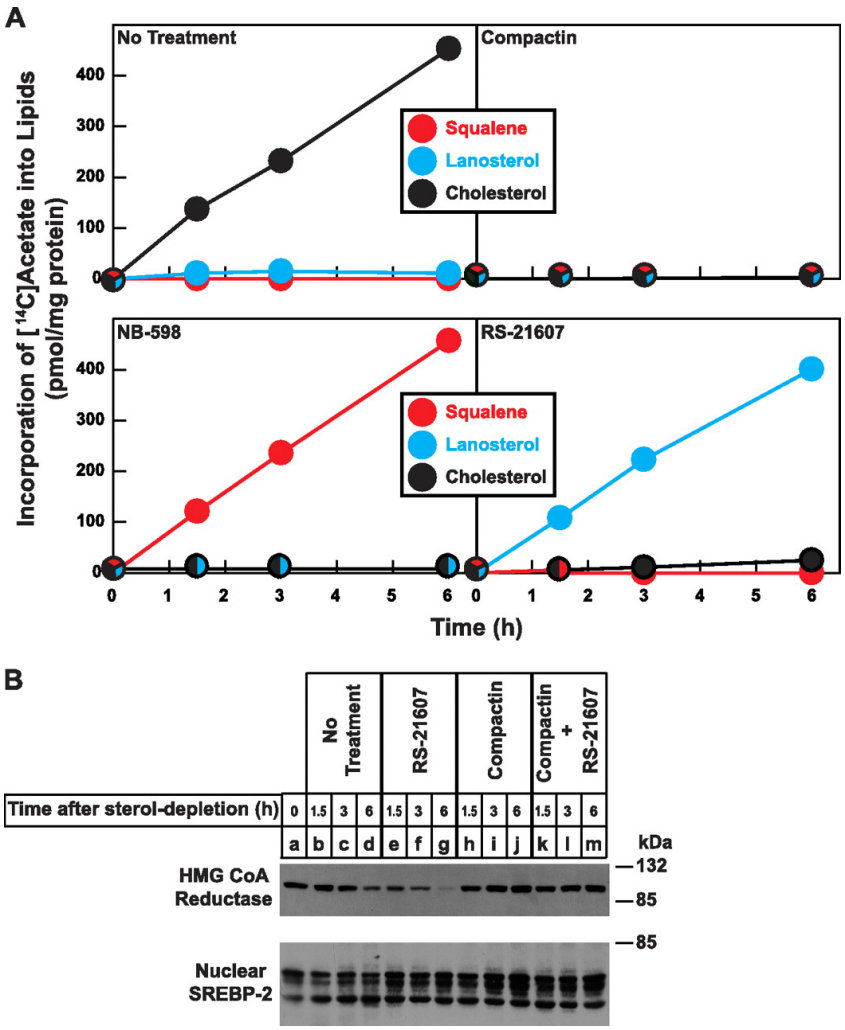

Figure 1-2. Inhibition of lanosterol 14α-demethylase causes accumulation of lanosterol and triggers degradation of HMG CoA reductase in CHO cells. *A*, CHO-7 cells were set up for experiments on day 0 at 5×10^5 cells per 60-mm dish in medium A supplemented with 5% lipoprotein-deficient serum. On day 1, the cells were refed 2 ml of the identical medium containing 10 μCi of [^{14}C]acetate; cold acetate was added to achieve a final concentration of 0.5 mM. Some of the dishes also received 10 μM sodium compactin, 30 μM NB-598, or 0.1 μM RS-21607. Following incubation at 37 °C for the indicated periods of time, cell lysates were prepared, and lipids were extracted. Aliquots of the resulting lipid extracts were then subjected to TLC in parallel with authentic standards for squalene, lanosterol, and cholesterol. Incorporation of [^{14}C]acetate into squalene, lanosterol, and cholesterol was determined by scintillation counting. Data are presented as mean values from triplicate dishes. *B*, CHO-7 cells were set up on day 0 at 5×10^5 cells per 100-mm dish in medium A with 5% lipoprotein-deficient serum. On day 3,

cells were subjected to treatment for 1 h at 37 °C in medium A containing 1% (w/v) hydroxypropyl-β-cyclodextrin. The cells were subsequently switched back to medium A containing 5% lipoprotein-deficient serum and incubated at 37 °C for an additional 5-6 h. The cells were then subjected to treatments in the identical medium containing various combinations of 0.1 μM RS-21607 and 10 μM compactin. After incubation at 37 °C for the indicated times, cells were harvested, lysed, and subjected to cell fractionation. Aliquots of protein from the membrane (12 μg of protein/lane) and nuclear extract (40 μg of protein/lane) fractions were separated by 8% SDS-PAGE and transferred to nitrocellulose membranes. Immunoblot analysis was carried out with 1 μg/ml monoclonal IgG-A9 (against reductase) or 5 μg/ml monoclonal IgG-7D4 (against SREBP-2).

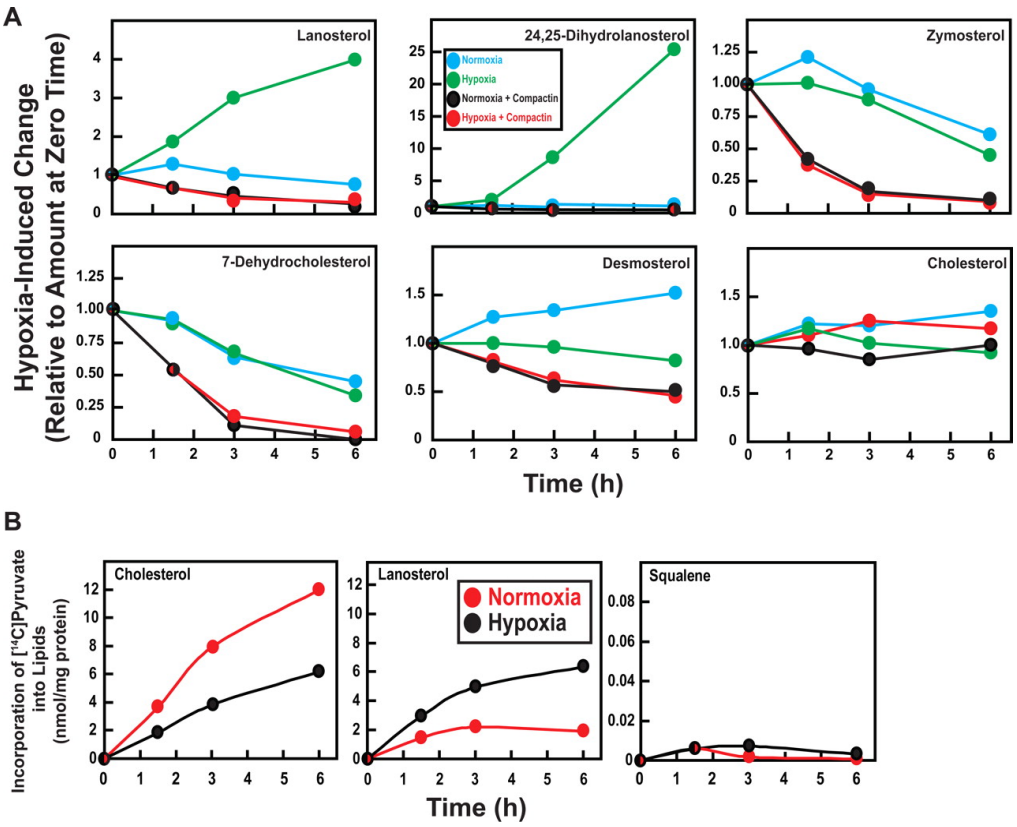

Figure 1-3. Hypoxia triggers accumulation of lanosterol and 24,25-dihydrolanosterol in CHO cells. *A*, CHO-7 cells were set up for experiments on day 0 and subjected to cyclodextrin treatment on day 3 as described in the legend to Figure 1-2B. The cells were then incubated at 37 °C with medium A containing 5% lipoprotein-deficient serum in the absence or presence of 10 μM compactin under normoxic (21% O_2) or hypoxic (1% O_2) conditions. After the indicated periods of time, cells were harvested, cell lysates were prepared, and lipids were extracted with chloroform/methanol. The amounts of cholesterol and sterol precursors in the resulting lipid extracts were determined by HPLC-MS and normalized for protein content. The data are presented as fold changes relative to the amount of the indicated sterol prior to hypoxia treatment (t = 0 h). These values per mg of protein were 5.1 μg of lanosterol, 2.0 μg of 7-dehydrocholesterol, 6.3 μg of desmosterol, and 41.9 μg of cholesterol. 24,25-Dihydrolanosterol and zymosterol were not quantified; relative fold changes were calculated based on peak areas. *B*, CHO-7 cells were set up on day 0 as described in the legend to Figure 1-2A. On day 1, cells were subjected to cyclodextrin treatment at 37 °C for 1 h. Cells were subsequently incubated for 6 h under normoxic or hypoxic conditions, after which they were labeled with 6.25 μCi of [^{14}C]pyruvate as described in the Experimental Methods section. Following incubation at 37 °C for the indicated periods of time, incorporation of [^{14}C]pyruvate into squalene, lanosterol, and cholesterol was determined as described in the legend to Figure 1-2A.

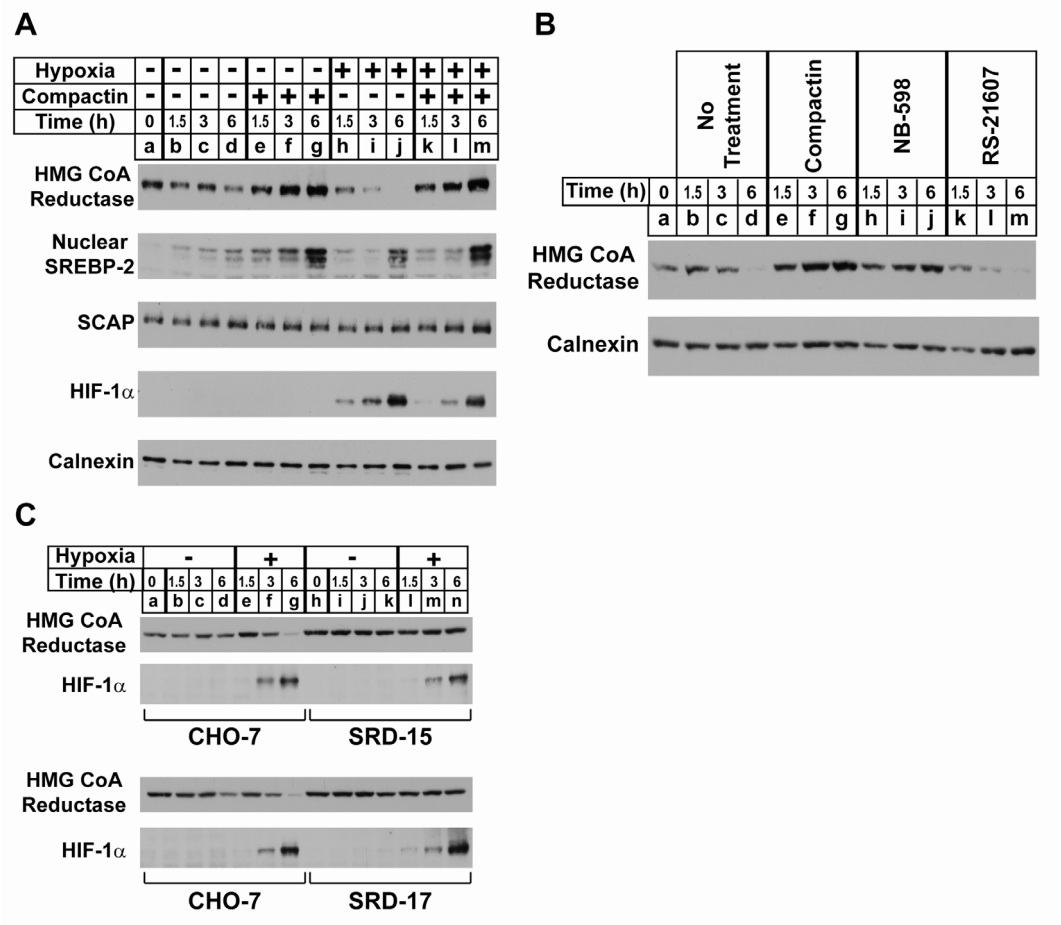

Figure 1-4. Hypoxia increases degradation of HMG CoA reductase through an Insig-dependent mechanism. CHO-7, SRD-15, and SRD-17 cells were set up for experiments on day 0 and subjected to cyclodextrin treatment on day 3 as described in the legend to Figure 1-2B. The cells were subsequently refed medium A containing 5% lipoprotein-deficient serum in the absence or presence of either 10 μM compactin, 30 μM NB-598, or 0.1 μM RS-21607. Following the indicated times of incubation at 37 °C under normoxic or hypoxic conditions, cells were harvested, lysed, and subjected to cell fractionation. Aliquots of the membrane (12 μg of protein/lane) and nuclear extract (40 μg of protein/lane for SREBP-2, 10 μg of protein/lane for HIF-1α) fractions were subjected to 8% SDS-PAGE, and immunoblot analysis was performed with 1 μg/ml IgG-A9 (against reductase), 5 μg/ml IgG-7D4 (against SREBP-2), 2 μg/ml monoclonal anti-HIF-1α IgG, 5 μg/ml polyclonal IgG-R139 (against SCAP), or polyclonal antibody against calnexin (1:2000 dilution).

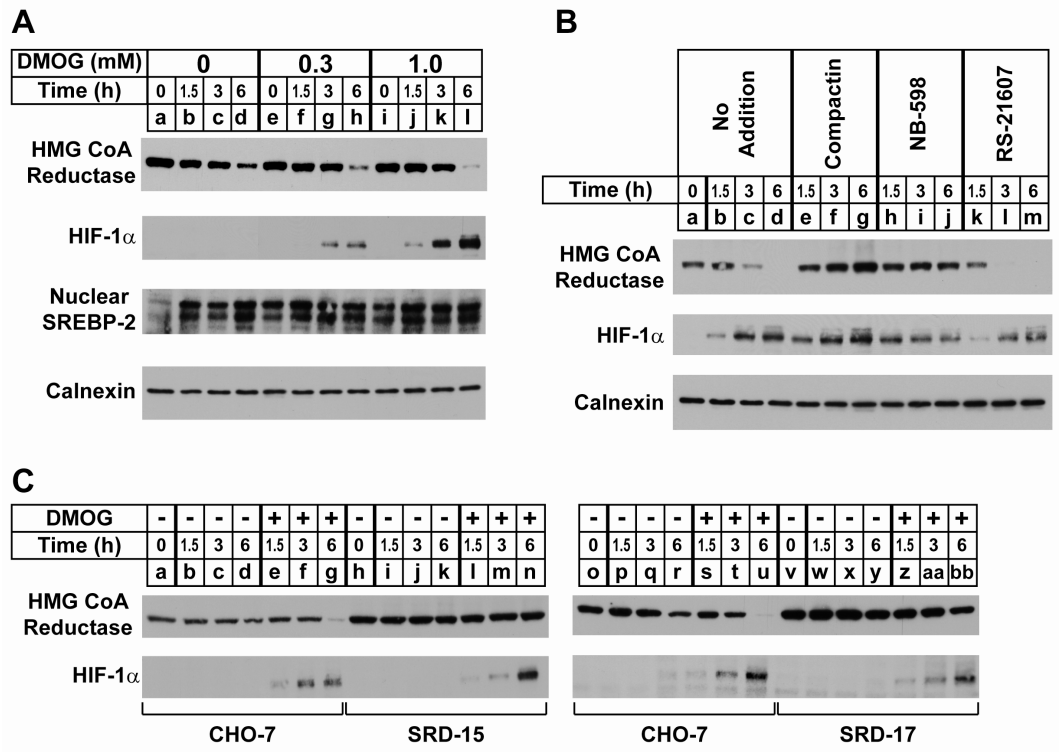

Figure 1-5. 2-Oxoglutarate-dependent dioxygenase inhibition stimulates Insig-mediated degradation of HMG CoA reductase. CHO-7, SRD-15, and SRD-17 cells were set up for experiments on day 0 and treated with cyclodextrin on day 3 as described in the legend to Figure 1-2B. The cells were subsequently incubated at 37 °C under normoxic conditions for various periods of time in medium A containing 5% lipoprotein-deficient serum with or without DMOG (0.3 and 1.0 mM in *A*; 1 mM in *B* and *C*) in the absence or presence of 10 μM compactin. After the indicated times of incubation, cells were harvested, lysed, and subjected to cell fractionation. Aliquots of membrane (12 μg of protein/lane) and nuclear extract (40 μg of protein/lane for SREBP-2, 10 μg of protein/lane for HIF-1α) fractions were subjected to 8% SDS-PAGE, and immunoblot analysis was performed with 1 μg/ml IgG-A9 (against reductase), 5 μg/ml IgG-7D4 (against SREBP-2), 2 μg/ml monoclonal anti-HIF-1α IgG, 5 μg/ml polyclonal IgG-R139 (against SCAP), or polyclonal antibody against calnexin (1:2000 dilution).

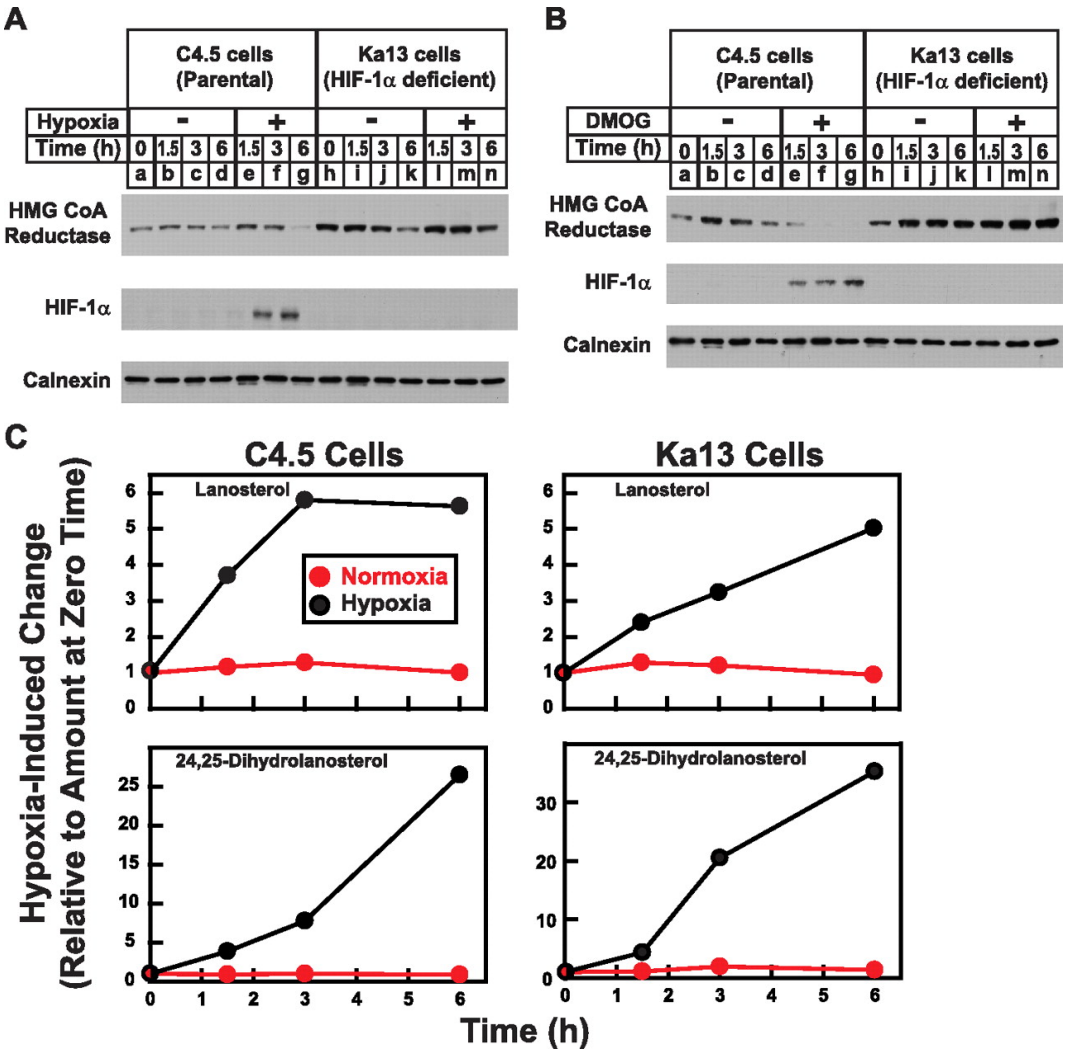

Figure 1-6. HIF-1α-deficient CHO cells fail to stimulate degradation of HMG CoA reductase in response to hypoxia and 2-oxoglutarate-dependent dioxygenase inhibition. Parental C4.5 and HIF-1α-deficient Ka13 cells were set up on day 0 at 5×10^5 cells per 100-mm dish in medium A containing 5% fetal calf serum and switched to medium A containing 5% lipoprotein-deficient serum on day 1. On day 3, cells were treated with cyclodextrin as described in the legend to Figure 1-2B. The cells were then subjected to incubation in medium A supplemented with 5% lipoprotein-deficient serum at 37 °C under normoxic or hypoxic conditions for the indicated periods of time. In *B*, cells were incubated under normoxic conditions in the absence or presence of 1 mM DMOG. *A* and *B*, after the indicated times of incubation, cells were harvested, lysed, and subjected to cell fractionation. Aliquots of membrane (12 μg of protein/lane) and nuclear extract (10 μg of protein/lane) fractions were subjected to 8% SDS-PAGE, and immunoblot analysis was performed with 1 μg/ml IgG-A9 (against reductase), 2 μg/ml

monoclonal anti-HIF-1α IgG, or polyclonal antibody against calnexin (1:2000 dilution). *C*, after the indicated periods of time, cells were harvested, cell lysates were prepared, and lipids were extracted with chloroform/methanol. The amount of lanosterol and 24,25-dihydrolanosterol in the resulting lipid extracts was determined by HPLC-MS and normalized for protein content. The data are presented as fold changes relative to the amount of the indicated sterol prior to hypoxia treatment (t = 0 h).

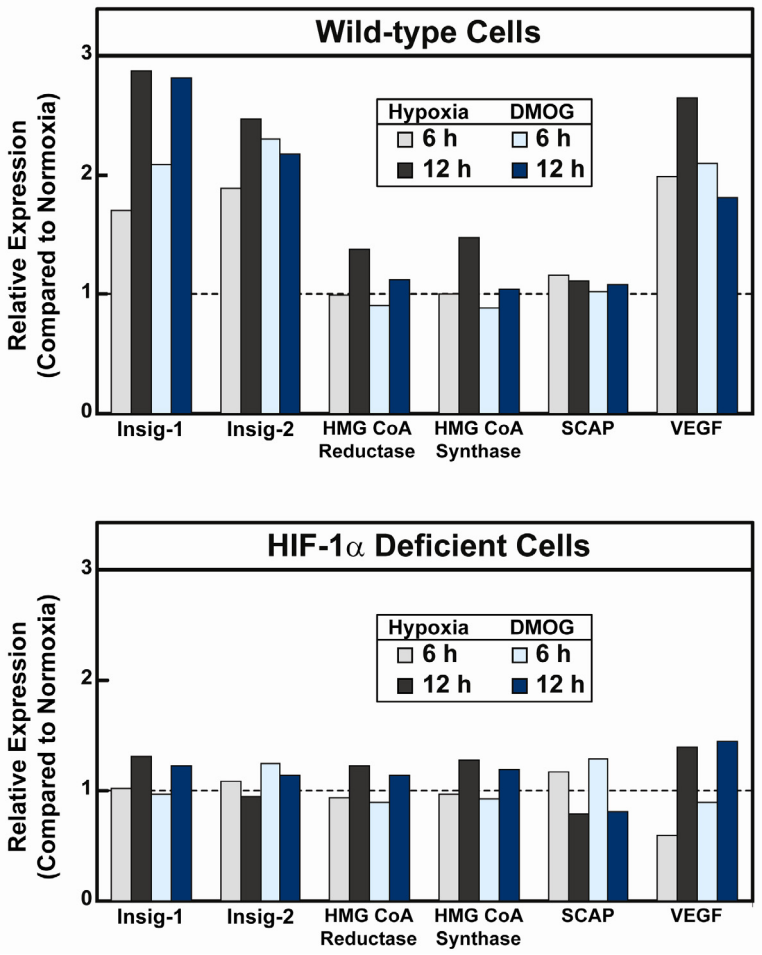

Figure 1-7. Hypoxia and 2-oxoglutarate-dependent dioxygenase inhibition enhance Insig expression through a HIF-1α-dependent mechanism. C4.5 cells (*A*) and Ka13 cells (*B*) were set up for experiments as described in the legend to Figure 1-6. The cells were switched to medium A containing 5% lipoprotein-deficient serum on day 1. On day 2, cells were refed the identical medium and incubated for the indicated periods of time at 37 °C under normoxic or hypoxic conditions; some of the cells cultured under normoxic conditions received 1 mM DMOG. Following incubations, cells were harvested, and total RNA was isolated and subjected to reverse transcription reactions. Aliquots of the resulting cDNA were then subjected to real-time PCR analysis using specific primer pairs for the indicated genes and an invariant control gene. Each value represents the expression of the indicated gene relative to that in cells cultured under normoxic conditions in the absence of DMOG.

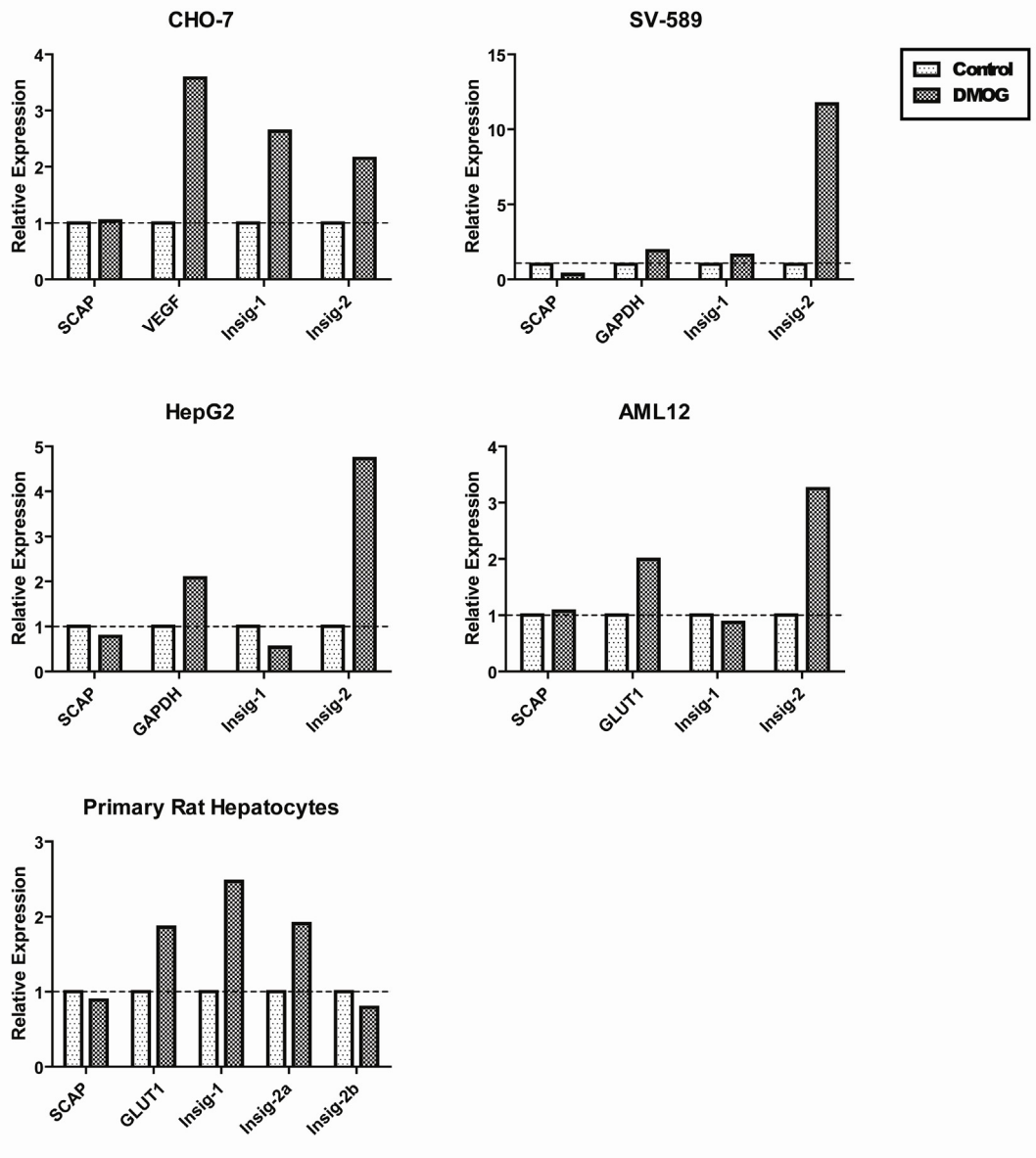

Figure 1-8. 2-Oxoglutarate-dependent dioxygenase inhibition induces expression of Insig-2 in various cell lines. Cells were set up on day 0 at a density of 5×10^5 cells per 100-mm dish (CHO-7, SV-589, HepG2, and AML12 cells) or 1.5×10^6 cells per well in 6-well plates (primary rat hepatocytes) in the respective culture medium described in the Experimental Methods section. On day 1, cells were treated in the identical medium without or with 1 mM DMOG. On day 2, RNA was isolated and real-time PCR analysis was carried as described in the legend of Figure 1-7. Each value represents the expression of the indicated gene relative to that in the control cells.

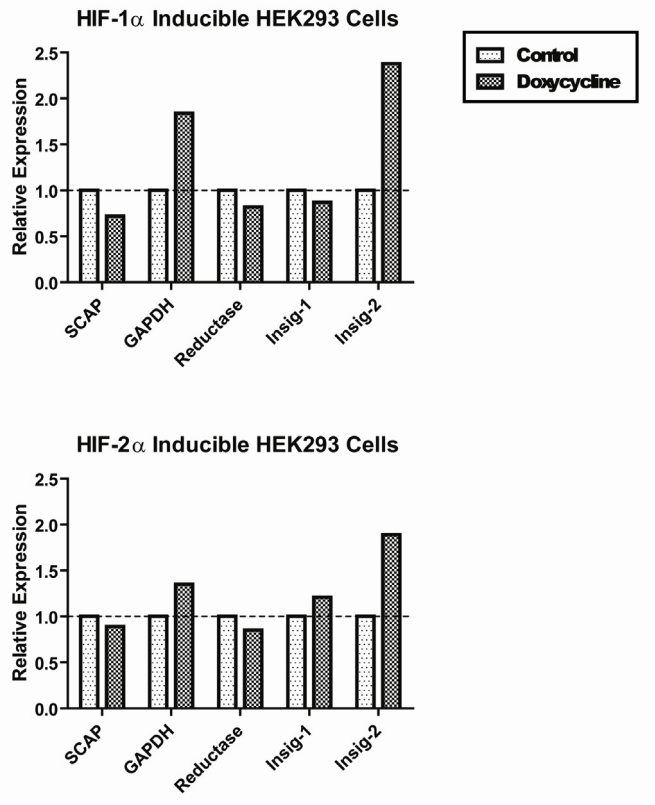

Figure 1-9. Doxycycline treatment of HIF-1α- and HIF-2α-inducible HEK293 cell lines results in elevated Insig-2 mRNA levels. On day 0, cells were set up in 100-mm dishes in medium B supplemented with 10% fetal calf serum. On day 2, cells were treated without or with 1 μg/ml doxycycline in the same medium. On day 3, RNA was isolated from cells and real-time quantitative PCR analysis was carried out as described in the legend of Figure 1-7. Each value represents the expression of the indicated gene relative to that in the control cells.

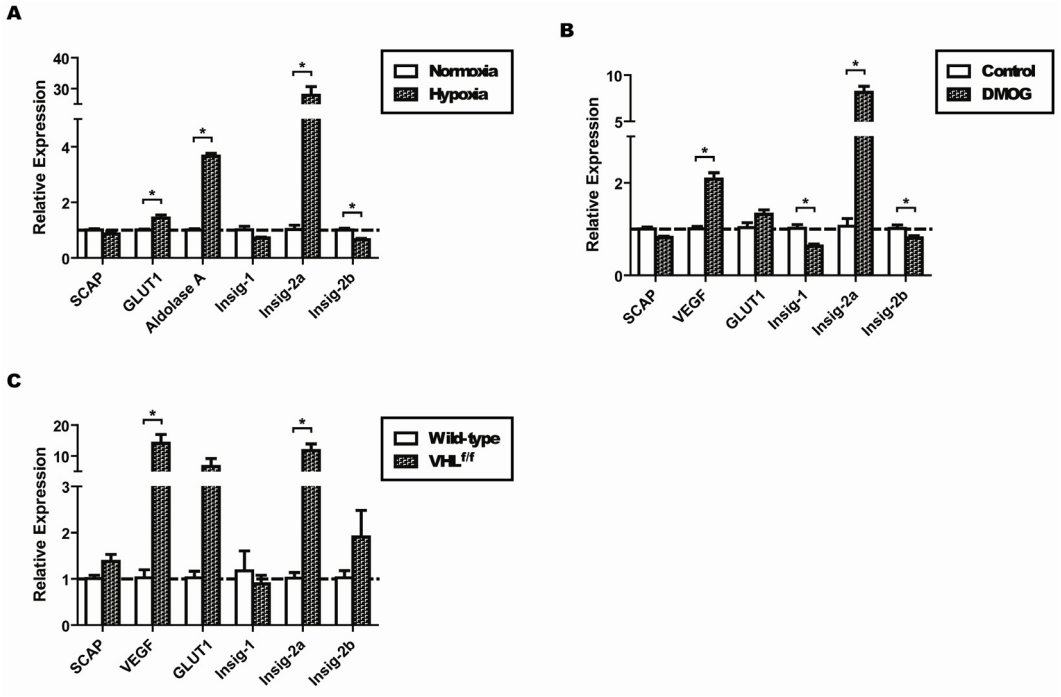

Figure 1-10. Hepatic Insig-2a expression is upregulated in mouse models of hypoxia. *A*, wild-type mice were exposed to normoxia (21% O_2) or hypoxia (6% O_2) for 6 h as described in the Experimental Methods section. *B*, wild-type mice were administered with 8 mg/day of DMOG in PBS by oral gavage for 5 consecutive days. Control mice received the vehicle PBS. *C*, wild-type or *VHL*$^{f/f}$ mice were injected with adenovirus encoding for Cre recombinase driven by an albumin promoter. Mice were analyzed 4 days after injection. At the end of the treatment periods, mice were sacrificed; RNA was isolated from the liver and quantitative real-time PCR analysis was performed as described in the legend of Figure 1-7. Each value represents the expression of the indicated gene relative to that in the control group. Data are presented as means ± SEM (n=3 for each group in *A* and *B*, n=6 for each group in *C*). * $p < 0.05$ compared to the control group.

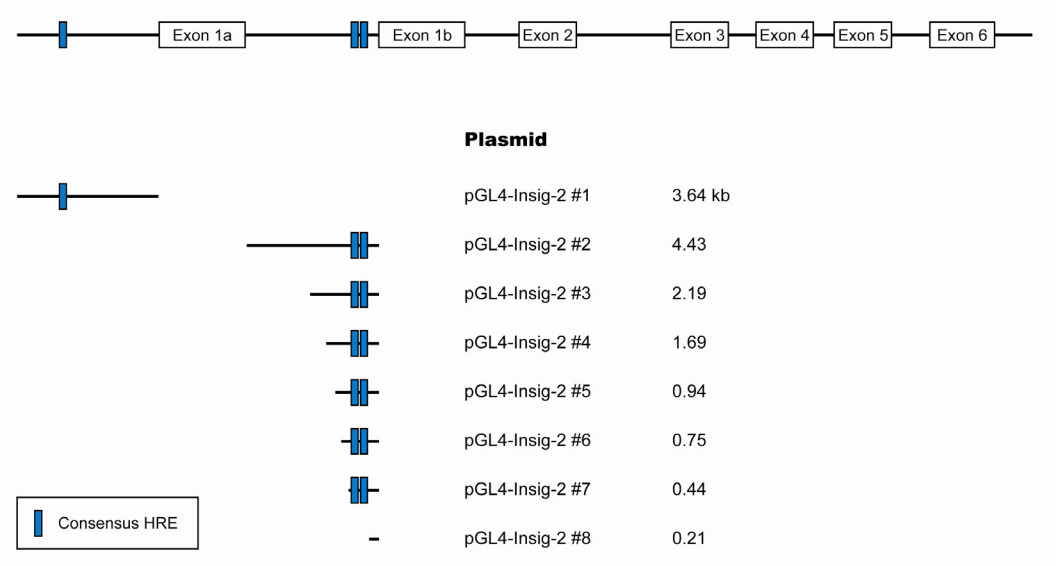

Figure 1-11. Schematic representation of the mouse *Insig-2* gene and reporter plasmids used for promoter analysis. Sequences conforming to the consensus HRE (5'-CGTGX$_{(1-8)}$CAC-3') are indicated in blue.

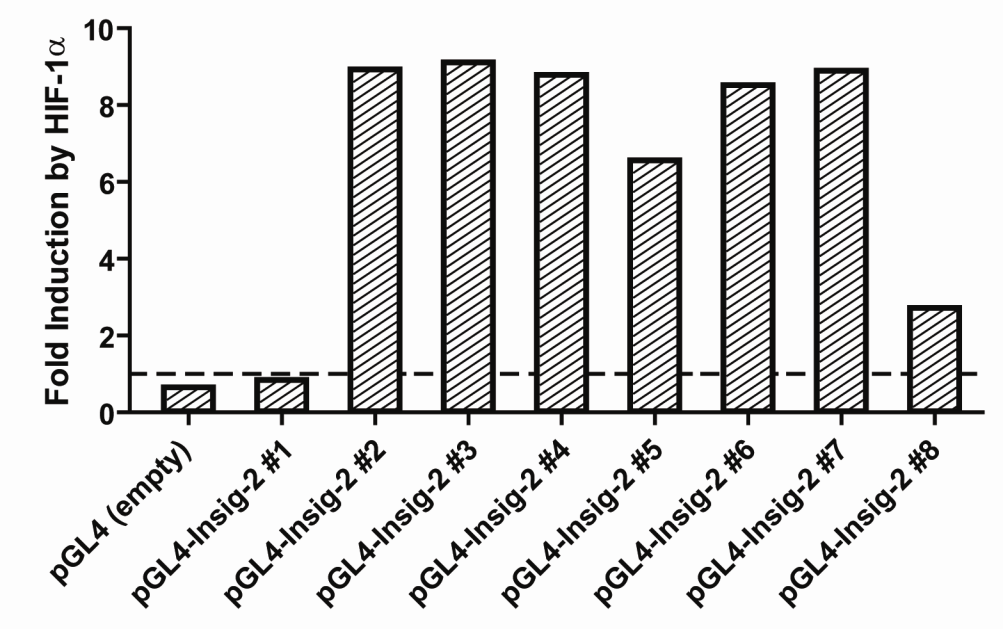

Figure 1-12. Localization of an HRE to a 234-nucleotide region upstream of exon 1b of the mouse *Insig-2* gene. On day 0, primary rat hepatocytes were isolated and plated in 6-well plates at a density of 5×10^5 cells per well in medium B supplemented with 5% fetal calf serum. After 4 h, cells were switched to medium C supplemented with 1 nM insulin, 100 nM dexamethasone, and 100 nm 3,3′,5-triiodo-L-thyronine. On day 1, cells were transfected with 4 μg DNA (1.8 μg of the indicated reporter plasmid and 0.4 μg of pGL4-tk-Renilla Luciferase, without or with 1.8 μg of pCMV-HIF-1α) per well in medium D. After 6 h, cells were refed medium C containing 100 nM insulin, 100 nM dexamethasone, and 100 nM 3,3′,5-triiodo-L-thyronine for 36 h. At the end of the incubation period, cells were harvested and lysed in a detergent-containing buffer. Firefly and Renilla luciferase activities were measured as described in the Experimental Methods section. Firefly luciferase activities were normalized to Renilla luciferase activities, and data are presented as the fold induction by HIF-1α.

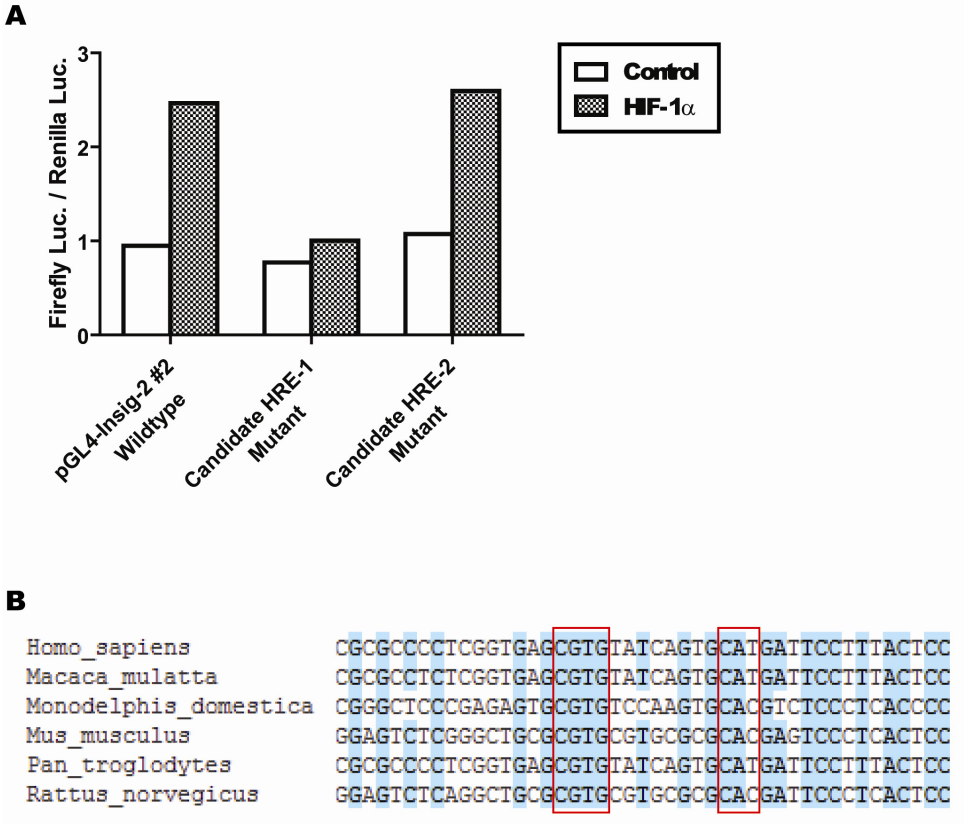

Figure 1-13. Identification of a functional HRE in the mouse *Insig-2* gene. *A*, mutation of candidate HRE-1 abolishes HIF-mediated induction of the Insig-2 reporter plasmid. Primary rat hepatocytes were isolated, transfected, and treated as described in the legend of Figure 1-12. Data are presented as the normalized ratio of firefly luciferase activities divided by Renilla luciferase activities. *B*, sequence alignment of the *Insig-2* HRE in various species. Sequence data and alignment were obtained from Ensembl (www.ensembl.org). The core components of the consensus HRE are boxed in red.

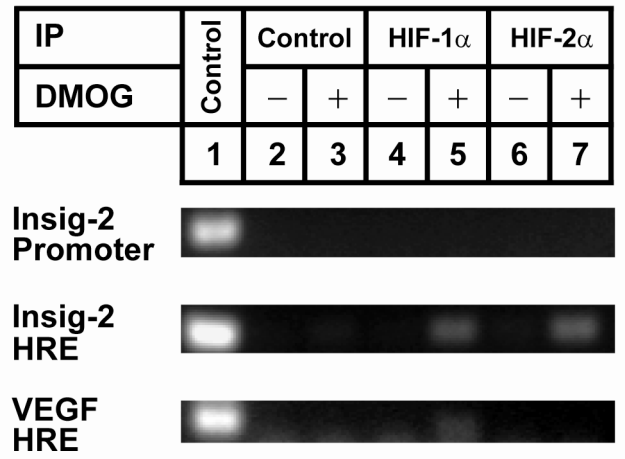

Figure 1-14. The *Insig-2* HRE physically interacts with HIF-1α and HIF-2α in human fibroblast cells. SV-589 cells were set up on day 0 at a density of 2×10^5 cells per 100-mm dish in medium B supplemented with 10% fetal calf serum. On day 2, cells were refed the identical medium without or with 2 mM DMOG. On day 3, Cells were treated with 1% formaldehyde for 10 min to crosslink chromatin, harvested, and chromatin immunoprecipitation was carried out with the indicated antibodies as described in the Experimental Methods section.

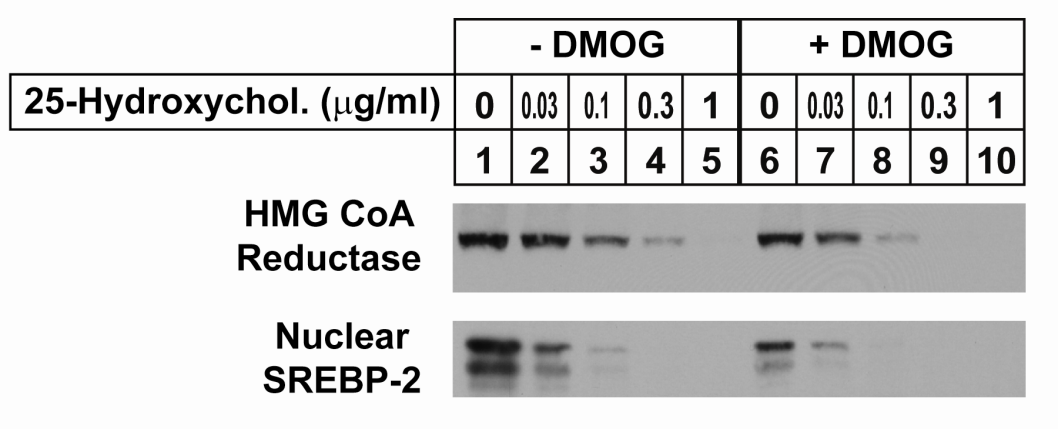

Figure 1-15. Prolonged inhibition of 2-oxoglutarate-dependent dioxygenases enhances sensitivity of HMG CoA reductase degradation and SREBP-2 processing to 25-hydroxycholesterol in CHO cells. CHO-7 cells were set up for experiments on day 0 at 5×10^5 cells per 100-mm dish in medium A containing 5% lipoprotein-deficient serum. On day 2, cells were refed the same medium containing 10 μM compactin and 50 μM mevalonate, without or with 1 mM DMOG. Following incubation for 24 h, cells were treated with medium A containing 5% lipoprotein-deficient serum containing 10 μM compactin, 10 mM mevalonate, without or with 1 mM DMOG, in the absence or presence of the indicated concentrations of 25-hydroxycholesterol. After 5 h, cells were harvested, lysed, and subjected to cellular fractionation. Aliquots of membrane (12 μg) and nuclear extract (40 μg) fractions were separated by 8% SDS-PAGE and immunoblot analysis was performed with 1 μg/ml IgG-A9 (against reductase) or 5 μg/ml IgG-7D4 (against SREBP-2).

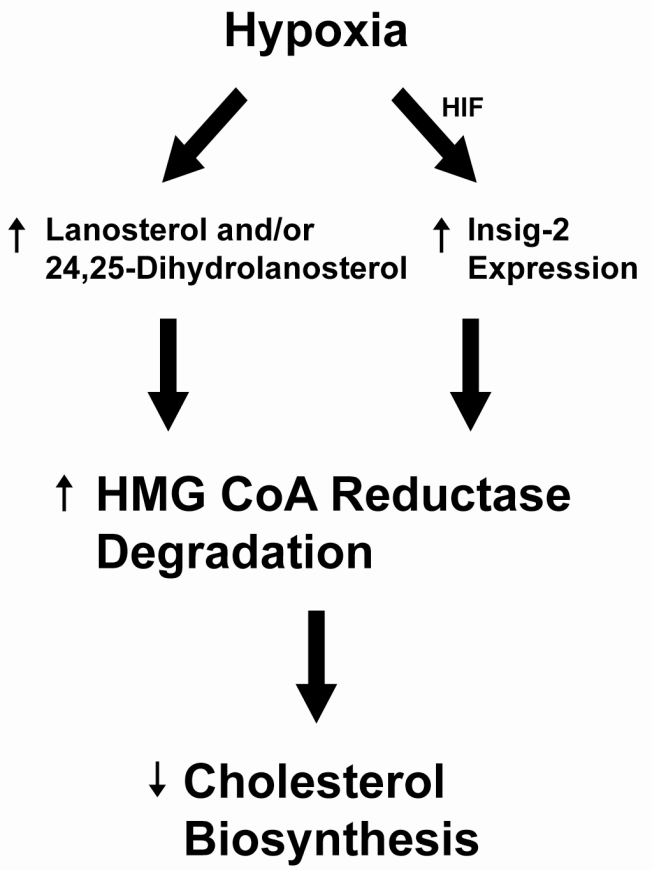

Figure 1-16. Model for oxygen-mediated regulation of cholesterol biosynthesis through accelerated degradation of HMG CoA reductase. Hypoxia triggers accumulation of lanosterol and its reduced metabolite 24,25-dihydrolanosterol, due to inhibition of lanosterol 14α-demethylase. The accumulation of these methylated sterols serves as one signal for rapid degradation of reductase. The other signal is provided by the HIF-mediated induction of Insig-2, which confers cells with enhanced sensitivity to sterol-induced degradation of reductase. Together, these signals lead to accelerated degradation of reductase, which ultimately reduces flow through early steps of the cholesterol synthesis pathway when oxygen is limiting.

CHAPTER TWO

INSIG-MEDIATED, STEROL-ACCELERATED DEGRADATION OF THE MEMBRANE DOMAIN OF MAMMALIAN HMG COA REDUCTASE IN INSECT CELLS

ABSTRACT

Sterol-accelerated, ER-associated degradation (ERAD) of the enzyme HMG CoA reductase is one of several mechanisms through which cholesterol synthesis is controlled in mammalian cells. This degradation results from the binding of the membrane domain of reductase to ER membrane proteins called Insigs, which are carriers of a ubiquitin ligase called gp78. The gp78-dependent ubiquitination of reductase marks for rapid, 26S proteasome-mediated degradation from ER membranes, thereby slowing a rate-limiting step in cholesterol synthesis. Here, we report that sterols accelerate the degradation of the membrane domain of hamster reductase in *Drosophila* S2 cells even though they lack Insigs and their own reductase is not subjected to sterol-accelerated degradation. Degradation of reductase in S2 cells mimics the reaction that occurs in mammalian cells with regard to its absolute requirement for the action of human Insig-1 or Insig-2, sensitivity to proteasome inhibitors, augmentation by nonsterol isoprenoids, and sterol specificity. Moreover, RNA interference (RNAi) studies reveal that sterol-accelerated ERAD of reductase in S2 cells requires the *Drosophila* homolog of the *S. cerevisiae* ubiquitin ligase Hrd1 and several other proteins, including a putative substrate selector, that are associated with the enzyme in yeast and mammalian systems. These studies define Insigs as the minimal requirement for sterol-accelerated degradation of the membrane domain of reductase in *Drosophila* S2 cells.

INTRODUCTION

In mammalian cells, the enzyme HMG CoA reductase catalyzes the reduction of HMG CoA to mevalonate, a rate-limiting step in the synthesis of cholesterol and essential nonsterol isoprenoids such as the farnesyl and geranylgeranyl groups that become covalently attached to many cellular proteins, thereby increasing their association with membranes (Goldstein and Brown, 1990). Reductase is a resident glycoprotein of the ER that consists of a hydrophobic N-terminal domain that contains eight membrane-spanning segments followed by a hydrophilic C-terminal domain that projects into the cytosol where it exerts enzymatic activity (Gil et al., 1985; Liscum et al., 1985; Roitelman et al., 1992). The membrane domain plays a key role in accelerated ER-associated degradation (ERAD) of reductase (Gil et al., 1985; Sever et al., 2003b), one of several mechanisms through which sterols and nonsterol isoprenoids exert stringent feedback control on the enzyme (Brown and Goldstein, 1980). When certain sterols build up in ER membranes, reductase becomes ubiquitinated through a reaction that is mediated by the membrane domain of the enzyme (Ravid et al., 2000; Sever et al., 2003a; Sever et al., 2003b). This sterol-regulated ubiquitination is an obligatory reaction for the recognition and delivery of reductase to cytosolic 26S proteasomes for degradation from the ER membrane. Sterol-induced ERAD reduces the half-life of the reductase protein from 12 h in sterol-deprived cells to less than 1 h when intracellular sterols are abundant, thereby ensuring a constant supply of essential nonsterol isoprenoids while at the same time avoiding toxic over-accumulation of cholesterol or one of its sterol precursors.

Accelerated ERAD of reductase is mediated by sterol-induced binding of its membrane domain to one of two polytopic ER membrane proteins called Insig-1 and Insig-2 (Sever et al., 2003b). Specific point mutations within the membrane domain of reductase markedly reduce its binding to Insigs, rendering the mutant enzymes resistant to sterol-accelerated degradation (Lee et al., 2007; Sever et al., 2003a). A subset of Insig molecules are found associated with a membrane-anchored ubiquitin ligase named gp78, which mediates transfer of ubiquitin from the ubiquitin-conjugating enzyme Ubc7 to a pair of cytosolically exposed lysine residues in the membrane domain of reductase (Sever et al., 2003a; Song et al., 2005b). Once ubiquitinated, reductase presumably becomes extracted from membranes and delivered to proteasomes through an as yet undefined mechanism that likely involves gp78-bound AAA-ATPase VCP/p97 and its associated cofactors. Current evidence indicates this extraction is augmented by the 20-carbon isoprenoid geranylgeraniol (Sever et al., 2003a).

The Insig proteins also mediate sterol regulation of another protein called SCAP (Goldstein et al., 2006; Yang et al., 2002), which like reductase, contains a hydrophobic N-terminal domain with eight membrane-spanning segments and a large C-terminal domain located in the cytosol (Nohturfft et al., 1998; Sakai et al., 1997). SCAP is a sterol-regulated escort protein that associates with SREBPs, a family of transcription factors that enhance transcription of all of the genes required for cholesterol synthesis (including reductase) as well as the LDL receptor (Horton et al., 2002a; Horton et al., 2002b). In sterol-deprived cells, SCAP facilitates translocation of SREBPs from the ER to Golgi, where active fragments of SREBPs are proteolytically released from membranes (DeBose-Boyd et al., 1999; Nohturfft et al., 2000; Rawson et al., 1999).

These fragments then migrate from the cytosol into the nucleus to enhance transcription of target genes, thereby increasing the synthesis and uptake of cholesterol. Sterol accumulation causes binding of Insigs to the membrane domain of SCAP, which traps the protein in the ER and prevents delivery of its associated SREBP to the Golgi for release. Without this release, expression of SREBP target genes falls and cholesterol synthesis declines.

Cultured *Drosophila* cell lines have become a popular model system in which to study fundamental processes in biology. One of the most commonly used lines, Schneider S2 cells, offers a number of advantages over mammalian cells including ease of culture and transgene expression; less functional redundancy of the *Drosophila* genome compared to mammalian genomes; and high susceptibility to RNA interference (RNAi) after treatment with large double-stranded RNAs (dsRNAs). With regard to sterol regulation, *Drosophila* cells lack a recognizable *Insig* gene and cannot synthesize cholesterol or other sterols *de novo* owing to the absence of many of the enzymes in the cholesterol biosynthetic pathway (Clark and Block, 1959; Clayton, 1964).

Sterol-mediated regulation of mammalian SREBP-2, one of the two SREBP isoforms expressed in mammalian cells, has been reconstituted in S2 cells (Dobrosotskaya et al., 2003). In these experiments, S2 cells were transfected with cDNAs encoding human SREBP-2, hamster SCAP, and human Insig-1 or Insig-2. Hamster SCAP mediated transport of human SREBP-2 from the ER to Golgi where the protein was processed by *Drosophila* proteases. Importantly, ER to Golgi transport of SREBP-2 was inhibited by sterols, but only when human Insig-1 or Insig-2 was co-expressed. Thus, SCAP and Insigs are the minimal requirements for sterol-regulated transport of

mammalian SREBPs from the ER to the Golgi in insect cells. Taken together with the advantages of the insect cell system, the ability to reconstitute sterol-regulated transport of SCAP in S2 cells suggests they could be an excellent model system in which mechanisms for Insig-mediated, sterol-accelerated degradation of mammalian reductase can be examined.

In the current studies, we reconstitute sterol-accelerated degradation of hamster reductase in *Drosophila* S2 cells. For this purpose, we transfect the S2 cells with cDNAs encoding either human Insig-1 or Insig-2 and the membrane domain of hamster reductase, which is necessary and sufficient for accelerated degradation in mammalian cells (Gil et al., 1985; Sever et al., 2003b; Skalnik et al., 1988). In the presence of sterols, the membrane domain of hamster reductase becomes rapidly degraded in S2 cells through a process that is augmented by geranylgeraniol and blocked by inhibitors of the 26S proteasome. Importantly, this degradation only occurs when human Insig-1 or Insig-2 is co-expressed and coincides with sterol-induced binding of the membrane domain of reductase to these proteins. RNAi experiments reveal an important role for the *Drosophila* homolog of the *S. cerevisiae* protein Hrd1 in sterol-induced degradation of reductase in S2 cells. Hrd1 is a membrane-anchored RING-H2 ubiquitin ligase that exists in a large multiprotein complex in both yeast and mammalian systems (Carvalho et al., 2006; Denic et al., 2007; Lilley and Ploegh, 2005; Schulze et al., 2005). In addition to *Drosophila* Hrd1, a subset of its associated proteins, including the putative substrate selector, is required for sterol-accelerated degradation of reductase in S2 cells. These results demonstrate that Insig is sufficient to cause the membrane domain of reductase to

become ubiquitinated and subsequently degraded through mechanisms mediated by the *Drosophila* Hrd1 ubiquitin ligase complex.

EXPERIMENTAL METHODS

Materials

We obtained 25-hydroxycholesterol and 24,25-dihydrolanosterol from Steraloids; lanosterol from Sigma; MG-132 and digitonin from Calbiochem; and horseradish peroxidase-conjugated, donkey anti-mouse IgG (affinity-purified) from Jackson ImmunoResearch Laboratories. SR-12813 and Apomine were synthesized by the Core Medicinal Chemistry Laboratory at the University of Texas Southwestern Medical Center. Stock solutions of palmitate were made up in 0.15 M NaCl and 10% (w/v) fatty acid-free bovine serum albumin at pH 7.4 as described (Hannah et al., 2001; Seegmiller et al., 2002). Stock solutions of ethanolamine were made up in H_2O. Other reagents, including lipoprotein-deficient serum (d > 1.215 g/ml), sodium compactin, and sodium mevalonate, were prepared or obtained from sources as described previously (DeBose-Boyd et al., 1999).

Expression Plasmids

The previously described plasmids pAc-Insig-1-Myc and pAc-Insig-2-Myc encode amino acids 1-277 and 1-225 of human Insig-1 and Insig-2, respectively, followed by six copies of a c-Myc epitope under control of the *Drosophila* actin 5C promoter (Dobrosotskaya et al., 2003). The following plasmids were constructed by subcloning the indicated open reading frame from mammalian expression vectors into pAc5.1/V5-HisB: pAc-HMG-Red (TM1-8)-T7 encodes amino acids 1-346 of hamster HMG CoA reductase tagged with three copies of a T7 epitope (Sever et al., 2003b); pAc-HMG-Red (TM1-8)-T7

(K89R/K248R) encodes amino acids 1-346 of hamster HMG CoA reductase tagged with three copies of a T7 epitope and harbors substitutions of arginine for lysines 89 and 248 (Sever et al., 2003a).

The membrane domain of *Drosophila* HMG CoA reductase (amino acids 1-391) and the open reading frames for *Drosophila* homologs of Hrd1 and Trc8 were amplified by PCR with the Phusion DNA polymerase kit (New England Biolabs) using first strand cDNA obtained by RT-PCR of total RNA isolated from *Drosophila* S2 cells. The primers and templates used are listed in Appendix D. The PCR products were gel purified, subjected to restriction enzyme digestion, and subcloned into the insect cell expression vector pAc5.1/V5-HisB (Invitrogen). All of the proteins encoded by these plasmids contain three tandem copies of a T7 epitope at the C-terminus. The integrity of all plasmids constructed above was confirmed by DNA sequencing.

Culture and Transfection of Drosophila S2 Cells

Stock cultures of *Drosophila* S2 cells were maintained in monolayer at 23 °C in medium A (Schneider's Drosophila medium containing 100 units/ml penicillin and 100 μg/ml streptomycin sulfate) supplemented with 10% (v/v) heat-inactivated fetal calf serum. Cells were set up for experiments on day 0 in 6-well plates at a density of 1×10^6 cells per well in medium A supplemented with 10% heat-inactivated fetal calf serum. After 3-4 h, the cells were washed with PBS and transfected with 2-3 μg DNA per well using 10 μl of Cellfectin transfection reagent (Invitrogen) in 2 ml of Medium B (Drosophila SFM medium). The total amount of DNA was kept constant in each well by the addition of empty vector DNA. On day 1, cells were washed with PBS and switched to medium C

(IPL-41 containing 100 units/ml penicillin and 100 μg/ml streptomycin sulfate) supplemented with 10% heat-inactivated lipoprotein-deficient serum. On day 3, cells were subjected to treatments as described in the figure legends, after which they were harvested and pooled for analysis as described below. Sterols were added in ethanol at a final concentration of 0.1% (v/v); MG-132 was added in DMSO at a final concentration of 0.1%.

Preparation of Cell Lysates and Immunoblot Analysis

Conditions of the incubations are described in the figure legends. At the end of the incubations, the cells were harvested by scraping in PBS and collected by centrifugation at 1000 × g for 5 min at 4 ºC. Cell pellets from triplicate wells were combined, resuspended in RIPA buffer (50 mM Tris-HCl pH 8.0, 150 mM NaCl, 0.1% (v/v) SDS, 1.5% (v/v) NP-40, 0.5% (w/v) sodium deoxycholate, and 2 mM $MgCl_2$) containing protease inhibitors (0.1 mM leupeptin, 5 μg/ml pepstatin A, 2 μg/ml aprotinin, 25 μg/ml *N*-acetyl-leucinal-leucinal-norleucinal, 0.5 mM phenylmethylsulfonylfluoride, 0.5 mM Pefabloc, and 0.25 mM dithiothreitol), disrupted by passing through a 22-gauage needle, and rotated at 4 ºC for 30 min. Following removal of insoluble material by centrifugation at 20,000 × g for 5 min at 4 ºC, aliquots of clarified lysates were subjected to 8% SDS-PAGE and transferred to nitrocellulose membranes. Immunoblot analysis was carried out with 1 μg/ml monoclonal anti-T7 IgG (Novagen), 2 μg/ml monoclonal IgG-9E10, 0.4 μg/ml monoclonal IgG-P4D1 (Santa Cruz Biotechnology), or 2 μg/ml monoclonal IgG-3B2 (Seegmiller et al., 2002).

Immunoprecipitation

Following the treatments described in the figure legends, cells were harvested and lysed in PBS containing 0.2% or 1% digitonin plus 5 mM EDTA and 5 mM EGTA supplemented with protease inhibitors as described above. The clarified lysates were then subjected to immunoprecipitation with either 50 µl of monoclonal anti-T7 IgG-coupled agarose beads (Novagen) or 5 µg of polyclonal anti-Myc IgG plus 50 µl protein A/G-coupled agarose beads (Santa Cruz Biotechnology) as described previously (Sever et al., 2003b). Aliquots of the pellet or supernatant fractions of the immunoprecipitation were subjected SDS-PAGE and analyzed by western immunoblot analysis as described above.

Ubiquitination of HMG CoA reductase

Ubiquitination of hamster HMG CoA reductase in *Drosophila* S2 cells was assessed as previously described (Sever et al., 2003a). Briefly, S2 cells were harvested and lysed in PBS containing 1% NP-40, 1% deoxycholate, 5 mM EDTA, and 5 mM EGTA; the buffer was also supplemented with protease inhibitors and 10 mM N-ethyl maleimide. Clarified lysates were subjected to immunoprecipitation with anti-T7 IgG-coupled agarose beads as described above. Aliquots of the immunoprecipitates were subjected to SDS-PAGE, followed by immunoblot analysis was with 0.4 µg/ml monoclonal IgG-P4D1 (against ubiquitin) and 1 µg/ml monoclonal anti-T7 IgG (against reductase).

Ubiquitination of HMG CoA Reductase in vitro

SV-589 human fibroblast cells were maintained in medium D (Dulbecco's modified Eagle's medium containing 100 units/ml penicillin and 100 µg/ml streptomycin sulfate)

supplemented with 10% fetal calf serum at 37 ºC and 5% CO_2. Ubiquitination of endogenous HMG CoA reductase was carried out *in vitro* using permeabilized SV-589 cells as previously described (Song et al., 2005a). Briefly, cells were incubated with 0.025% (w/v) digitonin for 10 min, and the resulting permeabilized cells were resuspended in a permeabilization buffer containing protease inhibitors, MG-132, an ATP-regenerating system, FLAG-ubiquitin, ubiquitin-aldehyde, and rat liver cytosol. Sterols were added to reactions in ethanol at a final concentration of 1%. Reactions were carried out at 37 °C for 30 min. Subsequently, the cell pellets were lysed and subjected to immunoprecipitation with 30 μg of polyclonal IgG directed against the C-terminus of human HMG CoA reductase (Sato et al., 1993). Immunoblot analysis was carried out using 0.4 μg/ml monoclonal IgG-P4D1 (against ubiquitin) and 5 μg/ml monoclonal IgG-A9 (against reductase) (Liscum et al., 1983).

Production of dsRNA and RNAi-Mediated Knockdown in Drosophila S2 Cells

DNA templates used for synthesis of dsRNA were amplified by PCR with the Phusion DNA polymerase kit (New England Biolabs) using first strand cDNA obtained by RT-PCR of total RNA isolated from *Drosophila* S2 cells; sequences of the primers used in the amplifications are shown in Appendix E. The resulting PCR products (~700 bp) were purified with the QIAquick PCR Purification kit (Qiagen) and subsequently used to synthesize dsRNA with the MEGAscript T7 kit (Ambion); products of these reactions were purified using the RNeasy Mini kit (Qiagen). RNAi was performed as previously described with minor modifications (Clemens et al., 2000; Seegmiller et al., 2002). S2 cells were set up in 6-well plates on day 0 at a density of 1×10^6 cells per well in 1 ml of

medium B. Immediately after plating, each well received 15 µg of dsRNA and was incubated for 1 h. Subsequently, 2 ml of medium A containing 10% heat-inactivated fetal calf serum was added to each well. Cells were transfected on day 1 as described above and subsequently treated on day 3 as described in the figure legends.

Isolation of Total RNA and Quantitative Real-Time PCR Analysis

Total RNA was prepared from *Drosophila* S2 cells using the RNeasy kit (Qiagen) and used as a template for cDNA synthesis employing the Taqman Reverse Transcription Reagents (Applied Biosystems) and random hexamer primers. Quantitative real-time PCR was performed as previously described (Liang et al., 2002) using the primers listed in Appendix F. Relative expression was calculated using the comparative C_T method. *Drosophila* acetaldehyde dehydrogenase mRNA was used as an internal control for variations in amounts of mRNA.

RESULTS

Figure 2-1A shows an experiment designed to determine whether Insig is the minimal requirement for sterol-accelerated degradation of hamster reductase in *Drosophila* S2 cells. Considering our previous findings that establish the membrane domain of reductase necessary and sufficient for regulated degradation (Gil et al., 1985; Sever et al., 2003b; Skalnik et al., 1988), we transfected S2 cells with an expression plasmid encoding the entire membrane domain of hamster reductase (transmembrane helices 1-8), followed by three tandem copies of the T7 epitope. Expression is driven by the *Drosophila* actin 5c promoter and the plasmid is designated pAc-HMG-Red (TM1-8)-T7. Some of the dishes were also transfected with pAc-Insig-1-Myc or pAc-Insig-2-Myc, expression plasmids that encode amino acids 1-277 of human Insig-1 and 1-225 of human Insig-2, respectively. Following transfection, the cells were subjected to treatments in the absence or presence of the regulatory oxysterol 25-hydroxycholesterol plus mevalonate, which provides a source of nonsterol isoprenoids that combine with sterols to maximally accelerate degradation of reductase in mammalian cells (Correll and Edwards, 1994; Nakanishi et al., 1988; Roitelman and Simoni, 1992; Sever et al., 2003a). The cells were subsequently harvested and detergent lysates were prepared; aliquots of the resulting lysates were then subjected to SDS-PAGE and immunoblotted with anti-T7 and anti-Myc monoclonal antibodies to detect the membrane domain of reductase and Insigs, respectively. The results show that when pAc-HMG-Red (TM1-8)-T7 was transfected alone, the protein resisted degradation in the presence of 25-hydroxycholesterol plus mevalonate (*top panel*, *lanes 1-2*). Co-expression of pAc-Insig-

1-Myc or pAc-Insig-2-Myc (*bottom panel*, *lanes 3-6*) led to the disappearance of the membrane domain of hamster reductase, but only when the cells were treated with 25-hydroxycholesterol plus mevalonate (*top panel*, *lanes 3-6*). We transfected parallel sets of dishes with an expression plasmid encoding the membrane domain of *Drosophila* reductase. This protein failed to become degraded in the presence of 25-hydroxycholesteorl plus mevalonate (*top panel*, *lanes 7-12*), regardless of co-expression of either Insig-1-Myc or Insig-2-Myc (*bottom panel*, *lanes 9-12*). The inability of 25-hydroxycholesterol to stimulate rapid of the membrane domain of *Drosophila* reductase is consistent with previous observations that endogenous reductase in either *Drosophila* S2 or Kc cells does not become degraded in the presence of sterols (Brown et al., 1983; Gertler et al., 1988).

In the experiment of Figure 2-1B, we used co-immunoprecipitation to determine whether 25-hydroxycholesterol and mevalonate triggers binding of the membrane domain of hamster reductase to Insig, a key event in regulated degradation of the enzyme (Sever et al., 2003b). S2 cells transfected with pAc-HMG-Red (TM1-8)-T7 in the absence or presence of pAc-Insig-1-Myc were treated with MG-132 (to block degradation of reductase); some of the dishes were also received 25-hydroxycholesterol plus mevalonate. Following treatments, the cells were harvested and the overexpressed membrane domain of reductase was immunoprecipitated from detergent lysates with anti-T7-coupled agarose beads. Immunoblot analysis of the pellet and supernatant fractions revealed that immunoprecipitation of the membrane domain of reductase was essentially complete (*top two panels*, *lanes 1-4*). When co-expressed with the membrane domain of reductase, Insig-1-Myc appeared in the pellet fraction (*third panel*, *lane 3*) and this co-

immunoprecipitation was enhanced when the cells were treated with 25-hydroxycholesterol plus mevalonate (*lane 4*).

To directly address the requirement for nonsterol isoprenoids in sterol-regulated degradation of hamster reductase in S2 cells, we designed the experiment of Figure 2-1C in which 25-hydroxycholesterol and mevalonate were added to cells individually or in combination. As expected, the membrane domain of reductase was fully resistant to sterol-induced degradation in the absence of Insig-1-Myc co-expression (*top panel*, *lanes 1-4*). In the presence of Insig-1-Myc (*bottom panel*, *lanes 5-8*), neither 25-hydroxycholesterol nor mevalonate treatment alone stimulated degradation of the membrane domain of reductase (*top panel*, *lanes 5-7*). However, the protein became completely degraded when the cells were subjected to treatment with both 25-hydroxycholesterol and mevalonate (*lane 8*). Consistent with our previous findings in mammalian cells (Sever et al., 2003a), the mevalonate requirement for complete degradation of the membrane domain of reductase in S2 cells was satisfied by the addition of the 20-carbon nonsterol isoprenoid geranylgeraniol (Figure 2-1D, *top panel*, compare *lanes 1-2* with *lanes 5-6*).

The next set of experiments was designed to establish a role for the ubiquitin-proteasome pathway in sterol-accelerated degradation of the membrane domain of hamster reductase in S2 cells. In Figure 2-2A, we explored a role for the 26S proteasome in reductase degradation using the inhibitor MG-132. The results show that Insig-mediated, sterol-induced degradation of the membrane domain of reductase (*top panel*, compare *lanes 1-2* with *lanes 3-4*) was completely blocked when the cells were treated with MG-132 (compare *lanes 3-4* with *lanes 7-8*). It is notable that MG-132 also

stabilized Insig-1-Myc (*bottom panel*, compare *lanes 3-4* with *lanes 7-8*), indicating that the protein is subjected to rapid, proteasome-mediated degradation in S2 cells as well as mammalian cells (Gong et al., 2006; Lee and Ye, 2004). To determine the ubiquitination status of the membrane domain of reductase, transfected S2 cells were subjected to MG-132 treatment in the absence or presence of 25-hydroxycholesterol plus mevalonate. Following treatments, the cells were harvested and the membrane domain of reductase was immunoprecipitated from detergent extracts with anti-T7-coupled agarose beads. Aliquots of the precipitated material were then subjected to SDS-PAGE, followed by immunoblot analysis with anti-ubiquitin IgG (Figure 2-2B). The results show that in the absence of Insig-1-Myc co-expression, the membrane domain of reductase did not become ubiquitinated in the presence of 25-hydroxycholesterol plus mevalonate (*top panel*, *lanes 1-2*). Co-expression of Insig-1-Myc led to the appearance of ubiquitinated forms of reductase, but only in 25-hydroxycholesterol plus mevalonate-treated cells (*lanes 3-4*). Evidence in mammalian cells indicates that two cytosolically exposed lysine residues (amino acids 89 and 248) adjacent to transmembrane helices 3 and 7 are sites of Insig-mediated, sterol-induced ubiquitination. To determine whether modification of these lysine residues is required for degradation of the membrane domain of hamster reductase in S2 cells, we generated a mutant version of pAc-HMG-Red (TM1-8)-T7 that harbors conservative substitutions of arginine for lysines 89 and 248. Figure 2-2C shows that the wild-type membrane domain of reductase (*top panel*, *lanes 3-4*), but not the lysine mutant of the protein (*lanes 7-8*) was subjected to Insig-mediated, sterol-induced degradation.

To further characterize degradation of hamster reductase in S2 cells, we next examined the specificity of the reaction. Previous studies from our group and others have established that in addition to 25-hydroxycholesterol, the cholesterol synthesis intermediate 24,25-dihydrolanosterol and the 1,1-bisphosphonate esters SR-12813 and Apomine trigger rapid degradation of reductase in mammalian cells (Berkhout et al., 1997; Berkhout et al., 1996; Roitelman et al., 2004; Sever et al., 2004; Song et al., 2005a; Ylitalo, 2000). Figure 2-3A shows that 25-hydroxycholesterol, 24,25-dihydrolanosterol, SR-12813, and Apomine stimulated rapid degradation of the membrane domain of reductase in transfected S2 cells (*top panel*, *lanes 2, 4, 5, and 6*, respectively). The inability of lanosterol to stimulate degradation of the membrane domain of reductase (*lane 3*) contrasts our previous results (Song et al., 2005a). To clarify this issue, we tested the ability of lanosterol to stimulate ubiquitination of reductase *in vitro* using permeabilized mammalian cells. As shown in Figure 2-4, lanosterol did not promote ubiquitination of reductase (*top panel*, compare *lane 1* with *lanes 3-5*). In contrast, treatment with 25-hydroxycholesterol and 24,25-dihydrolanosterol led to robust ubiquitination of reductase (compare *lane 1* with *lane 2* and *lanes 6-8*). This discrepancy is likely due to the contamination of 24,25-dihydrolanosterol in the preparations of lanosterol that were used in those previous studies. It should be noted that purity of lanosterol and 24,25-dihydrolanosterol used in the current experiment was confirmed by gas chromatography-mass spectrometry (GC-MS) (data not shown).

ER to Golgi transport of *Drosophila* SCAP/SREBP is not inhibited by 25-hydroxycholesterol, but rather by a lipid derived from palmitate and ethanolamine (Dobrosotskaya et al., 2002; Seegmiller et al., 2002). This observation prompted us to

next determine the effect of palmitate plus ethanolamine treatment on degradation of the membrane domain of hamster reductase in S2 cells (Figure 2-3B). Neither 25-hydroxycholesterol and mevalonate (*top panel*, *lane 2*) nor the combination of palmitate and ethanolamine (*lane 3*) stimulated degradation of the membrane domain of hamster reductase in the absence of Insig-1. As expected, co-expression of Insig-1-Myc led to 25-hydroxycholesterol plus mevalonate-induced degradation of reductase (*lane 5*), but palmitate and ethanolamine continued to have no effect on the reaction (*lane 6*). Importantly, the membrane domain of *Drosophila* reductase was not subject to accelerated degradation regardless of the absence or presence of Insig-1, 25-hydroxycholesterol and mevalonate, and palmitate plus ethanolamine (*lanes 7-12*). It should be noted that palmitate plus ethanolamine was active in inhibiting processing of *Drosophila* SREBP as revealed by immunoblotting extracts with anti-dSREBP antibody.

In mammalian cells, Insigs bridge reductase to the membrane-bound ubiquitin ligase gp78 when sterols accumulate (Goldstein et al., 2006; Song et al., 2005b). Faithful reconstitution of sterol-accelerated degradation of the membrane domain of reductase in S2 cells (see Figure 2-1) points to the existence of a *Drosophila* ubiquitin ligase that is capable of binding to human Insig-1 and initiating reductase ubiquitination. Database searches failed to identify a recognizable homolog of mammalian gp78 in the *Drosophila* genome. Instead, these searches revealed the existence of three membrane-bound ubiquitin ligases: dTrc8, dTeb4, and dHrd1. *Drosophila* Trc8 (dTrc8) has not been extensively studied, but the enzyme has been implicated as a tumor suppressor in mammalian cells (Brauweiler et al., 2007; Gemmill et al., 2002; Gemmill et al., 1998); substrates for mammalian Trc8 have yet to be identified. A recent study in the yeast *S.*

cerevisiae revealed that the Teb4 homolog (Doa10) and Hrd1 exist in distinct multiprotein complexes (Carvalho et al., 2006). The Doa10 ubiquitin ligase complex contains Doa10, the cytosolic ubiquitin conjugating enzyme Ubc7 and its membrane anchor Cue1, and the UBX domain-containing protein Ubx2, which aids in recruitment of an AAA-ATPase called cdc48. Hrd1 associates with a large complex that contains its cofactor Hrd3, Ubc7 and Cue1, the polytopic ER membrane protein Der1 and its recruitment factor Usa1, Ubx2/cdc48, and the Hsp70 chaperone Kar2 bound to the lectin Yos9. Mammalian Hrd1 likely exists in a similar multi-protein complex (Lilley and Ploegh, 2005; Schulze et al., 2005).

Figure 2-6A shows an experiment in which we used RNA interference (RNAi) to determine a possible role for dTrc8, dHrd1, and dTeb4 in sterol-induced degradation of the membrane domain of hamster reductase in S2 cells. In untreated cells and in those treated with a control dsRNA against an irrelevant mRNA (mouse Cyp7A1), the membrane domain of reductase became degraded in the presence of 25-hydroxycholesterol and mevalonate (*top panel*, *lanes 1-4*). The protein was similarly degraded in cells subjected to treatment with dsRNA against mRNAs for dTrc8 and dTeb4 (*lanes 5-6 and 9-10*); however, RNAi-mediated knockdown of dHrd1 completely blocked sterol-accelerated degradation of the membrane domain of reductase (*lanes 7-8*). It should be noted that quantitative real-time PCR analysis revealed that RNAi reduced expression of dTrc8, dHrd1, and dTeb4 by 75%, 76%, and 85%, respectively. The effects of dHrd1 knockdown on degradation of the membrane domain of reductase appear to be specific as indicated by the experiment of Figure 2-6B. Here, we compared the ability of wild-type and a mutant form of dHrd1 to restore degradation of reductase in dHrd

knockdown cells. The cDNA for dHrd1 predicts a 626 amino acid protein consisting of a hydrophobic N-terminal domain with six transmembrane helices and a cytosolic C-terminal domain that includes a RING-H2 motif. The mutant form of dHrd1 evaluated in Figure 2-5B harbors a substitution of Ser for Cys-327. The correponding Cys residue in yeast and human Hrd (Cys-399 and Cys-329, respectively) is a key zinc coordinating residue in the RING-H2 domain; mutation of this cysteine residue in yeast and human Hrd1 abolishes *in vitro* and *in vivo* ubiquitin ligase activity of the enyzmes (Bays et al., 2001; Bordallo and Wolf, 1999; Deak and Wolf, 2001; Kikkert et al., 2003). Consistent with the result of Figure 2-6A, knockdown of dHrd1 abolished sterol-induced degradation of the membrane domain of reductase (*top panel*, compare *lanes 1-2* with *lanes 3-4*). Sterol-accelerated degradation of the membrane domain of reductase was restored by the overexpression of wild-type, T7-tagged dHrd1 (*lanes 5-8*), but not the inactive C327S mutant (*lanes 9-12*). A role for dHrd1 in sterol-accelerated degradation of reductase is further supported by its co-immunoprecipitation with Insig-1 (Figure 2-6C, *top panel*, *lanes 6-7*). Insig-1 failed to co-immunoprecipitate with dTrc8 (*lanes 8-9*), which does not participate in degradation of reductase in S2 cells (see Figure 2-6A).

Although a C-terminal fragment of yeast Hrd1 that includes the RING-H2 motif catalyzes polyubiquitination of itself and other substrates *in vitro* (Bays et al., 2001; Bordallo et al., 1998; Hampton et al., 1996), the ubiquitin ligase function of the Hrd1 in cells requires the presence of Hrd3, which forms a 1:1 stoichiometric complex with the enzyme (Gardner et al., 2000). Considering the requirement of dHrd1 for sterol-accelerated degradation of the membrane domain of reductase in S2 cells, we next designed an experiment to determine whether the *Drosophila* homolog of Hrd3 (dSel1) is

required for the reaction. As shown in Figure 2-7A, the membrane domain of reductase was subject to Insig-mediated, sterol-accelerated degradation in control cells (*top panel*, *lanes 1-2*). RNAi-mediated knockdown of dSel1 abrogated this degradation (compare *lanes 1-2* with *lanes 3-4*); similar results were obtained in dHrd1-knockdown cells (*lanes 5-6*).

In the next set of experiments, we used RNAi to identify *Drosophila* homologs of other Hrd1 complex components that are required for the degradation of reductase in S2 cells. As expected, the membrane domain of reductase was subjected to sterol-induced degradation in cells treated with dsRNA against mouse Cyp7A1 or dTrc8 (Figure 2-7B, *top panels*, *lanes 1-4*), but not in cells treated with dsRNA against dHrd1 and dSel1 (*lanes 5-8*). Degradation of the membrane domain of reductase was also significantly blunted by RNAi-mediated knockdown of dHerp (*lanes 9-10*), dUbxd8 (*lanes 21-22*), and the VCP/p97 cofactors dNpl4 (*lanes 23-24*) and dUfd1 (*lanes 25-26*). Sterol-accelerated degradation of reductase continued in cells treated with dsRNA against the two *Drosophila* homologs of yeast Der1, dDerlin-1 and dDerlin-2/3 (*lanes 11-14*); a similar result was obtained when expression of both dDerlin-1 and dDerlin-2/3 were reduced by RNAi (Figure 2-7C, *top panel*, *lanes 11-14*). Figure 2-7D shows that knockdown of the ubiquitin-conjugating enzyme dUbc7 partially blocked regulated degradation of the membrane domain of reductase (*top panel*, *lane 9-10*); this partial effect is likely due to incomplete knockdown (53%) of dUbc7. Finally, knockdown of lectin-like dOs9 failed to inhibit sterol-induced degradation of the membrane domain of reductase in S2 cells (Figure 2-7E, *top panel*, *lanes 5-6*). A summary of the results from Figures 2-6 and 2-7 is shown in Table 2-1.

DISCUSSION

The current results establish that Insig is the minimal requirement for sterol-accelerated degradation of the membrane domain of hamster HMG CoA reductase in *Drosophila* S2 cells. This Insig-mediated degradation (see Figure 2-1A) precisely mirrors the reaction that occurs in mammalian cells. For example, the membrane domain of reductase binds to Insig-1 through a reaction that is stimulated by the oxysterol 25-hydroxycholesterol (Figure 2-1B); nonsterol isoprenoids derived from mevalonate combine with sterols to maximally stimulate reductase degradation (Figure 2-1, C and D); inhibition of proteasome activity blocks degradation of reductase, leading to the accumulation of ubiquitinated forms of the enzyme (Figure 2-2, A and B); and mutation of lysine residues required for ubiquitination of reductase blocks the enzyme's degradation in S2 cells (Figure 2-2C). Remarkably, the selectivity of reductase degradation is also preserved in the *Drosophila* system: the reaction is stimulated by not only 25-hydroxychoesterol, but also by the cholesterol synthesis intermediate 24,25-dihydrolanosterol and the 1,1-bisphosphonate esters SR-12813 and Apomine (Figure 2-3A). The action of 25-hydroxycholesterol in S2 cells can be explained by the important finding that the oxysterol directly binds to Insig, which allows the protein to bind to and modulate the activities of SCAP and reductase (Radhakrishnan et al., 2007). The mechanism through which 24,25-dihydrolanosterol, SR-12813, and Apomine accelerate degradation of reductase is unknown, but is likely distinct from that of 25-hydroxycholesterol. This is indicated by the inability of these compounds to bind Insig *in vitro* and inhibit SCAP-mediated processing of SREBPs (Radhakrishnan et al., 2007;

Sever et al., 2004; Song et al., 2005a) (unpublished observations). Considering that cholesterol binds directly to the membrane domain of SCAP and induces SCAP/Insig complex formation (Radhakrishnan et al., 2004), we reason the most likely mode of action for 24,25-dihydrolanosterol, SR-12813, and Apomine involves their direct binding to the membrane domain of reductase. This scenario is supported by the fact that *Drosophila* cells are cholesterol auxotrophs and would not be expected to express protein(s) that bind cholesterol synthesis intermediates. Moreover, our current results and those of others indicate that the *Drosophila* reductase is not subject to sterol-induced degradation (Figure 2-1A) (Brown et al., 1983; Gertler et al., 1988). It is noteworthy that palmitate and ethanolamine failed to stimulate reductase degradation in S2 cells (Figure 2-3B) even though these treatments were previously found to block ER to Golgi transport of mammalian SCAP/SREBP in *Drosophila* cells through an Insig-mediated mechanism (Dobrosotskaya et al., 2003). These results provide another example of differential, Insig-mediated regulation of SCAP and reductase, which likely reflects differences in the binding specificities of the membrane domains of the two proteins.

RNAi experiments reveal a key role for the *Drosophila* homolog of the yeast RING-H2 ubiquitin ligase Hrd1 in sterol-accelerated degradation of hamster reductase in S2 cells (Figure 2-6A). Hrd1 was first identified in genetic studies of regulated degradation of Hmg2p, one of two reductase isozymes in yeast (Hampton et al., 1996). High flux through the mevalonate pathway stimulates rapid degradation of Hmg2p, while diminished flux through the pathway stabilizes the enzyme (Hampton and Rine, 1994). The stability of the other isozyme, Hmg1p, is not regulated. Although the membrane domains of yeast Hmg2p and mammalian reductase are necessary and sufficient for

accelerated degradation (Gil et al., 1985; Hampton and Rine, 1994; Sever et al., 2003b; Skalnik et al., 1988), they bear limited sequence identity (<20% over 340 amino acids). This limited conservation may explain the observation that accelerated degradation of Hmg2p in yeast is stimulated by a nonsterol isoprenoid, whereas degradation of mammalian reductase requires sterols in addition to nonsterol isoprenoids (see Figure 2-1, C and D). It should be noted that the yeast Insig (called Nsg1p) appears to play a role opposite to that of its mammalian counterpart by stabilizing Hmg2p, even when nonsterol isoprenoids accumulate (Flury et al., 2005). Despite these differences, regulated ubiquitination and degradation of reductase is employed by yeast and mammals to control flux through the mevalonate pathway.

Together with its binding partner Hrd3, Hrd1 exists in a multiprotein complex (see Figure 2-5) that mediates ER-associated degradation of Hmg2p and a variety of misfolded ER lumenal and membrane proteins (Carvalho et al., 2006; Denic et al., 2007; Kostovaa et al., 2007). Recent evidence indicates that this ensemble of proteins coordinates the degradation of two classes of ERAD substrates: proteins with misfolded lumenal domains (ERAD-L substrates) and proteins with misfolded intramembrane domains (ERAD-M substrates). An emerging model for Hrd1-mediated degradation of glycosylated ERAD-L substrates involves their recognition by the chaperone Kar2, which in turn associates with the lumenal lectin Yos9 (Figure 2-5). These substrates are then presented to the Hrd1 complex for ubiquitination, retrotranslocation, and dislocation into the cytosol through a mechanism that is mediated by interactions between Yos9 and Hrd3. Translocation of lumenal substrates across the ER membrane has been proposed to be mediated by the polytopic Hrd1 complex component Der1 (Carvalho et al., 2006;

Taxis et al., 2003). Following this, the cytosolic AAA-ATPase cdc48 and its associated cofactors Npl4 and Ufd1 are required for dislocation of both lumenal and membrane-bound ERAD substrates into the cytosol; energy derived from ATP hydrolysis is likely used to drive this reaction. A similar model applies to Hrd1-mediated degradation of ERAD-L substrates in mammalian cells (Christianson et al., 2008; Lilley and Ploegh, 2004; Lilley and Ploegh, 2005; Ye et al., 2004).

The prevailing view for selection of ERAD-L substrates involves Kar2/Yos9-mediated sensing of structural features indicative of misfolding such as the presence of immature glycans or exposure of hydrophobic patches and reactive thiol groups that are normally sequestered from the hydrophilic environment. It is conceivable that selection of ERAD-M substrates involves intramembrane protein-protein interactions. Hmg2p is one of the few ERAD-M substrates that have been studied in detail and a "structural transition hypothesis" has been proposed in which Hmg2 adopts features of a misfolded protein when certain intermediates of mevalonate metabolism accumulate (Hampton, 2002). Binding of the apparently misfolded Hmg2 to Hrd1 requires the presence of Hrd3, which is consistent with a role for Hrd3 in degradation of ERAD-M as well as ERAD-L substrates. By analogy to the model for recognition/selection of ERAD-L substrates, it is reasonable to speculate the existence of molecular chaperones that recognize misfolded intramembrane regions and intermediary protein(s) that bridge Hmg2 and other ERAD-M substrates to the Hrd1 complex through Hrd3-mediated interactions.

Considering the current understanding of Hrd1-dependent ERAD in yeast, we used RNAi to examine a role for dHrd1 complex components in degradation of reductase in S2 cells (Figure 2-7). These studies reveal that Insig-mediated degradation of reductase

requires a subset of the dHrd1 complex including dSel1 (the *Drosophila* homolog of Hrd3), dHerp (Usa1p), dUbxd8 (Ubx2), dUbc7 (Ubc7), dNpl4, and dUfd1 (see Table 2-1 for summary). A role for dUbxd8, dNpl4, and dUfd1 in degradation of reductase in S2 cells is not surprising considering their well-established roles in the action of VCP/p97. Unfortunately, we could not directly address the role of VCP/p97 in the current studies owing to cellular toxicity of the protein's RNAi-mediated knockdown (data not shown).

The requirement of dHerp in degradation of reductase is somewhat surprising in light of previous observations (Carvalho et al., 2006; Denic et al., 2007). In these studies, degradation of ERAD-M substrates such as Hmg2p did not require Usa1p, the yeast equivalent of dHerp. Degradation of Hmg2p was also unaffected by the absence of Der1, for which Usa1p acts as an adaptor to the Hrd1 complex (Carvalho et al., 2006). The requirement of dHerp, but not the *Drosophila* Derlin proteins (dDerlin-1 and dDerlin-2/3) in the degradation of reductase in S2 cells (see Figure 7, B and C) indicates a role for dHerp that is distinct from recruitment of Derlins to the Hrd1 complex. This notion is consistent with the recent finding that mammalian Herp binds to a family of proteins called ubiquilins (Kim et al., 2008). Ubiquilins contain an N-terminal ubiquitin-like domain that binds to proteasomes and a C-terminal domain that recognizes polyubiquitin chains. The yeast equivalent of ubiquilins, Dsk2, is known to play a key role in ERAD by guiding substrates to the proteasome (Ko et al., 2004; Walters et al., 2004). Determining whether dHerp mediates reductase degradation in S2 cells through a mechanism involving *Drosophila* ubiquilin will be a goal of future studies.

It should be noted that while the membrane domain of reductase contains a single N-linked glycan, its degradation does not require the presence of dOs9 (Figure 2-7E).

This is consistent with the observation that a mutant form of reductase that cannot become N-glycosylated is subjected to Insig-mediated degradation in S2 cells (data not shown).

Based on the results of this study and those of Hrd3-mediated degradation of Hmg2p in yeast, we propose a working model for sterol-induced degradation of reductase in S2 cells that predicts Insigs nucleate a dSel1-reductase interaction. This interaction results in the transfer of the enzyme to the dHrd1 complex for ubiquitination and subsequent degradation. An important feature of this model is the proposed role of Insig as the intermediary protein that bridges the ERAD substrate (reductase) to the ubiquitin ligase complex. Thus, mammalian reductase should bind to dHrd1 in an Insig-dependent, sterol-induced fashion and the reductase-Insig complex should bind to dHrd1 through a dSel1-mediated mechanism. Although Insig-1 co-immunoprecipitates with dHrd1 in a specific manner (see Figure 2-6C), we have been unable to demonstrate this interaction requires the presence of dSel1 (data not shown). Moreover, attempts to demonstrate Insig-dependent binding of reductase to dHrd1 have been so far unsuccessful. A likely explanation may be provided by the observation that overexpression of Hrd1 restores degradation of ERAD substrates in yeast lacking Hrd3 (Bordallo and Wolf, 1999; Gardner et al., 2000), suggesting the ubiquitin ligase has an intrinsic affinity for these substrates that is enhanced by Hrd3. To guard against potential artifacts generated by overexpression of dHrd1 and dSel1, future co-immunoprecipitation studies will employ antibodies against the endogenous proteins to define interactions between reductase, Insigs, dSel1, and dHrd1.

In conclusion, the ability to reconstitute sterol-accelerated degradation of the membrane domain of hamster reductase in S2 cells provides a new tool to delineate the molecular mechanisms of the reaction. A thorough understanding of how Insigs mediate selection and delivery of mammalian reductase to the multiprotein dHrd1 complex in S2 cells should provide important insights into how Insigs arbitrate gp78-mediated ubiquitination and degradation of reductase in mammalian cells. Moreover, information gleaned from understanding of the molecular interactions between dSel1 and Insig that result in selection of reductase as an ERAD-M substrate will likely be applicable to the selection of similar types of substrates in both yeast and mammalian systems.

FIGURES

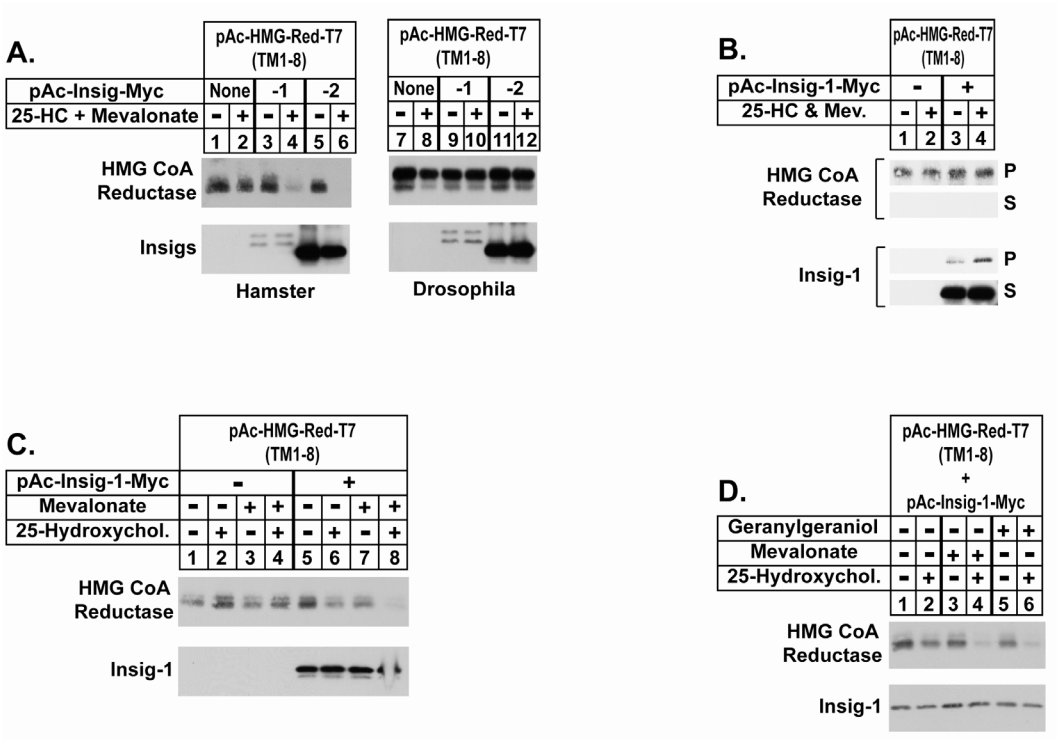

Figure 2-1. Insig-mediated, sterol-accelerated degradation of the membrane domain of mammalian HMG CoA reductase in *Drosophila* S2 cells. *A-D*, S2 cells were set up on day 0 at 1×10^6 cells per well of 6-well plates in medium A supplemented with 10% heat-inactivated fetal calf serum. Several hours later, cells were washed with PBS and transfected in medium B with 1.8 μg hamster pAc-HMG-Red (TM1-8)-T7, 50 ng *Drosophila* pAc-HMG-Red (TM1-8)-T7, and 0.2 μg pAc-Insig-1-Myc or pAc-Insig-2-Myc as indicated using Cellfectin reagent. The total amount of DNA was adjusted to 2 μg/well by the addition of empty vector. On day 1, cells were switched to medium C supplemented with 10% heat-inactivated lipoprotein-deficient serum. On day 3, cells were treated with the identical medium in the absence (-) or presence (+) of 2.5 μM 25-hydroxycholesterol plus 10 mM mevalonate (*A*, *B*); in *C* and *D*, cells were treated with various combinations of 2.5 μM 25-hydroxycholesterol, 10 mM mevalonate, and 30 μM geranylgeraniol. In *B*, the proteasome inhibitor MG-132 was also present at a concentration of 10 μM. *A*, *C*, and *D,* following incubation for 6 h, the cells were harvested and detergent lysates were prepared as described in the Experimental Methods section. Aliquots of the lysates (40 μg protein/lane for reductase and 10 μg protein/lane for Insig) were fractionated by 8% SDS-PAGE and transferred to nitrocellulose membranes. Immunoblot analysis was carried out with 1 μg/ml anti-T7 IgG (against reductase) and 2 μg/ml IgG-9E10 (against Insig). *B*, following incubation for 2 h, the

cells were harvested, lysed in PBS containing 1% digitonin, and immunoprecipitation was carried out with anti-T7 IgG-coupled agarose beads as described in the Experimental Methods section. Aliquots of the pellet and supernatant fractions were subjected to SDS-PAGE and immunoblot analysis was performed as described above.

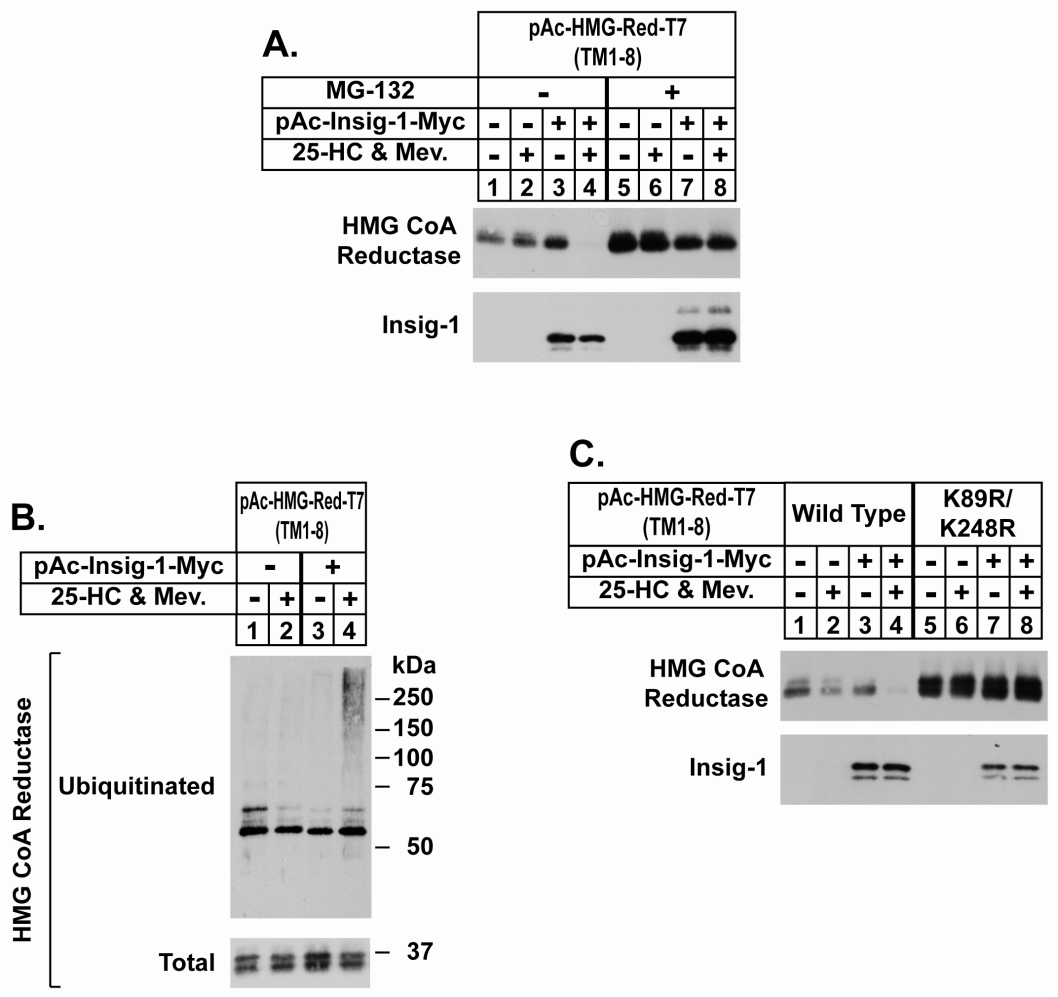

Figure 2-2. Sterols stimulate Insig-dependent ubiquitination and degradation of the membrane domain of mammalian HMG CoA reductase in *Drosophila* S2 cells. *A-C*, S2 cells were set up and transfected on day 0 and refed on day 1 as described in the legend of Figure 2-1. On day 3, the cells were treated with medium C supplemented with 10% heat-inactivated lipoprotein-deficient serum in the absence of presence of 2.5 μM 25-hydroxycholesterol and 10 mM mevalonate. Some cells also received 10 μM MG-132 (*A*, lanes 5-8). *A* and *C,* following incubation for 6 h, the cells were harvested; detergent lysates were prepared and immunoblot analysis was carried out as described in the legend of Figure 1. *B*, following incubation for 2 h, the cells were lysed in PBS containing 1% NP-40, 1% deoxycholate, and 10 mM N-ethyl maleimide, and transfected reductase was immunoprecipitated with anti-T7-coupled agarose beads as described in the Experimental Methods section. Aliquots of the immunoprecipitated material were subjected to SDS-PAGE followed by immunoblot analysis with 1 μg/ml anti-T7 IgG (against reductase) and 0.4 μg/ml IgG-P4D1 (against ubiquitin).

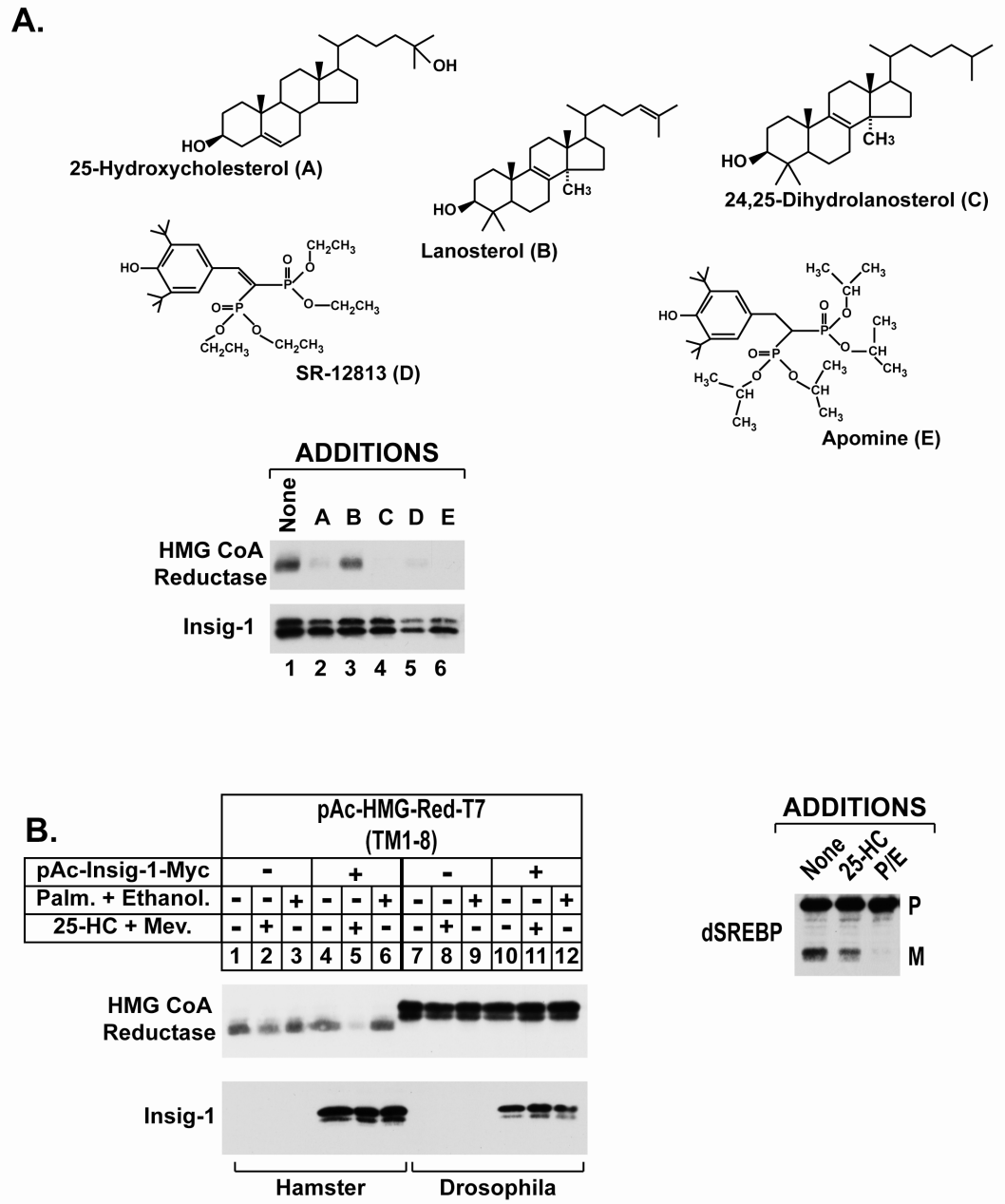

Figure 2-3. Specificity of Insig-mediated degradation of the membrane domain of mammalian HMG CoA reductase in *Drosophila* S2 cells. *A* and *B,* S2 cells were set up and transfected on day 0 and treated on day 1 as described in the legend of Figure 2-1. *A*, cells were treated on day 3 for 6 h with medium C containing 10% heat-inactivated lipoprotein-deficient serum and 10 mM mevalonate in the absence or presence of 2.5 μM 25-hydroxycholesterol, 25 μM lanosterol, 25 μM 24,25-dihydrolanosterol, 30 μM SR-

12813, or 10 μM Apomine. In *B*, the cells were treated for 6 h with medium C containing 10% heat-inactivated lipoprotein-deficient serum in the absence or presence of 2.5 μM 25-hydroxycholesterol plus 10 mM mevalonate or 100 μM palmitate plus 100 μM ethanolamine. At the end of the incubations, cells were harvested; detergent lysates were prepared and subjected to immunoblot analysis as described in the legend of Figure 2-1. Proteolytic processing of dSREBP was assessed by immunoblot analysis using 2 μg/ml IgG-3B2. P denotes the precursor form and M denotes the mature nuclear form.

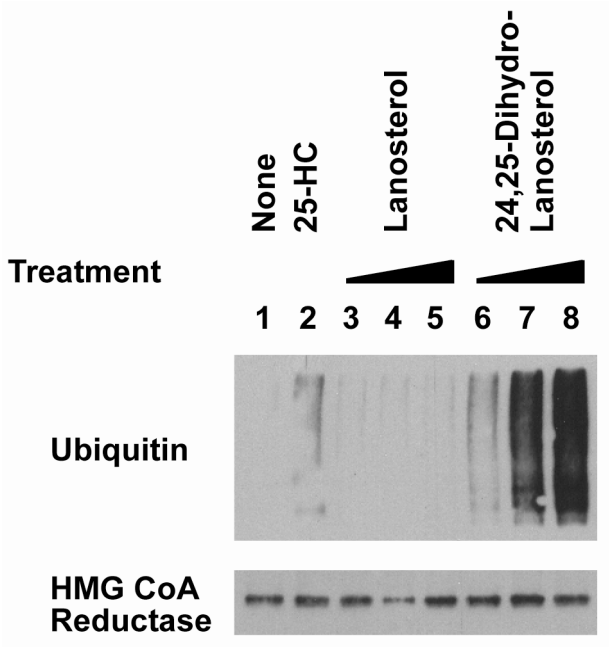

Figure 2-4. 24,25-Dihydrolanosterol, and not lanosterol, stimulates ubiquitination of HMG CoA reductase *in vitro*. Human SV-589 fibroblast cells were set up on day 0 at a density of 2×10^5 cells per 100-mm dish in medium D supplemented with 10% fetal calf serum. On day 2, the cells were switched to medium D supplemented with 10% lipoprotein-deficient serum, 50 μM compactin, and 50 μM mevalonate. On day 3, cells were harvested and permeabilized with 0.025% digitonin. Ubiquitination reactions were carried out for 30 min at 37 °C as described in the Experimental Methods section. 25-Hydroxycholesterol was added at a final concentration of 25 μg/ml; lanosterol and 24,25-dihydrolanosterol were added at concentrations of 6.25, 25, and 62.5 μM. Subsequently, the cell pellets were lysed and subjected to immunoprecipitation with 30 μg of polyclonal anti-HMG CoA reductase IgG. Immunoblot analysis was carried out using 0.4 μg/ml IgG-P4D1 (against ubiquitin) and 5 μg/ml IgG-A9 (against reductase).

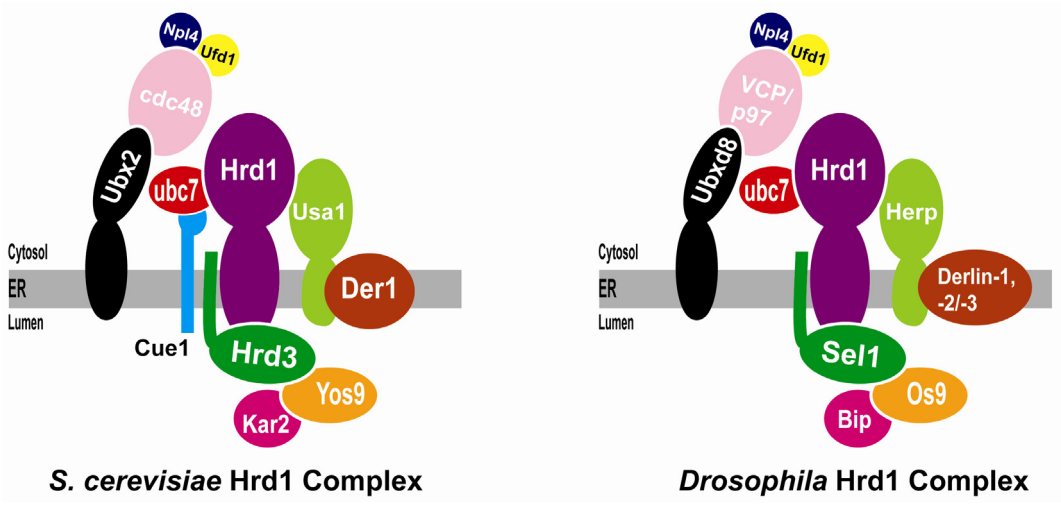

Figure 2-5. The *S. cerevisiae* and *Drosophila* Hrd1 ubiquitin ligase complexes. Schematic representation of the Hrd1 complexes including the lumenal factors Kar2 and Yos9 that, together with Hrd3, function in the initial steps of substrate recognition and recruitment.

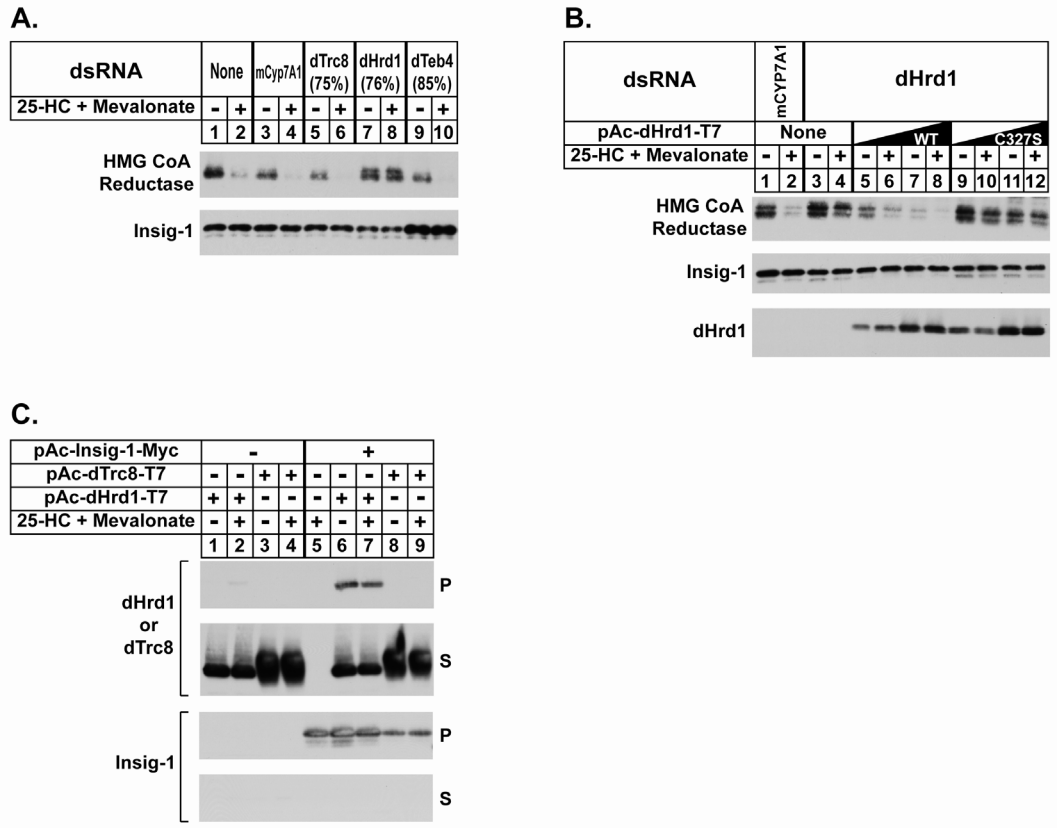

Figure 2-6. *Drosophila* Hrd1 (dHrd1) is the ubiquitin ligase required for sterol-accelerated degradation of the membrane domain of mammalian HMG CoA reductase in *Drosophila* S2 cells. *A* and *B*, S2 cells were set up on day 0 at 1×10^6 cells per well of 6-well plates in 1 ml medium B. Immediately after plating, the cells were incubated for 1 h with 15 μg of dsRNA targeted against the indicated endogenous mRNAs. Following this incubation, each well received 2 ml of medium A supplemented with 10% heat-inactivated fetal calf serum. On day 1, the cells were washed with PBS and transfected with Cellfectin reagent in medium B as follows: *A*, 1.8 μg pAc-HMG-Red (TM1-8)-T7 and 0.2 μg pAc-Insig-1-Myc per well and *B*, 1.8 μg pAc-HMG-Red (TM1-8)-T7, 0.2 μg pAc-Insig-1-Myc, and 0.3 μg or 1 μg pAc-dHrd1-T7 per well (total amount of DNA was adjusted to 3 mg/well by addition of empty vector). On day 2, the cells were switched to medium C supplemented with 10% heat-inactivated lipoprotein-deficient serum and subsequently treated for 6 h on day 3 with the identical medium in the absence or presence of 2.5 μM 25-hydroxycholesterol and 10 mM mevalonate. Following this incubation, cells were harvested; detergent lysates were prepared and subjected to immunoblot analysis as described in the legend of Figure 2-1. The efficiency of RNAi-mediated knockdown was determined in parallel wells by quantitative real-time PCR analysis and the extent of knockdown of the indicated mRNA relative to that in control-treated cells is indicated in parentheses. *C*, S2 cells were set up on day 0 in 6-

well plates and transfected with 1 μg pAc-Insig-1-Myc and 0.5 μg pAc-dHrd1-T7 or 0.5 μg pAc-dTrc8-T7 per well in medium B; the cells were subsequently treated on day 1 as described in the legend to Figure 2-1. On day 3, the cells were refed medium C supplemented with 10% heat-inactivated lipoprotein-deficient serum without or with 2.5 μM 25-hydroxycholesterol plus 10 mM mevalonate. After 2 h, cells were harvested and lysed in PBS containing 0.2% digitonin. Immunoprecipitation was carried out using anti-myc IgG and protein A/G-coupled agarose beads. Aliquots of the resulting pellet (P) and supernatant (S) fractions of the immunoprecipitation were subjected to immunoblot analysis with 1 μg/ml anti-T7 IgG (against dHrd1 or dTrc8) and 2 μg/ml IgG-9E10 (against Insig).

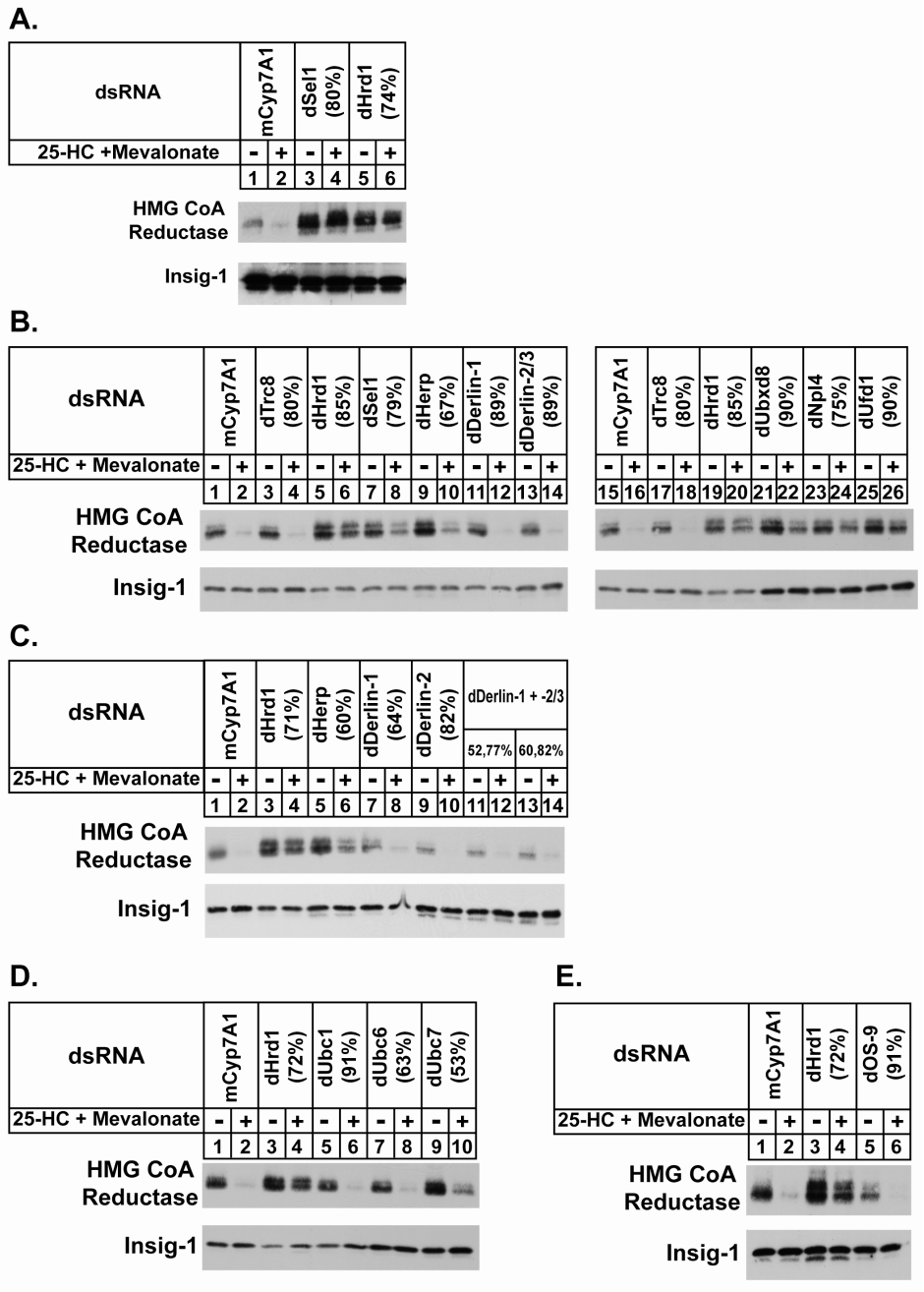

Figure 2-7. Requirement of dHrd1 complex components for sterol-induced degradation of the membrane domain of mammalian HMG CoA reductase in *Drosophila* S2 cells. *A-E*, S2 cells were set up, transfected, and subjected to RNAi-mediated knockdown as described in the legend of Figure 2-6A. The efficiency of RNAi-mediated knockdown for each mRNA is indicated in parentheses.

TABLES

Table 2-1. Role of dHrd1 complex components in sterol-accelerated degradation of mammalian HMG CoA reductase in *Drosophila* S2 cells.

S. cerevisiae	**Mammalian cells**	**Required for degradation of HMG CoA Reductase in *Drosophila* S2 cells**
Hrd1	Hrd1	Yes
Hrd3	Sel1 or Sel1L	Yes
Usa1	Herp	Yes
Yos9	Os9	No
Kar2	Bip	Not Determined
cdc48	VCP/p97	Not Determined (Cell Toxicity)
Ubx2	Ubxd8	Yes
Npl4	Npl4	Yes
Ufd1	Ufd1	Yes
Ubc7	Ubc7	Yes
Der1	Derlin-1, -2, and -3	No
Cue1	None	-

CHAPTER THREE

CONCLUSIONS AND PERSPECTIVES

Physiological Relevance of Oxygen-Mediated Regulation of Cholesterol Synthesis

Although cultured cells are routinely maintained at atmospheric oxygen levels (21% O_2, 160 mm Hg), cells within the body are exposed to considerably lower oxygen levels. The oxygen tension that a given cell encounters is determined by a number of factors including the oxygen tension of the blood, the perfusion rate, the distance from the capillary, and the rate of oxygen consumption by neighboring cells (Tsai et al., 2003). Under physiological conditions, the oxygen tensions of arterial and venous blood are approximately 100 mm Hg and 40 mm Hg, respectively (Boron and Boulpaep, 2003). Oxygen levels are markedly lower in the liver because it is oxygenated by the portal circulation. The structure of the portal triad gives rise to an oxygen gradient with higher oxygen concentrations in the periportal zone and lower concentrations in the perivenous zone. The intracellular oxygen tensions of cells in these zones has been estimated to be 45-50 mm Hg and 15-20 mm Hg, respectively (Jungermann and Kietzmann, 2000). Recent studies using transgenic mice expressing an oxygen-regulated fusion protein has provided evidence that HIF is active in certain tissues under normal oxygen conditions (Safran et al., 2006). The oxygen dependent degradation (ODD) domain of HIF-1α (amino acids 530-652) contains the minimal requirements for degradation in the presence of oxygen. These authors used a fusion protein containing the ODD domain linked to firefly luciferase as a probe to measure HIF activity *in vivo*. In mice breathing atmospheric air, luminescence was observed in the kidneys. Moreover, with

pharmacological inhibition of HIF degradation, luminescence was also observed in the liver. These and other studies suggest that HIF is active in certain tissues under physiological conditions. Moreover, HIF is known to be activated in a number of pathological situations including sleep apnea, ischemic states, and genetic conditions such as von Hippel-Lindau disease (Kaelin, 2007). Therefore, hypoxia- and HIF-mediated pathways are physiologically relevant under a variety of settings.

A number of small population studies have found relationships between high altitude and plasma cholesterol levels. In Venezuela and Kyrgyzstan, populations living at a higher altitudes were found to have significantly lower levels of total cholesterol, compared to groups living nearby at lower altitudes (Aitbaev, 1985; de Mendoza et al., 1979). Moreover, in several studies examining cardiovascular disease, populations living at higher altitudes have been reported to have lower mortality rates (Ashouri et al., 1994; Mortimer et al., 1977). However, it should be noted that these studies are difficult to control and one of these studies was very controversial (Mortimer et al., 1977). There are also several reports of decreased total cholesterol levels in people following migration to higher altitudes (Aitbaev et al., 1990; Ferezou et al., 1988). These studies are consistent with our cell-based observations that cholesterol production is inhibited when oxygen availability is reduced.

In the current studies, we are unable to assess the rate of degradation of reductase in the mouse liver. Reductase is subjected to feedback regulation through multiple mechanisms, including at the levels of transcription, translation of reductase mRNA, and protein degradation (Brown and Goldstein, 1980). In cultured cells, we are able to study reductase degradation in isolation by inhibiting the other mechanisms. However, this is

not possible at the level of the whole animal. Addressing the role of reductase degradation *in vivo* will require the generation of a transgenic mouse which constitutively expresses the N-terminal membrane domain of reductase. Previous studies have shown that fusion proteins containing the membrane domain of reductase linked to either β-galactosidase (Chun and Simoni, 1992) or luciferase (unpublished observation) are subject to sterol-induced degradation. Therefore, it should be possible to monitor degradation of a reductase-luciferase fusion protein in real-time by bioluminescent imaging. The stability of this fusion protein can be examined noninvasively following a variety of treatments including cholesterol feeding, administration of 24,25-dihydrolanosterol, and exposure to hypoxia. These experiments are necessary to establish a role for sterol-accelerated degradation of reductase *in vivo*.

Dysregulation of Cholesterol Homeostasis in Renal Clear Cell Carcinoma

Inactivating mutations of the *VHL* tumor suppressor gene leads to development of a variety of neoplasias including renal cell carcinoma (RCC), hemangioblastomas, and pheochromocytomas (Kaelin, 2004). Mutations in the *VHL* gene have been found in >50% of sporadic cases of RCC; moreover, silencing of *VHL* due to hypermethylation has been found in an additional 19% of cases (Herman et al., 1994). Under these settings, HIF is hyperactivated as HIF-α subunits are no longer subject to rapid degradation.

Interestingly, lipid accumulation is one of the hallmark features of RCC (Gonzalez et al., 1981). In tumor samples obtained from patients with RCC, levels of total and esterified cholesterol were elevated by 8- and 35-fold, respectively, compared to levels in normal kidneys (Gebhard et al., 1987). Studies using two different *in vivo*

models of RCC found that the rate of cholesterol synthesis was 5-fold higher in tumors compared to normal kidneys (Clayman et al., 1986a; Clayman et al., 1986b). Paradoxically, mRNA levels of reductase and LDL receptor, which are both SREBP target genes, have been reported to be significantly decreased in RCC samples from patients (Rudling and Collins, 1996). Consistent with the gene expression data, reductase enzymatic activity levels are reduced in tumor samples (Gebhard et al., 1987). These observations raise the question of how RCC cells are able to escape feedback regulatory mechanisms to maintain high rates of cholesterol synthesis while accumulating large amounts of cholesterol.

Mechanisms of Oxygen-Sensing in Sterol Biosynthetic Pathways

In our studies, we find that mammalian cells adapt to hypoxia by stimulating rapid degradation of HMG CoA reductase, which is a rate-determining enzyme in the cholesterol biosynthetic pathway. Two signals trigger this degradation: 1) accumulation the cholesterol precursor 24,25-dihydrolanosterol and 2) HIF-mediated induction of Insig-2, which confers cells with enhanced sensitivity to sterol-induced degradation of reductase. Together, these signals lead to accelerated degradation of reductase, and consequently cholesterol production is markedly decreased (Figure 1-16). Recent work in the fission yeast *S. pombe* found that Sre1 and Scp1, orthologs of mammalian SREBP and SCAP, respectively, function together in a mechanism that uses sterol synthesis as a measure of oxygen availability (Hughes et al., 2005). Hypoxia inhibits production of the fungal sterol ergosterol, which in turn leads to Scp1-dependent proteolytic activation of Sre1. These activated forms of Sre1 migrate to the nucleus and activate transcription of

genes encoding for enzymes that catalyze oxygen-dependent steps in ergosterol production in order to maintain sterol homeostasis. Additional Sre1 target genes include those that encode for oxygen-requiring enzymes involved in heme, sphingolipid, and ubiquinone synthesis (Todd et al., 2006). Importantly, Sre1 is a principal activator of anaerobic gene expression and is required for proper adaptation of *S. pombe* to low oxygen conditions (Hughes et al., 2005; Todd et al., 2006).

Despite these differences, it is intriguing nonetheless that mechanisms exist in both yeast and mammalian cells to incorporate oxygen availability into the regulation of sterol biosynthesis. In an analogous way, yeast and mammalian cells have distinct mechanisms for optimizing mitochondrial respiration under different oxygen conditions. When mammalian cells encounter hypoxic conditions, HIF activates transcription of genes encoding for the cytochrome *c* oxidase (COX)4-2 subunit and the mitochondrial protease LON (Fukuda et al., 2007). LON, in turn, increases the rate of degradation of the COX4-1 subunit. This switching of COX4 subunits results in more efficient respiration under low oxygen conditions. Yeast cells also respond to hypoxia by altering the composition of COX subunits; however, the mechanism is different than that of mammalian cells. In yeast, the regulation is entirely at the transcriptional level. At high oxygen concentrations, the COX5a subunit is expressed and COX5b subunit is repressed; conversely, at low oxygen concentrations, the COX5b subunit is expressed and the COX5a subunit is repressed (Forsburg and Guarente, 1989; Lowry and Zitomer, 1984). The presence of hypoxia-responsive regulatory mechanisms in both yeast and mammalian cells suggests that these adaptive changes in sterol biosynthesis and

mitochondrial respiration are critical for cell function and survival under low oxygen conditions.

Sterol Specificity of Insig-Mediated Accelerated Degradation of HMG CoA Reductase

After reconstituting the process of sterol-induced, Insig-dependent degradation of the membrane domain of mammalian reductase in *Drosophila* S2 cells (Figures 2-1 and 2-2), we applied this system to test sterol specificity in the context of reductase degradation. As with other insects, *Drosophila* S2 cells are cholesterol auxotrophs (Clayton, 1964). This inability to synthesize cholesterol *de novo* is attributable to multiple blocks in the cholesterol biosynthetic pathway (Clark and Block, 1959). In agreement with this, bioinformatics searches of the *Drosophila* genome failed to identify homologs of the mammalian genes encoding for the following enzymes: squalene synthase, squalene epoxidase, lanosterol synthase, lanosterol 14α-demethylase, lathosterol oxidase, 7-dehydrocholesterol reductase, and 24-dehydrocholesterol reductase. As such, this provides a clean system for testing sterol specificity; exogenously added sterols cannot be metabolized into other species, which is a concern in studies employing mammalian cells. Importantly, *Drosophila* S2 cells lack 24-dehydrocholesterol reductase, which is the enzyme that converts lanosterol to 24,25-dihydrolanosterol, thereby allowing us to separate the activities of these two sterols in promoting reductase degradation. These studies revealed that 24,25-dihydrolanosterol, but not lanosterol, stimulates degradation of reductase (Figures 2-3 and 2-4). We believe that earlier studies implicating a role for lanosterol in the ubiquitination and degradation of reductase were confounded by the

presence of significant amounts of contaminating 24,25-dihydrolanosterol in the batches of commercially available lanosterol that were used (data not shown).

The results of these studies in *Drosophila* S2 cells suggest that 24,25-dihydrolanosterol binds to the membrane domain of reductase. In this reconstituted system, only two mammalian proteins are co-expressed: the membrane domain of hamster reductase and human Insig. Sterol binding studies have shown that 24,25-dihydrolanosterol cannot compete for binding of [^{3}H]25-hydroxycholesterol to Insig (Radhakrishnan et al., 2007), indicating that 24,25-dihydrolanosterol does not bind to Insig. Moreover, since *Drosophila* S2 cells cannot synthesize cholesterol, it is unlikely that they express a protein that specifically binds 24,25-dihydrolanosterol and is able to confer regulated degradation to the membrane domain of reductase. Taken together, the results of these studies strongly support the idea that 24,25-dihydrolanosterol directly binds to the membrane domain of reductase.

We have recently obtained [^{3}H]24,25-dihydrolanosterol, which was previously not available. With this reagent, we can test for binding of 24,25-dihydrolanosterol to purified reductase *in vitro*. Infante at al. have recently performed similar binding assays using a recombinant form of the membrane protein Niemann-Pick, Type C1 (NPC1) purified from transiently transfected mammalian cells (Infante et al., 2008). Importantly, purifying NPC1 from mammalian cells allowed for the use of a variety of detergents. In an earlier purification of the membrane domain of SCAP from insect cells, only detergents from the Fos-Choline class were able to appreciably solubilize the recombinant protein from the pelleted membrane fraction (Radhakrishnan et al., 2004). This presents a major limitation because Fos-Choline detergents are harsh and could

potentially disrupt sterol binding. Based on these studies, we plan to purify the membrane domain of reductase from transfected mammalian cells and test for [^{3}H]24,25-dihydrolanosterol *in vitro*.

Recognition of HMG CoA Reductase as an ERAD Substrate

Although many of the molecular events involved in the sterol-induced degradation of reductase are now understood, a fundamental question that remains is how sterols cause reductase to be recognized as an ERAD substrate. Consistent with previous results from mammalian cells, our current studies in *Drosophila* S2 cells support a model in which sterols trigger the binding of the membrane of reductase to Insig, which in turn is associated with an E3 ligase. This reductase/Insig interaction initiates the ubiquitination of reductase by bringing the E3 ligase into proximity with the membrane domain of reductase. In this scenario, Insig serves the role of a substrate selector for the ERAD of reductase. If this is the case, then are there other ERAD substrates that require Insig for recognition?

Alternatively, in a simplistic model, sterols may induce a conformational change in the membrane domain of reductase in such a way that lysine 89 and lysine 248 become exposed. The topology model of reductase predicts that these two lysine residues are located in short cytosolic loops that are adjacent to transmembrane helices 3 and 7. Importantly, the lysine residues are situated at the border of the cytosol and the ER membrane. As such, it is possible that in the absence of sterols the lysine residues are buried, to some degree, within the ER membrane. In contrast, in the presence of sterols, the membrane domain of reductase may undergo a conformational change that causes

these lysine residues to shift away from the membrane to a more cytosolic position such that the lysine residues are assessable to the E3 ligase.

Such a sterol-induced conformational change has not been observed thus far for reductase. However, Adams et al. have shown that cholesterol binding to SCAP causes a conformational change in SCAP that can be detected by trypsin cleavage assays (Adams et al., 2003). A similar approach may be undertaken to determine if the conformation of reductase also changes in the presence of sterols. Importantly, 24,25-dihydrolanosterol should be used to stimulate this process. Another way to test this idea is to generate mutant forms of reductase in which lysine residues 89 and 248 are moved either towards the cytosol or towards the membrane. Moreover, additional lysine residues can be inserted into the cytosolic loops adjacent to lysines 89 and 248. The hypothesis predicts that these exposed lysine residues will cause the mutant protein to rapidly degrade in a sterol-independent manner. If this hypothesis is correct, then what is the role of Insig in this process? Answering these basic questions may lead to a better understanding of not only how reductase is recognized, but perhaps also how other substrates that undergo regulated ERAD are recognized and targeted for degradation.

Using the Membrane Domain of HMG CoA Reductase as a Model Substrate to Study ERAD

Degradation of a T-cell receptor subunit in a "non-lysosomal, pre-Golgi compartment" was first reported in 1988 (Lippincott-Schwartz et al., 1988). These early studies led to the creation of new field, which was termed ERAD ~13 years ago. Early characterization of this system was carried out largely in yeast. Much of this work is applicable to humans

because the pathway is highly conserved. For example, the yeast and human ubiquitin molecules differ in only two of their 76 amino acids; moreover, the *Drosophila* and human proteins are identical. Despite rapid growth of the field, many fundamental questions still remain to be answered. For example, how are ERAD substrates recognized? And how are integral membrane substrates dislocated from the ER membrane into the cytosol where they are assessable to proteasomes?

We plan to use the *Drosophila* cell system to carry out genetic and biochemical studies to address these and other outstanding questions about ERAD. For the genetic studies, this system offers several key advantages. RNAi is simple and effective in the S2 cells. Large dsRNAs can be synthesized by *in vitro* transcription and directly added to the culture medium; cells take up these dsRNAs through scavenger receptors and process them into active small interfering RNAs (siRNAs). Therefore, unlike with mammalian cells, no transfection reagents are required to perform RNAi in *Drosophila* cells. Additionally, the *Drosophila* genome is less redundant compared to mammalian genomes. This is likely to, at least in part, explain the robust effects on reductase degradation that we see in RNAi-treated cells. Another advantage of this system is that it is regulated; we can add sterols and observe rapid degradation of reductase. Our initial characterization of the system has confirmed much of the previous work done on yeast. At the same time, these studies validate our system as an approach to study ERAD. Based on this, we plan to perform a genome-wide RNAi screen to identify novel proteins involved in the ERAD process.

APPENDIX A

Primers Used for Real-Time PCR Analysis for Mammalian Cells

Gene	**Species**	**Primers** (Forward and Reverse)
β-Actin (control)	Hamster	GGCTCCCAGCACCATGAA GCCACCGATCCACACAGAGT
HMG CoA Reductase	Hamster	CAATTCTGGGCCCCACATT CCCTGACATGGTGCCAACTC
HMG CoA Synthase	Hamster	CCTGGGTCACTTCCTTTGAATG GATCTCAAGGGCAACGATTCC
Insig-1	Hamster	GGCTTGTGGTGGACATTCG GGCGATGGTGATCCCAAGT
Insig-2	Hamster	GGGTGGTGCTCTTCTTCATTG CAGGTGGAAAAAGTGTCACGTTT
SCAP	Hamster	GTACCTGCAGATGATGTCCATTG CTGCCATCCCGGAAAGTG
VEGF	Hamster	AGCGGAGAAAGCATTTGTTTG CCAAGATCCGCAGACGTGTAAATGTTCC
36B4 (control)	Human	TGCATCAGTACCCCATTCTATCA AAGGTGTAATCCGTCTCCACAGA
GAPDH	Human	GCCCCAGCGTCAAAGGT GGCATCCTGGGCTACACTGA
HMG CoA Reductase	Human	CAAGGAGCATGCAAAGATAATCC GCCATTACGGTCCCACACA
Insig-1	Human	CCCAGATTTCCTCTATATTCGTTCTT CACCCATAGCTAACTGTCGTCCTA
Insig-2	Human	TGTCTCTCACACTGGCTGCACTA CTCCAAGGCCAAAACCACTTC
SCAP	Human	GGGTCAGCCATGTGTTTGC TGCTGCGGTCCCAGATG
36B4 (control for cells)	Mouse	CACTGGTCTAGGACCCGAGAAG GGTGCCTCTGGAGATTTTCG
Cyclophilin B (control for mice)	Mouse	TGGAGAGCACCAAGACAGACA TGCCGGAGTCGACAATGAT
Aldolase A	Mouse	TCCCTTCCCCCAAGTTATCAA GGCACCACACCCTTATCTACCT

GLUT1	Mouse	GGTGTGCAGCAGCCTGTGTA CAACAAACAGCGACACCACAGT
Insig-1	Mouse	TCACAGTGACTGAGCTTCAGCA TCATCTTCATCACACCCAGGAC
Insig-2	Mouse	CGGAAGATGCTGGAACCTGA TGTGCTCTCCATACGCTCTCC
Insig-2a	Mouse	CCCTCAATGAATGTACTGAAGGATT TGTGAAGTGAAGCAGACCAATGT
Insig-2b	Mouse	CCGGGCAGAGCTCAGGAT GAAGCAGACCAATGTTTCAATGG
SCAP	Mouse	ATTTGCTCACCGTGGAGATGTT GAAGTCATCCAGGCCACTACTAATG
VEGF	Mouse	CACGACAGAAGGAGAGCAGAA CGCTGGTAGACGTCCATGA
36B4 (control)	Rat	TTCCCACTGGCTGAAAAGGT CGCAGCCGCAAATGC
GLUT1	Rat	CAGTGTATCCTGTTGCCCTTCTG CCCGGTTCTCCTCGTTACG
Insig-1	Rat	TGCAGATCCAGCGGAATGT CCAGGCGGAGGAGAAGATG
Insig-2a	Rat	GACGGATGTGTTGAAGGATTTCT TGGACTGAAGCAGACCAATGTC
Insig-2b	Rat	CCGGCAGAGCTCAGGATTT AACTGTGGACTGAAGCAGACCAA
SCAP	Rat	TGCTCACCGTGGAGATGTCA TCGGTCCCAGATGTTGATGA

APPENDIX B

Primers Used for Generation of Mammalian Cell Plasmids

Plasmid	**Primers** (Forward and Reverse)
Cloning	
pGL4-Insig-2 #1	CAGGACCCAAACAACAGCACATTC GAGGCAATGGCAGGGGTCAGA
pGL4-Insig-2 #2	GGTGTCGAATTCAGAGGGGTTAGG CGTCCCCGGCCAAATAAGC
pGL4-Insig-2 #3	GCAGGGCAACAGCAGAACTATCAA CGTCCCCGGCCAAATAAGC
pGL4-Insig-2 #4	CCATTGGGGCTGCTCACATCC CGTCCCCGGCCAAATAAGC
pGL4-Insig-2 #5	CTCCCCACTTCCCTGACACATCTC CGTCCCCGGCCAAATAAGC
pGL4-Insig-2 #6	GGAAGGTCTTAGCTGGGCGTGGTG CGTCCCCGGCCAAATAAGC
pGL4-Insig-2 #7	TGCAGGCGACAACCGTGGAG CGTCCCCGGCCAAATAAGC
pGL4-Insig-2 #8	GAAGTCCTTTTGCCCCGTCTCC CGTCCCCGGCCAAATAAGC
pCMV-HIF-1α	ATGGAGGGCGCCGGC CTAAATAATTCCTACTGCTTGAAAAAGTGAACCATCATGTTCCA
Mutagenesis	
Candidate HRE-1 Mutant	GCTGCGTACTTACTCGCGGTAGAGTCC GGACTCTACCGCGAGTAAGTACGCAGC
Candidate HRE-2 Mutant	GACAACTACTGAGCCTGTGTACCGGC GCCGGTACACAGGCTCAGTAGTTGTC

APPENDIX C

Primers Used for Chromatin Immunoprecipitation Assays

Region	**Primers** (Forward and Reverse)	**Size** (bp)
Insig-2 Promoter	AACGCGCTCCTTTCGGCTAC CGTAGGTAATGACGGATGCCCAGAC	131
Insig-2 HRE	CAATGATGTTACTTTCACTCAGTCTCTCAGGC ACAAAGGCAATGGCAGAGGATACAAAG	125
VEGF HRE	TGTCTGCCCAGCTGCCTC GGAGCTGAGAACGGGAAGCTG	129

APPENDIX D

Primers Used for Generation of Insect Cell Plasmids

Gene	**Template**	**Primers** (Forward and Reverse)
Hamster Reductase (X00494)	pCMV-HMG-Red-T7 (TM1-8) (Sever et al., 2003b)	ATGTTGTCACGACTTTTCCGTATGCAT GGACTCTGTCTCTGCTTGTTCAAAGAA
Drosophila Reductase (NM_170089)	cDNA	ATGATAGGACGTTTGTTTCGCGCC CGGCAGAGGATCACGATTGTCAA
Drosophila Hrd1 (NM_143637)	cDNA	ATGCAGCTGCTCTTATCGTCCGTT TTCCGCTGTCGTGCGTTCATTAGT
Drosophila Trc8 (NM_170413)	cDNA	ATGTCCGTGCGGACGAAGG CTGCTGGTCCTGCGACATCC

APPENDIX E

Primers Used for Generation of dsRNAs

Gene		**Nucleotides**	**Primers** (Forward and Reverse)
mouse CYP7A1 (control)		317-339 1044-1065	CGAAGGCATTTGGACACAGAAGC CCGCAGAGCCTCCTTGATGATG
Derlin-1	CG10908-RA	33-51 670-689	CCGCTTCACCCGCTACTGG TGCCTAGGTGGTGCTCTGCT
Derlin-2/3	CG14899-RA	105-127 733-754	GCCGCTGCAGCTCTACTTCAATC GATTCGCTGGCTCCTCATCCTG
Herp	CG14536-RA	696-714 1350-1373	CTTGCCGCCACCGACTCAA AGCGAGGTGAAGAACGTGATGACA
Hrd1	CG1937-RA	220-243 892-915	CATCTGCTGGAGCGCTTTTGGTAT GCAGGGCAGTTTCTTTGAGTGATT
Npl4	CG4673-RA	67-90 810-831	GTGCGCCATCGTCTGTTTGTGTTA GGTGCGCCAGTAGTTGAGGAAG
Os9	CG6766-RA	111-138 802-825	TGATTTCGAAGTGCCGGATTTAGATGTG CGCCTCGGATTCAACCCATTCCTT
Sel1	CG10221-RA	80-101 822-842	ACATTGATGGTACGGGCAGCAG TGGATCAGCGCCTTCTCACAG
Teb4	CG1317-RB	823-846 1524-1548	GTTTTTCTGGAGCACGTCTTCTGG CAGCAATTGCAAGTTAACCGCTGAA
TER94	CG2331-RC	1713-1733 2452-2477	CATGTGGTTCGGCGAGTCTGA CTGTAAAGATCATCGTCGCCGTTGT
Trc8	CG2304-RA	1052-1074 1617-1638	TCGACGGCTGTGAGACTATGACG GATGCCGAAGCAGAACTCCACT
Ubc1	CG8284-RA	1-22 577-599	ATGGCGAACATGGCAGTGTCGC TAACTGAACAGGCCCTCGGTGGC
Ubc6	CG5823-RA	48-71 699-717	GTCGCGCATGAAGCAGGACTATAT TCCTCCGCCGCTGGCCAAA
Ubc7	CG4443-RA	1-20 478-504	ATGGCTGGGTCCGCACTGCG TTACGCCGGTAAACCAAGAGTTTTGCG
Ubxd2	CG8042-RA	540-566 1198-1218	GGAGGCCAAGACGAATCCACCAAATTC TCGGATCTGCAGCCTCGTCTC
Ubxd8	CG10372-RA	20-42 654-675	CCAACGAACAGACGGAGAAGGTC GGCTACGTCGCATCCCCATAAC
Ufd1	CG6233-RA	163-187 853-878	CGCCTGAATGTCGAGTATCCAATGC GCTACGGCATCATCTTCTTGGCTTCT

Forward and reverse primers contain the T7 binding site: GAATTAATACGACTCACTA TAGGGAGA

APPENDIX F

Primers Used for Real-Time PCR Analysis for Insect Cells

Gene		**Nucleotides**	**Primers** (Forward and Reverse)
Acetaldehyde Dehydrogenase	CG3752-RA (control)	1180-1254	GAGGGCCTACCCGGCTACT CTCCCTTGCAATGGTCATATCA
Derlin-1	CG10908-RA	642-701	TCAAGTTCCAATACTCGCAGGAT AGAACTGCGGCGTTTCCA
Derlin-2/3	CG14899-RA	1072-1138	ATGAGCACATCGAACGCAACT CCGCCCCAAGGAAATCC
Herp	CG14536-RA	1142-1217	CCTGCTGATCCTCAGATTAATGG CGTGCATTTCCGGTTCCT
Hrd1	CG1937-RA	1562-1635	CGGCTTGCCCAATGGA GCGAAATCATGGGCATTACTG
Os9	CG6766-RA	1477-1546	AGCCGAAGACGTGCCAGTATA TCGGCGTTGTGGATGAGAT
SEL1L	CG10221-RA	2944-3035	TCGATCCCACTGGTTAGTCTTAGTAA TCGGGCGAAATTAGATGATAAATAT
Teb4	CG1317-RB	2815-2884	TCGAGCCTACATGGATGGATT GACCGGCACAGCCAAGTCT
TER94	CG2331-RC	1673-1745	AGGCGAACTTCATCTCAGTCAAG CGCACGTTGGCCTCAGA
Trc8	CG2304-RA	1966-2036	CTGCTGCACTTCCTGCACAA CGCGAGGGATTCCGTG
Ubc1	CG8284-RA	956-1020	TCCCAGCCGCACTAGCAT GAAGTTGGCCGGTGTTCTTG
Ubc6	CG5823-RA	1047-1111	CCTGCGCAACACCAACTTCT GCAGCCGCTGCTTGATCT
Ubc7	CG4443-RA	458-516	CCTGAGGGCACTTGTTTCGA GGATAGTCGGTCGGAAAGATGA
Ubxd2	CG8042-RA	1895-1960	TCCGCCGGCTCATAACAC CCGGGTCGCTGTTGGA
Ubxd8	CG10372-RA	1367-1432	AGGCATACGAGCAGAGTTTGC CATCCCGCTCCCTTTGC
Ufd1	CG6233-RA	499-568	GTGGCCACCTTCTCAAAGTTTC GCACCGCCTTGGGATTG

BIBLIOGRAPHY

Adams, C.M., Goldstein, J.L., and Brown, M.S. (2003). Cholesterol-induced conformational change in SCAP enhanced by Insig proteins and mimicked by cationic amphiphiles. Proc. Natl. Acad. Sci. U. S. A. *100*, 10647-10652.

Adams, C.M., Reitz, J., De Brabander, J.K., Feramisco, J.D., Li, L., Brown, M.S., and Goldstein, J.L. (2004). Cholesterol and 25-hydroxycholesterol inhibit activation of SREBPs by different mechanisms, both involving SCAP and Insigs. J. Biol. Chem. *279*, 52772-52780.

Aitbaev, K.A. (1985). The levels of high density lipoprotein cholesterol and other lipids in the native population of the mountain region of Kirghizia. Vopr. Med. Khim. *31*, 58-61.

Aitbaev, K.A., Madaminov, I.K., Meimanaliev, T.S., Shleifer, E.A., and Kim, N.M. (1990). Study of the effect of migration to high-mountain regions on the blood lipoprotein system. Kosm. Biol. Aviakosm. Med. *24*, 45-46.

Ashouri, K., Ahmed, M.E., Kardash, M.O., Sharif, A.Y., Abdalsattar, M., and al Ghozeim, A. (1994). Acute myocardial infarction at high altitude: the experience in Asir Region, southern Saudi Arabia. Ethn. Dis. *4*, 82-86.

Bays, N.W., Gardner, R.G., Seelig, L.P., Joazeiro, C.A., and Hampton, R.Y. (2001). Hrd1p/Der3p is a membrane-anchored ubiquitin ligase required for ER-associated degradation. Nat. Cell Biol. *3*, 24-29.

Berkhout, T.A., Simon, H.M., Jackson, B., Yates, J., Pearce, N., Groot, P.H., Bentzen, C., Niesor, E., Kerns, W.D., and Suckling, K.E. (1997). SR-12813 lowers plasma cholesterol in beagle dogs by decreasing cholesterol biosynthesis. Atherosclerosis *133*, 203-212.

Berkhout, T.A., Simon, H.M., Patel, D.D., Bentzen, C., Niesor, E., Jackson, B., and Suckling, K.E. (1996). The novel cholesterol-lowering drug SR-12813 inhibits cholesterol synthesis via an increased degradation of 3-hydroxy-3-methylglutaryl-coenzyme A reductase. J. Biol. Chem. *271*, 14376-14382.

Bligh, E.G., and Dyer, W.J. (1959). A rapid method of total lipid extraction and purification. Can. J. Biochem. Physiol. *37*, 911-917.

Bloch, K. (1952). Biological synthesis of cholesterol. Harvey Lect. *48*, 68-88.

Bordallo, J., Plemper, R.K., Finger, A., and Wolf, D.H. (1998). Der3p/Hrd1p is required for endoplasmic reticulum-associated degradation of misfolded lumenal and integral membrane proteins. Mol. Biol. Cell *9*, 209-222.

Bordallo, J., and Wolf, D.H. (1999). A RING-H2 finger motif is essential for the function of Der3/Hrd1 in endoplasmic reticulum associated protein degradation in the yeast Saccharomyces cerevisiae. FEBS Lett. *448*, 244-248.

Boron, W.F., and Boulpaep, E.L. (2003). Medical Physiology, 1st edn (Philadelphia, Saunders).

Brauweiler, A., Lorick, K.L., Lee, J.P., Tsai, Y.C., Chan, D., Weissman, A.M., Drabkin, H.A., and Gemmill, R.M. (2007). RING-dependent tumor suppression and G2/M arrest induced by the TRC8 hereditary kidney cancer gene. Oncogene *26*, 2263-2271.

Brown, A.J., Sun, L., Feramisco, J.D., Brown, M.S., and Goldstein, J.L. (2002). Cholesterol addition to ER membranes alters conformation of SCAP, the SREBP escort protein that regulates cholesterol metabolism. Mol. Cell *10*, 237-245.

Brown, K., Havel, C.M., and Watson, J.A. (1983). Isoprene synthesis in isolated embryonic Drosophila cells. II. Regulation of 3-hydroxy-3-methylglutaryl coenzyme A reductase activity. J. Biol. Chem. *258*, 8512-8518.

Brown, M.S., Faust, J.R., and Goldstein, J.L. (1978). Induction of 3-hydroxy-3-methylglutaryl coenzyme A reductase activity in human fibroblasts incubated with compactin (ML-236B), a competitive inhibitor of the reductase. J. Biol. Chem. *253*, 1121-1128.

Brown, M.S., and Goldstein, J.L. (1980). Multivalent feedback regulation of HMG CoA reductase, a control mechanism coordinating isoprenoid synthesis and cell growth. J. Lipid Res. *21*, 505-517.

Bruick, R.K., and McKnight, S.L. (2001). A conserved family of prolyl-4-hydroxylases that modify HIF. Science *294*, 1337-1340.

Carvalho, P., Goder, V., and Rapoport, T.A. (2006). Distinct ubiquitin-ligase complexes define convergent pathways for the degradation of ER proteins Cell *126*, 361-373.

Christianson, J.C., Shaler, T.A., Tyler, R.E., and Kopito, R.R. (2008). OS-9 and GRP94 deliver mutant alpha1-antitrypsin to the Hrd1-SEL1L ubiquitin ligase complex for ERAD. Nat. Cell Biol. *10*, 272-282.

Chun, K.T., and Simoni, R.D. (1992). The role of the membrane domain in the regulated degradation of 3- hydroxy-3-methylglutaryl coenzyme A reductase. J. Biol. Chem. *267*, 4236-4246.

Clark, A.J., and Block, K. (1959). The absence of sterol synthesis in insects. J. Biol. Chem. *234*.

Clayman, R., Bilhartz, L., Buja, L., Spady, D., and Dietschy, J. (1986a). Renal cell carcinoma in the Wistar-Lewis rat: a model for studying the mechanisms of cholesterol acquisition by a tumor in vivo. Cancer Res. *46*, 2958-2963.

Clayman, R., Bilhartz, L., Spady, D., Buja, L., and Dietschy, J. (1986b). Low density lipoprotein-receptor activity is lost in vivo in malignantly transformed renal tissue. FEBS Lett. *196*, 87-90.

Clayton, R. (1964). The utilization of sterols by insects. J. Lipid Res. *15*, 3-19.

Clemens, J.C., Worby, C.A., Simonson-Leff, N., Muda, M., Maehama, T., Hemmings, B.A., and Dixon, J.E. (2000). Use of double-stranded RNA interference in Drosophila cell lines to dissect signal transduction pathways. Proc. Natl. Acad. Sci. U. S. A. *97*, 6499-6503.

Correll, C.C., and Edwards, P.A. (1994). Mevalonic acid-dependent degradation of 3-hydroxy-3-methylglutaryl-coenzyme A reductase in vivo and in vitro. J. Biol. Chem. *269*, 633-638.

Damert, A., Ikeda, E., and Risau, W. (1997). Activator-protein-1 binding potentiates the hypoxia-inducible factor-1-mediated hypoxia-induced transcriptional activation of vascular-endothelial growth factor expression in C6 glioma cells. Biochem. J. *327*, 419-423.

de Mendoza, S., Nucete, H., Ineichen, E., Salazar, E., Zerpa, A., and Glueck, C.J. (1979). Lipids and lipoproteins in subjects at 1,000 and 3,500 meter altitudes. Arch. Environ. Health *34*, 308-311.

Deak, P.M., and Wolf, D.H. (2001). Membrane topology and function of Der3/Hrd1p as a ubiquitin-protein ligase (E3) involved in endoplasmic reticulum degradation. J. Biol. Chem. *276*, 10663-10669.

DeBose-Boyd, R.A., Brown, M.S., Li, W.-P., Nohturfft, A., Goldstein, J.L., and Espenshade, P.J. (1999). Transport-dependent proteolysis of SREBP: Relocation of Site-1 protease from Golgi to ER obviates the need for SREBP transport to Golgi. Cell *99*, 703-712.

Denic, V., Quan, E.M., and Weissman, J.S. (2007). A luminal surveillance complex that selects misfolded glycoproteins for ER-associated degradation. Cell *126*, 349-359.

Dobrosotskaya, I.Y., Goldstein, J.L., Brown, M.S., and Rawson, R.B. (2003). Reconstitution of sterol-regulated endoplasmic reticulum-to-Golgi transport of SREBP-2 in insect cells by co-expression of mammalian SCAP and Insigs. J. Biol. Chem. *278*, 35837-35843.

Dobrosotskaya, I.Y., Seegmiller, A.C., Brown, M.S., Goldstein, J.L., and Rawson, R.B. (2002). Regulation of SREBP processing and membrane lipid production by phospholipids in Drosophila. Science *296*, 879-883.

Dolt, K.S., Karar, J., Mishra, M.K., Salim, J., Kumar, R., Grover, S.K., and Qadar Pasha, M.A. (2007). Transcriptional downregulation of sterol metabolism genes in murine liver exposed to acute hypobaric hypoxia. Biochem. Biophys. Res. Commun. *354*, 148-153.

Ebert, B.L., and Bunn, H.F. (1998). Regulation of transcription by hypoxia requires a multiprotein complex that includes hypoxia-inducible factor 1, an adjacent

transcription factor, and p300/CREB binding protein. Mol. Cell. Biol. *18*, 4089-4096.

Elvidge, G.P., Glenny, L., Appelhoff, R.J., Ratcliffe, P.J., Ragoussis, J., and Gleadle, J.M. (2006). Concordant regulation of gene expression by hypoxia and 2-oxoglutarate-dependent dioxygenase inhibition: The role of HIF-1α, HIF-2α, and other pathways. J. Biol. Chem. *281*, 15215-15226.

Epstein, A.C.R., Gleadle, J.M., McNeill, L.A., Hewitson, K.S., O'Rourke, J., Mole, D.R., Mukherji, M., Metzen, E., Wilson, M.I., Dhanda, A.*, et al.* (2001). C. elegans egl-9 and mammalian homologs define a family of dioxygenases that regulate HIF by prolyl hydroxylation. Cell *107*, 43-54.

Ferezou, J., Richalet, J.P., Coste, T., and Rathat, C. (1988). Changes in plasma lipids and lipoprotein cholesterol during a high altitude mountaineering expedition (4800 m). Eur. J. Appl. Physiol. Occup. Physiol. *57*, 740-745.

Firth, J.D., Ebert, B.L., Pugh, C.W., and Ratcliffe, P.J. (1994). Oxygen-regulated control elements in the phosphoglycerate kinase 1 and lactate dehydrogenase A genes: similarities with the erythropoietin 3' enhancer. Proc. Natl. Acad. Sci. U. S. A. *91*, 6496-6500

Firth, J.D., Ebert, B.L., and Ratcliffe, P.J. (1995). Hypoxic regulation of lactate dehydrogenase A. J. Biol. Chem. *270*, 21021-21027.

Flury, I., Garza, R., Shearer, A., Rosen, J., Cronin, S., and Hampton, R.Y. (2005). INSIG: a broadly conserved transmembrane chaperone for sterol-sensing domain proteins. EMBO J. *24*, 3917-3926.

Forsburg, S.L., and Guarente, L. (1989). Communication between mitochondria and the nucleus in regulation of cytochrome genes in the yeast *Saccharomyces cerevisiae*. Annu. Rev. Cell Biol. *5*, 153-180.

Fukuda, R., Zhang, H., Kim, J.W., Shimoda, L., Dang, C.V., and Semenza, G.L. (2007). HIF-1 regulates cytochrome oxidase subunits to optimize efficiency of respiration in hypoxic cells. Cell *129*, 111-122.

Gardner, R.G., Swarbrick, G.M., Bays, N.W., Cronin, S.R., Wilhovsky, S., Seelig, L., Kim, C., and Hampton, R.Y. (2000). Endoplasmic reticulum degradation requires lumen to cytosol signaling: transmembrane control of Hrd1p by Hrd3p. J. Cell. Biol. *151*, 69-82.

Gaylor, J.L. (2002). Membrane-bound enzymes of cholesterol synthesis from lanosterol. Biochem. Biophys. Res. Commun. *292*, 1139-1146.

Gebhard, R.L., Clayman, R.V., Prigge, W.F., Figenshau, R., Staley, N.A., Reesey, C., and Bear, A. (1987). Abnormal cholesterol metabolism in renal clear cell carcinoma. J. Lipid Res. *28*, 1177-1184.

Gemmill, R.M., Bemis, L.T., Lee, J.P., Sozen, M.A., Baron, A., Zeng, C., Erickson, P.F., Hooper, J.E., and Drabkin, H.A. (2002). The TRC8 hereditary kidney cancer gene suppresses growth and functions with VHL in a common pathway. Oncogene *21*, 3507-3516.

Gemmill, R.M., West, J.D., Boldog, F., Tanaka, N., Robinson, L.J., Smith, D.I., Li, F., and Drabkin, H.A. (1998). The hereditary renal cell carcinoma 3;8 translocation fuses FHIT to a patched-related gene, TRC8. Proc. Natl. Acad. Sci. U. S. A. *95*, 9572-9577.

Gertler, F.B., Chiu, C.Y., Richter-Mann, L., and Chin, D.J. (1988). Developmental and metabolic regulation of the Drosophila melanogaster 3-hydroxy-3-methylglutaryl coenzyme A reductase. Mol. Cell. Biol. *8*, 2713-2721.

Gil, G., Faust, J.R., Chin, D.J., Goldstein, J.L., and Brown, M.S. (1985). Membrane-bound domain of HMG CoA reductase is required for sterol-enhanced degradation of the enzyme. Cell *41*, 249-258.

Goldstein, J.L., and Brown, M.S. (1990). Regulation of the mevalonate pathway. Nature *343*, 425-430.

Goldstein, J.L., DeBose-Boyd, R.A., and Brown, M.S. (2006). Protein sensors for membrane sterols. Cell *124*, 35-46.

Gong, Y., Lee, J.N., Lee, P.C.W., Goldstein, J.L., Brown, M.S., and Ye, J. (2006). Sterol-regulated ubiquitination and degradation of Insig-1 creates a convergent mechanism for feedback control of cholesterol synthesis and uptake. Cell Metab. *3*, 15-24.

Gonzalez, R., Clayman, R.V., and Dempsey, M.E. (1981). Cholesterol accumulation in renal cell cancer: a review. Invest. Urol. *19*, 1-3.

Haase, V.H., Glickman, J.N., Socolovsky, M., and Jaenisch, R. (2001). Vascular tumors in livers with targeted inactivation of the von Hippel–Lindau tumor suppressor. Proc. Natl. Acad. Sci. U. S. A. *98*, 1583-1588.

Hampton, R.Y. (2002). ER-associated degradation in protein quality control and cellular regulation Curr. Opin. Cell Biol. *14*, 476-482.

Hampton, R.Y., Gardner, R.G., and Rine, J. (1996). Role of 26S proteasome and HRD genes in the degradation of 3-hydroxy-3- methylglutaryl-CoA reductase, an integral endoplasmic reticulum membrane protein. Mol. Biol. Cell *7*, 2029-2044.

Hampton, R.Y., and Rine, J. (1994). Regulated degradation of HMG-CoA reductase, an integral membrane protein of the endoplasmic reticulum, in yeast. J. Cell Biol. *125*, 299-312.

Hannah, V.C., Ou, J., Luong, A., Goldstein, J.L., and Brown, M.S. (2001). Unsaturated fatty acids down-regulate SREBP isoforms 1a and 1c by two mechanisms in HEK-293 cells. J. Biol. Chem. *276*, 4365-4372.

Herman, J.G., Latif, F., Weng, Y., Lerman, M.I., Zbar, B., Liu, S., Samid, D., Duan, D.S., Gnarra, J.R., and Linehan, W.M. (1994). Silencing of the VHL tumor-suppressor gene by DNA methylation in renal carcinoma. Proc. Natl. Acad. Sci. U. S. A. *91*, 9700-9704.

Horie, M., Tsuchiya, Y., Hayashi, M., Iida, Y., Iwasawa, Y., Nagata, Y., Sawasaki, Y., Fukuzumi, H., Kitani, K., and Kamei, T. (1990). NB-598: a potent competitive inhibitor of squalene epoxidase. J. Biol. Chem. *265*, 18075-18078.

Horton, J.D., Goldstein, J.L., and Brown, M.S. (2002a). SREBPs: activators of the complete program of cholesterol and fatty acid synthesis in the liver. J. Clin. Invest. *109*, 1125-1131.

Horton, J.D., Shah, N.A., Warrington, J.A., Anderson, N.N., Park, S.W., Brown, M.S., and L., G.J. (2002b). Combined analysis of oligonucleotide microarray data from transgenic and knockout mice identifies direct SREBP target genes. Proc. Natl. Acad. Sci. U. S. A. *100*, 12027-12032.

Horton, J.D., Shimano, H., Hamilton, R.L., Brown, M.S., and Goldstein, J.L. (1999). Disruption of LDL receptor gene in transgenic SREBP-1a mice unmasks hyperlipidemia resulting from production of lipid-rich VLDL. J. Clin. Invest. *103*, 1067-1076.

Hua, X., Nohturfft, A., Goldstein, J.L., and Brown, M.S. (1996). Sterol resistance in CHO cells traced to point mutation in SREBP cleavage-activating protein. Cell *87*, 415-426.

Huang, L.E., Gu, J., Schau, M., and Bunn, H.F. (1998). Regulation of hypoxia-inducible factor 1α is mediated by an O2-dependent degradation domain via the ubiquitin-proteasome pathway Proc. Natl. Acad. Sci. U. S. A. *95*, 7987-7992.

Hughes, A.L., Todd, B.L., and Espenshade, P.J. (2005). SREBP pathway responds to sterols and functions as an oxygen sensor in fission yeast. Cell *120*, 831-842.

Infante, R.E., Abi-Mosleh, L., Radhakrishnan, A., Dale, J.D., Brown, M.S., and Goldstein, J.L. (2008). Purified NPC1 protein. I. Binding of cholesterol and oxysterols to a 1278-amino acid membrane protein. J. Biol. Chem. *283*, 1052-1063.

Jaakkola, P., Mole, D.R., Tian, Y.-M., Wilson, M.I., Gielbert, J., Gaskell, S.J., Kriegsheim, A.v., Hebestreit, H.F., Mukherji, M., Schofield, C.J*., et al.* (2001). Targeting of HIF-α to the von Hippel-Lindau ubiquitylation complex by O2-regulated prolyl hydroxylation. Science *292*, 468-472.

Jungermann, K., and Kietzmann, T. (2000). Oxygen: modulator of metabolic zonation and disease of the liver. Hepatology *31*, 255-260.

Kaelin, W.G. (2007). Von Hippel-Lindau disease. Annu. Rev. Pathol. *2*, 145-173.

Kaelin, W.G., Jr. (2004). The von Hippel-Lindau tumor suppressor gene and kidney cancer. Clin. Cancer Res. *10*, 6290S-6295.

Kikkert, M., Doolman, R., Dai, M., Avner, R., Hassink, G., van Voorden, S., Thanedar, S., Roitelman, J., Chau, V., and Wiertz, E. (2003). Human HRD1 is an E3 ubiquitin ligase involved in degradation of proteins from the endoplasmic reticulum. J. Biol. Chem. *279*, 3525-3534.

Kilsdonk, E.P.C., Yancey, P.G., Stoudt, G.W., Bangerter, F.W., Johnson, W.J., Phillips, M.C., and Rothblat, G.H. (1995). Cellular cholesterol efflux mediated by cyclodextrins. J. Biol. Chem. *270*, 17250-17256.

Kim, H., Lee, D.-K., Choi, J.-W., Kim, J.-S., Park, S.C., and Youn, H.-D. (2003). Analysis of the effect of aging on the response to hypoxia by cDNA microarray. Mech. Ageing Dev. *124*, 941-949.

Kim, T.Y., Kim, E., Yoon, S.K., and Yoon, J.B. (2008). Herp enhances ER-associated protein degradation by recruiting ubiquilins. Biochem. Biophys. Res. Commun. *369*, 741-746.

Kim, W.Y., Safran, M., Buckley, M.R.M., Ebert, B.L., Glickman, J., Bosenberg, M., Regan, M., and Jr, W.G.K. (2006). Failure to prolyl hydroxylate hypoxia-inducible factor phenocopies VHL inactivation in vivo. EMBO J. *25*, 4650-4662.

Ko, H.S., Uehara, T., Tsuruma, K., and Nomura, Y. (2004). Ubiquilin interacts with ubiquitylated proteins and proteasome through its ubiquitin-associated and ubiquitin-like domains. FEBS Lett. *566*, 110-114.

Kostovaa, Z., Tsaia, Y.C., and Weissman, A.M. (2007). Ubiquitin ligases, critical mediators of endoplasmic reticulum-associated degradation Semin. Cell Dev. Biol. *18*, 770-779.

Lange, Y., Ory, D.S., Ye, J., Lanier, M.H., Hsu, F.-F., and Steck, T.L. (2008). Effectors of rapid homeostatic responses of endoplasmic reticulum cholesterol and 3-hydroxy-3-methylglutaryl-CoA reductase. J. Biol. Chem. *283*, 1445-1455.

Lee, J.N., and Ye, J. (2004). Proteolytic activation of sterol regulatory element-binding protein induced by cellular stress through depletion of Insig-1. J. Biol. Chem. *279*, 45257-45265.

Lee, P.C., Nguyen, A.D., and DeBose-Boyd, R.A. (2007). Mutations within the membrane domain of HMG CoA reductase confer resistance to sterol-accelerated degradation. J. Lipid Res. *48*, 318-327.

Lee, P.C., Sever, N., and DeBose-Boyd, R.A. (2005). Isolation of sterol-resistant Chinese hamster ovary cells with genetic deficiencies in both Insig-1 and Insig-2. J. Biol. Chem. *280*, 25242-25249.

Liang, G., Yang, J., Horton, J.D., Hammer, R.E., Goldstein, J.L., and Brown, M.S. (2002). Diminished hepatic response to fasting/refeeding and liver X receptor agonists in mice with selective deficiency of sterol regulatory element-binding protein-1c. J. Biol. Chem. *277*, 9520-9528.

Lilley, B.N., and Ploegh, H.L. (2004). A membrane protein required for dislocation of misfolded proteins from the ER. Nature *429*, 834-840.

Lilley, B.N., and Ploegh, H.L. (2005). Multiprotein complexes that link dislocation, ubiquitination, and extraction of misfolded proteins from the endoplasmic reticulum membrane. Proc. Natl. Acad. Sci. U. S. A. *102*, 14296-14301.

Lippincott-Schwartz, J., Bonifacino, J.S., Yuan, L.C., and Klausner, R.D. (1988). Degradation from the endoplasmic reticulum: disposing of newly synthesized proteins. Cell *54*, 209-220.

Liscum, L., Finer-Moore, J., Stroud, R.M., Luskey, K.L., Brown, M.S., and Goldstein, J.L. (1985). Domain structure of 3-hydroxy-3-methylglutaryl coenzyme A reductase, a glycoprotein of the endoplasmic reticulum. J. Biol. Chem. *260*, 522-530.

Liscum, L., Luskey, K.L., Chin, D.J., Ho, Y.K., Goldstein, J.L., and Brown, M.S. (1983). Regulation of 3-hydroxy-3-methylglutaryl coenzyme A reductase and its mRNA in rat liver as studied with a monoclonal antibody and a cDNA probe. J. Biol. Chem. *258*, 8450-8455.

Lowry, C.V., and Zitomer, R.S. (1984). Oxygen regulation of anaerobic and aerobic genes mediated by a common factor in yeast. Proc. Natl. Acad. Sci. U. S. A. *81*, 6129-6133.

Maxwell, P.H., Wiesener, M.S., Chang, G.-W., Clifford, S.C., Vaux, E.C., Cockman, M.E., Wykoff, C.C., Pugh, C.W., Maher, E.R., and Ratcliffe, P.J. (1999). The tumour suppressor protein VHL targets hypoxia-inducible factors for oxygen-dependent proteolysis. Nature *399*, 271-275.

Mense, S.M., Sengupta, A., Zhou, M., Lan, C., Bentsman, G., Volsky, D.J., and Zhang, L. (2006). Gene expression profiling reveals the profound upregulation of hypoxia-responsive genes in primary human astrocytes. Physiol. Genomics *25*, 435-449.

Metherall, J.E., Goldstein, J.L., Luskey, K.L., and Brown, M.S. (1989). Loss of transcriptional repression of three sterol-regulated genes in mutant hamster cells. J. Biol. Chem. *264*, 15634-15641.

Mortimer, E.A.J., Monson, R.R., and MacMahon, B. (1977). Reduction in mortality from coronary heart disease in men residing at high altitude. N. Engl. J. Med. *296*, 581-585.

Mukodani, J., Ishikawa, Y., and Fukuzaki, H. (1990). Effects of hypoxia on sterol synthesis, acyl-CoA:cholesterol acyltransferase activity, and efflux of cholesterol in cultured rabbit skin fibroblasts. Arteriosclerosis *10*, 106-110.

Nakanishi, M., Goldstein, J.L., and Brown, M.S. (1988). Multivalent control of 3-hydroxy-3-methylglutaryl coenzyme A reductase: mevalonate-derived product inhibits translation of mRNA and accelerates degradation of enzyme. J. Biol. Chem. *263*, 8929-8937.

Nohturfft, A., Brown, M.S., and Goldstein, J.L. (1998). Topology of SREBP cleavage-activating protein, a polytopic membrane protein with a sterol-sensing domain. J. Biol. Chem. *273*, 17243-17250.

Nohturfft, A., Yabe, D., Goldstein, J.L., Brown, M.S., and Espenshade, P.J. (2000). Regulated step in cholesterol feedback localized to budding of SCAP from ER membranes. Cell *102*, 315-323.

Radhakrishnan, A., Ikeda, Y., Kwon, H.J., Brown, M.S., and Goldstein, J.L. (2007). Sterol-regulated transport of SREBPs from endoplasmic reticulum to Golgi: oxysterols block transport by binding to Insig. Proc. Natl. Acad. Sci. U. S. A. *104*, 6511-6518.

Radhakrishnan, A., Sun, L.-P., Kwon, H.J., Brown, M.S., and Goldstein, J.L. (2004). Direct binding of cholesterol to the purified membrane region of SCAP: Mechanism for a sterol-sensing domain. Mol. Cell *15*, 259-268.

Ravid, T., Doolman, R., Avner, R., Harats, D., and Roitelman, J. (2000). The ubiquitin-proteasome pathway mediates the regulated degradation of mammalian 3-hydroxy-3-methylglutaryl-coenzyme A reductase. J. Biol. Chem. *275*, 35840-35847.

Rawson, R.B., DeBose-Boyd, R., Goldstein, J.L., and Brown, M.S. (1999). Failure to cleave sterol regulatory element-binding proteins (SREBPs) causes cholesterol auxotrophy in Chinese hamster ovary cells with genetic absence of SREBP cleavage-activating protein. J. Biol. Chem. *274*, 28549-28556.

Roitelman, J., Masson, D., Avner, R., Ammon-Zufferey, C., Perez, A., Guyon-Gellin, Y., Bentzen, C.L., and Niesor, E.J. (2004). Apomine, a novel hypocholesterolemic agent, accelerates degradation of 3-hydroxy-3-methylglutaryl-coenzyme A reductase and stimulates low density lipoprotein receptor activity. J. Biol. Chem. *279*, 6465-6473.

Roitelman, J., Olender, E.H., Bar-Nun, S., Dunn, W.A., Jr., and Simoni, R.D. (1992). Immunological evidence for eight spans in the membrane domain of 3- hydroxy-3-methylglutaryl coenzyme A reductase: implications for enzyme degradation in the endoplasmic reticulum. J. Cell Biol. *117*, 959-973.

Roitelman, J., and Simoni, R.D. (1992). Distinct sterol and nonsterol signals for the regulated degradation of 3-hydroxy-3-methylglutaryl-CoA reductase. J. Biol. Chem. *267*, 25264-25273.

Rudling, M., and Collins, V.P. (1996). Low density lipoprotein receptor and 3-hydroxy-3-methylglutaryl coenzyme A reductase mRNA levels are coordinately reduced in human renal cell carcinoma. Biochim Biophys Acta *1299*, 75-79.

Safran, M., Kim, W.Y., O'Connell, F., Flippin, L., Günzler, V., Horner, J.W., DePinho, R.A., and Kaelin, W.G. (2006). Mouse model for noninvasive imaging of HIF prolyl hydroxylase activity: Assessment of an oral agent that stimulates erythropoietin production. Proc. Natl. Acad. Sci. U. S. A. *103*, 105-110.

Sakai, J., Nohturfft, A., Cheng, D., Ho, Y.K., Brown, M.S., and Goldstein, J.L. (1997). Identification of complexes between the COOH-terminal domains of sterol regulatory element-binding proteins (SREBPs) and SREBP cleavage-activating protein. J. Biol. Chem. *272*, 20213-20221.

Salceda, S., and Caro, J. (1997). Hypoxia-inducible factor 1α (HIF-1α) protein is rapidly degraded by the ubiquitin-proteasome system under normoxic conditions: Its stabilization by hypoxia depends on redox-induced changes. J. Biol. Chem. *272*, 22642-22647.

Sato, R., Goldstein, J.L., and Brown, M.S. (1993). Replacement of serine-871 of hamster 3-hydroxy-3-methylglutaryl-CoA reductase prevents phosphorylation by AMP-activated kinase and blocks inhibition of sterol synthesis induced by ATP depletion. Proc. Natl. Acad. Sci. U. S. A. *90*, 9261-9265.

Schofield, C.J., and Ratcliffe, P.J. (2004). Oxygen sensing by HIF hydroxylases. Nat. Rev. Mol. Cell. Biol. *5*, 343-354.

Schulze, A., Standera, S., Buerger, E., Kikkert, M., van Voorden, S., Wiertz, E., Koning, F., Kloetzel, P.M., and Seeger, M. (2005). The ubiquitin-domain protein HERP forms a complex with components of the endoplasmic reticulum associated degradation pathway J. Mol. Biol. *354*, 1021-1027.

Seegmiller, A.C., Dobrosotskaya, I., Goldstein, J.L., Ho, Y.K., Brown, M.S., and Rawson, R.B. (2002). The SREBP pathway in Drosophila: regulation by palmitate, not sterols. Dev. Cell *2*, 229-238.

Semenza, G.L. (2004). Hydroxylation of HIF-1: oxygen sensing at the molecular level. Physiology (Bethesda) *19*, 176-182.

Sever, N., Lee, P.C., Song, B.L., Rawson, R.B., and DeBose-Boyd, R.A. (2004). Isolation of mutant cells lacking Insig-1 through selection with SR-12813, an agent that stimulates degradation of 3-hydroxy-3-methylglutaryl-coenzyme A reductase. J. Biol. Chem. *279*, 43136-43147.

Sever, N., Song, B.L., Yabe, D., Goldstein, J.L., Brown, M.S., and DeBose-Boyd, R.A. (2003a). Insig-dependent ubiquitination and degradation of mammalian 3-hydroxy-3-methylglutaryl-CoA reductase stimulated by sterols and geranylgeraniol. J. Biol. Chem. *278*, 52479-52490.

Sever, N., Yang, T., Brown, M.S., Goldstein, J.L., and DeBose-Boyd, R.A. (2003b). Accelerated degradation of HMG CoA reductase mediated by binding of Insig-1 to its sterol-sensing domain. Mol. Cell *11*, 25-33.

Shimomura, I., Shimano, H., Horton, J.D., Goldstein, J.L., and Brown, M.S. (1997). Differential expression of exons 1a and 1c in mRNAs for sterol regulatory element binding protein-1 in human and mouse organs and cultured cells. J. Clin. Invest. *99*, 838-845.

Skalnik, D.G., Narita, H., Kent, C., and Simoni, R.D. (1988). The membrane domain of 3-hydroxy-3-methylglutaryl-coenzyme A reductase confers endoplasmic reticulum localization and sterol-regulated degradation onto beta-galactosidase. J. Biol. Chem. *263*, 6836-6841.

Song, B.L., Javitt, N.B., and DeBose-Boyd, R.A. (2005a). Insig-mediated degradation of HMG CoA reductase stimulated by lanosterol, an intermediate in the synthesis of cholesterol. Cell Metab. *1*, 179-189.

Song, B.L., Sever, N., and DeBose-Boyd, R.A. (2005b). Gp78, a membrane-anchored ubiquitin ligase, associates with Insig-1 and couples sterol-regulated ubiquitination to degradation of HMG CoA reductase. Mol. Cell *19*, 829-840.

Spence, J.T., and Gaylor, J.L. (1977). Investigation of regulation of microsomal hydroxymethylglutaryl coenzyme A reductase and methyl sterol oxidase of cholesterol biosynthesis. J. Biol. Chem. *252*, 5852-5858.

Summons, R.E., Bradley, A.S., Jahnke, L.L., and Waldbauer, J.R. (2006). Steroids, triterpenoids and molecular oxygen. Philos. Trans. R. Soc. Lond. B Biol. Sci. *361*, 951-968.

Sung, F.L., Hui, E.P., Tao, Q., Li, H., Tsui, N.B.Y., Dennis Lo, Y.M., Ma, B.B.Y., To, K.F., Harris, A.L., and Chan, A.T.C. (2007). Genome-wide expression analysis using microarray identified complex signaling pathways modulated by hypoxia in nasopharyngeal carcinoma. Cancer Lett. *253*, 74-88.

Swinney, D.C., So, O.-Y., Watson, D.M., Berry, P.W., Webb, A.S., Kertesz, D.J., Shelton, E.J., Walker, K.A.M., and Burton, P.M. (1994). Selective inhibition of mammalian lanosterol 14α-demethylase by RS-21607 in vitro and in vivo. Biochemistry *33*, 4702-4713.

Taxis, C., Hitt, R., Park, S.-H., Deak, P.M., Kostova, Z., and Wolf, D.H. (2003). Use of modular substrates demonstrates mechanistic diversity and reveals differences in chaperone requirement of ERAD. J. Biol. Chem. *278*, 35903-35913.

Todd, B.L., Stewart, E.V., Burg, J.S., Hughes, A.L., and Espenshade, P.J. (2006). Sterol regulatory element binding protein is a principal regulator of anaerobic gene expression in fission yeast. Mol. Cell. Biol. *26*, 2817-2831.

Tsai, A.G., Johnson, P.C., and Intaglietta, M. (2003). Oxygen gradients in the microcirculation. Physiol. Rev. *83*, 933-963.

Walker, K.A.M., Kertesz, D.J., Rotstein, D.M., Swinney, D.C., Berry, P.W., So, O.Y., Webb, A.S., Watson, D.M., and Mak, A.Y. (1993). Selective inhibition of mammalian lanosterol 14α-demethylase: a possible strategy for cholesterol lowering. J. Med. Chem. *36*, 2235-2237.

Walters, K.J., Goh, A.M., Wang, Q., Wagner, G., and Howley, P.M. (2004). Ubiquitin family proteins and their relationship to the proteasome: a structural perspective. Biochim. Biophys. Acta. *1695*, 73-87.

Wang, G.L., and Semenza, G.L. (1993). Characterization of hypoxia-inducible factor 1 and regulation of DNA binding activity by hypoxia. J. Biol. Chem. *268*, 21513-21518.

Wang, G.L., and Semenza, G.L. (1995). Purification and characterization of hypoxia-inducible factor 1. J. Biol. Chem. *270*, 1230-1237.

Wenger, R.H., Stiehl, D.P., and Camenisch, G. (2005). Integration of oxygen signaling at the consensus HRE. Sci. STKE *306*, 1-13.

Williams, M.T., Gaylor, J.L., and Morris, H.P. (1977). Investigation of the rate-determining microsomal reaction of cholesterol biosynthesis from lanosterol in Morris hepatomas and liver. Cancer Res. *37*, 1377-1383.

Wood, S.M., Wiesener, M.S., Yeates, K.M., Okada, N., Pugh, C.W., Maxwell, P.H., and Ratcliffe, P.J. (1998). Selection and analysis of a mutant cell line defective in the hypoxia-inducible factor-1α-subunit (HIF-1α). Characterization of HIF-1α-dependent and -independent hypoxia-inducible gene expression. J. Biol. Chem. *273*, 8360-8368.

Wu, J., Merlino, G., and Fausto, N. (1994). Establishment and characterization of differentiated, nontransformed hepatocyte cell lines derived from mice transgenic for transforming growth factor alpha. Proc. Natl. Acad. Sci. U. S. A. *91*, 674-678.

Yabe, D., Brown, M.S., and Goldstein, J.L. (2002). Insig-2, a second endoplasmic reticulum protein that binds SCAP and blocks export of sterol regulatory element-binding proteins. Proc. Natl. Acad. Sci. U. S. A. *99*, 12753-12758.

Yabe, D., Komuro, R., Liang, G., Goldstein, J.L., and Brown, M.S. (2003). Liver-specific mRNA for Insig-2 down-regulated by insulin: Implications for fatty acid synthesis. Proc. Natl. Acad. Sci. U. S. A. *100*, 3155-3160.

Yang, J., Brown, M.S., Ho, Y.K., and Goldstein, J.L. (1995). Three different rearrangements in a single intron truncate sterol regulatory element binding protein-2 and produce sterol-resistant phenotype in three cell lines. J. Biol. Chem. *270*, 12152-12161.

Yang, T., Espenshade, P.J., Wright, M.E., Yabe, D., Gong, Y., Aebersold, R., Goldstein, J.L., and Brown, M.S. (2002). Crucial step in cholesterol homeostasis: Sterols promote binding of SCAP to Insig-1, a membrane protein that facilitates retention of SREBPs in ER. Cell *110*, 489-500.

Ye, Y., Shibata, Y., Yun, C., Ron, D., and Rapoport, T.A. (2004). A membrane protein complex mediates retro-translocation from the ER lumen into the cytosol. Nature *429*, 841-847.

Ylitalo, R. (2000). Bisphosphonates and atherosclerosis. Gen. Pharmacol. *35*, 287-296.